UNIVERSITA' DEGLI STUDI DI PADOVA
Sede amministrativa: Università degli Studi di Padova

Dipartimento di Chimica Biologica
Scuola di Dottorato in Biochimica e Biotecnologie
Indirizzo Biochimica e Biofisica
XX° Ciclo

Platelet interactions with α-thrombin and serotonin

Direttore : Prof. Lorenzo Pinna

Supervisore : Prof. Renzo Deana

Co-supervisore : Prof. Zaverio M. Ruggeri

Dottorando: Dr. Alessandro Zarpellon

31 Gennaio 2008

Index

“I do begin to have bloody thoughts”
William Shakespeare (1564 - 1616)
The Tempest, Act 4 Scene 1

Research project on : Role of the Tyr-sulfation of platelet GpIbα in the α-thrombin binding

Abstract

Glycoprotein Gp Ib, which is composed by the disulfide-linked α and β chains, associates with Gp IX and Gp V to form a noncovalent hetero-oligomeric complex expressed on the platelet membrane. The amino-terminal extracytoplasmic domain of GP Ibα contains binding sites for the adhesive protein, von Willebrand factor (vWF), and the platelet agonist α-thrombin, thus supporting two interactions relevant for normal hemostasis as well as the development of pathological thrombosis. Glycoprotein Ibα in the Gp Ib-IX-V receptor complex is the major binding site for α-thrombin associated to platelets, and through this function may support procoagulant activities and contribute to platelet activation and aggregation, as well as anticoaugulant activities, indeed platelets adherent to injured tissues provide a surface for the assembly of the prothrombinase complex that leads to the generation of α-thrombin, which in turn clots fibrinogen and induces platelet aggregation by signaling through protease-activated receptors (PARs), but in contrast, α-thrombin bound to endothelial cell thrombomodulin initiates the protein C pathway that inhibits clotting.

The region of GpIbα thought to be involved in interacting with and α-thrombin (residues 271-284) present three tyrosine residues (positions 276, 278, and 279) that have been shown to be potentially sulfated (Dong et al. 1994) and with recombinant protein has been demonstrated that the sulfation of these three residues is important for the formation of the complex between platelets GpIb and α-thrombin (Marchese et al. 1995).

The GpIbα interactions with α-thrombin are thought to be mediated by thrombin anion binding regions called exosites; several studies suggest that exosite II is relevant for the interactions of the two protein, whether is still matter of debate whereas a functional role for exosite I exist.

Aim of this study performed at the Scripps Research Institute (La Jolla, CA) in the laboratory directed by prof. Z.M. Ruggeri was to precisely define the functional role of tyrosine sulfation in the α-thrombin binding to GpIbα.

With this intent, we expressed a GP Ibα fragment (corresponding to the sequence 1-302 of the mature protein - GpIbN) that was digested with Abalonis sulfatase. Four peaks that differ in the level of sulfation were purified and tested for the ability to create a stable complex with α-thrombin. We arbitrarly named them Pk 4 (three sulfated tyrosine residues sTyr), Pk 3 (two sTyr), Pk 2 (one sTyr) and Pk 1 (no sTyr).

We found that the fully sulfated form of GPIbN Pk 4 generated the maximum amount of complex with α-thrombin, as proved by the shift of thrombin peak in gel filtration chromatograms. While Pk 3 and Pk 2 still retain the ability to generate a complex altough proportionately lower than Pk 4, Pk 1 does not generate any appreciable complex. We also found that stoichiometric ratio of the two proteins is relevant for the complex formation, since experiments with Pk 3 in excess to α-thrombin (3:1) generate more complex than when mixed equally (1:1) or in α-thrombin excess (1:3). To assess the specific role of any single sulfated Tyr we have introduced selected mutations in GPIbN and found that only GPIbN Y278F Pk 3 retains the ability to create stable and long lasting complex, while mutation Y276F and Y279F deeply impaired the binding of thrombin to GpIbN. These data were confirmed and developed by surface plasmon resonance experiments. The binding of thrombin to GPIbN Pk 4 involves the generation of two different binding site with affinity constant of 1.9 x 10^{-8} M for the high affinity site and 522 x 10^{-8} M for the low affinity site. As previosly reported by others (De Marco et al. 1990) we confirmed a temperature role on the binding of thrombin to GPIbN since at 4° C the affinity of the two sites increases. We also found that differently from what happens at 24° C no significant amount of α-thrombin was undissociable. Moreover we found that two sites are involved only when the receptor is present at high density, whereas at low density only the low affinity interaction takes place. We also observed that Pk 3 interacts with α-thrombin primarily using the low affinity site, in a density dependent manner. GPIbN Pk 2 still bind α-thrombin with affinity constant in the 10^{-8} M range, while Pk 1, in agreement with chromatographic data, does not bind α-thrombin significantly, proved by the inability of analysis software to generate reliable kinetic constants. The SPR analysis of the single mutations mirrored the chromatografic data. Indeed the mutation Y276F completely abolishes the formation of a stable complex. Furthermore Y278F is still able to bind α-thrombin with the low affinity site (Kd 100 x

10^{-8} M), whereas GPIbN Y279F Pk 3 binds α-thrombin with two sites of 10^{-8} M affinity. We also showed that both exosites are necessary for stronger interactions, since heparin and hirugen, inhibitors of exosite II and I respectively impaired the binding of α-thrombin to GPIbN.

Furthermore we studied cytofluorimetrically the binding of α-thrombin to the whole platelets. We found that human platelets bind to thrombin with a Kd of 104 nM, while the mutation Y279F deeply impairs the binding of α-thrombin to mice platelets, except at concentrations around the μM range, indicating a complexity of the binding mechanism. It might be worthy to note that this is the first experimental evidence with an ex-vivo approach, for a role of tyrosine sulfation on the binding of α-thrombin to platelets. Altough all these data clearly demonstrate with in vitro and ex-vivo approaches that the binding of α-thrombin is deeply modulated by the levels of tyrosine sulfation of GPIbα molecules, others ex-vivo and, expecially in vivo, experiments are necessary to finally clearly pinpoint the role of α-thrombin binding to GPIbα, and pave the way for the design of new effective drugs for the therapy of thrombotic diseases.

Riassunto

La glicoproteina GpIb, e` composta dalle catene α e β legate attraverso un ponte disolfuro, e associate con la GP IX e GP V a formare un complesso etero-oligomerico non covalente espresso sulla membrana piastrinica. Il dominio extracitoplasmatico N-terminale della GpIb contiene i siti di legame per la proteina adesiva fattore di von Willebrand (vWF) e per l`agonista piastrinico trombina, quindi supportando due interazioni rilevanti per la normale emostasi come per lo sviluppo di condizioni trombogeniche. La GpIb e` il maggior sito di legame per la trombina nelle piastrine, e attraverso questo legame puo` supportare attivita` procoaugulanti e proaggreganti. Le piastrine che aderiscono al vaso danneggiato forniscono una superficie ottimale per la generazione di trombina che attivera` successivamente il fibrinogeno e indurra` aggregazione piastrinica attraverso i recettori PAR. La trombina inoltre legandosi alla trombomodulina presente nelle cellule endoteliali converte la proteina C nella sua forma attivata dando il via a meccanismi anti coaugulatori.

La regione della GpIb coinvolta nella interazione con la trombina (residui aminoacidici 271-284) presenta tre tirosine che si e` dimostrato possano essere solfatate (Dong et al. 1994). Attraverso l`uso di proteine ricombinanti e` stato dimostrato un ruolo fondamentale per questi residui nel binding della trombina alla GpIb (Marchese et al. 1995).

Le interazioni tra queste due proteine sono mediate da due siti che legano residui anionici presenti sulla trombina, chiamate exosites. Diversi studi hanno suggerito un ruolo chiave per exosite II mentre e` ancora dibattuto se exosite I possa avere un ruolo importante in questa interazione.

Lo scopo di questo studio, condotto presso il laboratorio del prof. Ruggeri allo Scripps Institute (La Jolla, CA) e` stato quello di definire il ruolo funzionale della solfatazione tirosinica nel legame della trombina alla GpIb.

A questo scopo abbiamo espresso un frammento di GpIb (corrispondente alla sequenza 1-302 della proteina matura – GPIbN) che e` stato digerito con la Abalonis solfatasi. Quattro picchi che differiscono per il loro livello di solfatazione sono stati purificati e saggiati per la loro capacita` di creare complessi stabili con la trombina. Abbiamo arbitrariamente chiamato questi picchi Pk 4 (tre Tir solfatate), Pk 3 (due Tir solfatate), Pk 2 (una Tir solfatata) e Pk 1 (nessuna Tir solfatata).

La forma completamente solfatata Pk 4 genera la massima quantita di complesso, come dimostrato dallo spostamento del tempo di eluizione da una colonna di gel filtrazione del picco della trombina. Mentre Pk 3 e Pk 2 mantengono la capacita` di generare un complesso stabile, sebbene in quantita` minore, Pk 1 non genera apprezzabili quantita` di complesso.

Inoltre abbiamo dimostrato che il rapporto stechiometrico tra le due proteine e` rilevante ai fini della generazione del complesso, in quanto in eccesso di GPIbN se ne forma il maggiore quantitativo. Per capire il ruolo specifico di ogni singolo residuo abbiamo espresso mutanti per ognuna delle tre tirosine. Mentre Y278F Pk 3 mantiene la capacita` di legare trombina in maniera stabile e duratura, le mutazioni Y276F e Y279F, diminuiscono fortemente la capacita` della trombina di legarsi alla GPIbN. Questi dati sono stati ulteriormente confermati e approfonditi con la tecnica detta “surface plasmon resonance (SPR)”.

Con questa tecnica abbiamo trovato che il legame di trombina a GpIbα avviene attraverso due siti di legame con affinita nell ordine di 10^{-8} M, per il sito a bassa affinita' e 10^{-9} M per il sito a piu alta affinita`. Come precedentemente riportato da altri (De Marco et al. 1990) abbiamo confermato un ruolo della temperatura nel legame delle due proteine, in quanto a 4°C l`affinita` aumenta, sebbene sparisca una quota di complesso che a 24°C e` irreversibilmente associato.

Inoltre, abbiamo dimostrato che la densita` di GpIbα deve superare un determinato valore perche` l`interazione possa avvenire attraverso entrambi i siti di legame, in quanto a bassa densita`, solo il sito a bassa affinita` e` funzionalmente disponibile.

Con questa tecnica abbiamo visto che Pk 3 interagisce primariamente con la trombina attraverso il sito a bassa affinita` e anche per esso vi e` una correlazione con la densita` di GPIbN. Il Pk 2 lega ancora trombina con costante di affinita` nell ordine 10^{-8} M mentre Pk 1, in accordo con i dati ottenuti con tecniche cromatografiche, non genera una significativa quantita` di complesso stabile.

I mutanti analizzati con la tecnica SPR riproducono quanto visto con l`approccio cromatografico, infatti la mutazione Y276F abolisce la formazione di complesso stabile, mentre Y278F lega trombina con affinita` nell ordine del 10^{-8}M, cosi come fa, attraverso due siti di legame, il mutante Y279F. Abbiamo inoltre provato attraverso l`uso di inibitori che entrambi gli exosites sono importanti per la formazione di un legame stabile e duraturo tra trombina e GpIbα.

Inoltre abbiamo studiato anche il legame della trombina alle piastrine umane e murine. La trombina lega le piastrine umane con una Kd di 104 nM, mentre la mutazione Y279F abolisce quasi completamente il legame della trombina alle piastrine murine, almeno fino a concentrazioni attorno al μM, rafforzando l`ipotesi della presenza di due siti di legame.

Sebbene tutti questi dati dimostrino chiaramente, con diversi approcci, che il legame della trombina e` profondamente modulato dal livello di solfatazione tirosinica, ulteriori esperimenti sono necessari per delucidare completamente il ruolo e la funzione del legame della trombina alla GpIbα, aprendo cosi la strada alla progettazione di nuovi e piu potenti farmaci antitrombotici.

Research project on : Transport and action of serotonin in healthy and thrombocythemic subjects

Abstract

Polycythemia vera (PV), idiopathic myelofibrosis, and essential thrombocytosis (ET) have been traditionally classified under the category "chronic myeloproliferative disorders" (CMPDs) because they share the following features: involvement of a multipotent hematopoietic progenitor cell; dominance of the transformed clone over non transformed hematopoietic progenitor cells and overproduction of one or more of the elements of the blood in the absence of stimulus.

In our study we analyzed platelets from patients suffering essential thrombocytosis, where the abnormal proliferation of megacaryocites leds to an excessively high number of circulating platelets, however this disease is often asyntomatic, or can be even characterized by bleeding phenomena.

Platelets from ET patients present some well caractherized defects like a reduced number of surface receptor for thrombopoietin or integrin $\alpha_{2b}\beta_3$, enhanced syntesis of thromboxane TXA2, impaired procoaugulant response, an impaired release and stoarage of the consitutent of the dense granules. Recently it has been discovered a mutation in the JAK2 kinases, that seems to be present in the majority of patients with CMPDs Philadelphia negative.

Altough several authors tried to define the molecular mechanism that underlies these defects, there is no a general agreement. While some authors suggest a pre-activation of platelets, others argue against such an event. In this study we found that the impaired serotonin uptake is likely to be due by a defect in the mechanism that regulates the transport of 5-HT in the dense granules. Indeed serotonin uptake in platelets treated with reserpine, a well known inhibitor of the ΔpH driven uptake into granules, was not significantly different between platelets from patients with ET and control platelets. Lineweaver-Burk analysis of serotonin transport showed that while Kd was not different, the Vmax of 5-HT uptake was significantly less in ET platelets in comparison with those

from healthy people. Serotonin efflux induced by monensin, is not different in ET platelets from control platelets, arguing against a defect in SERT activity.

The numbers of granules evaluated with immunoistochemistry was not statistical different, thus it can not be ascribed to this parameter the differences found in serotonin uptake. We have ruled out also the involvement of ΔpH, since uptake of acridin orange, a probe that is accumulated in dense granules driven by the difference in pH as serotonin does, was the same in controls and ET patients. We next analized if the other granular components were present in a less amount too. We found that both ATP and Ca^{2+} amounts were lower in granules of ET patients; interestingly the decrease of Ca^{2+} concentration was more substantial than ATP (60% and 45% reduction respectively in comparison to controls).

Since the mutations of a tyrosine kinase (JAK) seems to be the link of all the Philadelphia negative CMPDs, we thought interesting to test the role of Tyr kinases in the uptake of serotonin. We found that whereas JAK kinase did not affect the uptake of serotonin, Src kinases inhibitors impaired the levels of serotonin stored in platelets from normal subjects, while no significant inhibition was found in ET platelets.

Since, on the one hand, $Ca2^{+}$ was the most dramatically impaired constituent of granules, and on the other, serotonin elicits platelet activation which is a higly debated process, we thought interesting to monitor the serotonin-induced cytosolic $Ca2^{+}$ concentration increase, chosen as activation parameter. We found that the increase in $[Ca^{2+}]_{cit}$ was higher in thrombocythemic platelets (400 vs 200 nM) with respect to the control ones.

All together these data suggest that the well known defect in granules uptake and storage of serotonin present in platelets from ET patients, are due by a disregulation of the signalling pathway that involves the VMAT2 transporter. Whether this is the main cause also for the impaired uptake of ADP and Ca^{2+} is not yet clear and further studies are needed to clarify this point as well as the mechanism by which the Tyr kinases differently regulate the serotonin transport in ET and healthy subjects.

Riassunto

Con il termine di patologie mieloproliferative croniche (MPD) si intende un gruppo di malattie a carico del midollo osseo, caratterizzate dalla proliferazione monoclonale di cellule staminali totipotenti ematopoietiche e/o cellule ad un grado di maturazione successivo. Nei quattro principali tipi di patologie mieloproliferative, classificati in base al particolare tipo cellulare coinvolto, sono comprese la policitemia vera (PV) in cui si ha iperproduzione di globuli rossi, spesso accompagnata da un'aumento della produzione della linea megacariocitaria e mieloide, e la trombocitemia essenziale (ET) caratterizzata da una elevata proliferazione monoclonale di megacariociti con iper-produzione di piastrine (mediamente oltre a 400.000 per μl), accompagnata da eventi trombotici ed emorragici, anche se spesso è asintomatica.

Le piastrine dei soggetti ET presentano numerosi difetti biochimici comprendenti una diminuizione dell'espressione recettoriale (per diversi agonisti, e meccanorecettori quali le integrine), della sintesi dei derivati dell'acido arachidonico e del contenuto granulare di nucleotidi adenilici e di serotonina. Recentemente è stata scoperta una mutazione nel dominio pseudochinasico della JAK chinasi, enzima implicato nei meccanismi di traduzione del segnale di molte citochine, che sembra essere presente nella maggior parte dei pazienti con disordini mieloproliferativi Philadelphia negativi.

Sebbene sia un dato universalmente accettato che i pazienti con ET abbiano granuli densi con un contenuto di serotonina e nucleotidi più basso rispetto ai soggetti sani, non sono sostanzialmente ancora chiare le cause di questo fenomeno.

La serotonina si accumula nelle piastrine attraverso l`azione di due trasportatori : il SERT, presente nelle membrana plasmatica, e il VMAT2 che accumula la serotonina nei granuli densi delle piastrine.

In questo studio abbiamo dimostrato che il dimuito accumulo di serotonina da parte dei soggetti malati rispetto a quello dei soggetti sani, molto probabilmente dipende da uno o piu` difetti nei meccanismi che regolano il trasporto di serotonina all` interno dei granuli densi. Infatti l'accumulo in presenza di reserpina, composto che inibisce il trasportatore VMAT2 e quindi l'accumulo del neurotrasmettitore all'interno dei granuli densi, non è significativamente diverso tra soggetti sani e malati. Inoltre anche l`efflusso di serotonina indotto da monensina, non e` diverso, suggerendo ancora una volta che non sia il SERT il

responsabile del minore accumulo. L`analisi di Lineweaver-Burk del trasporto di serotonina ha mostrato che la Kd non differisce tra i due gruppi analizzati, mentre diminuisce significativamente la Vmax di accumulo, suggerendo una disregolazione del transporto, piu` che una minore affinita` del trasportatore per la serotonina.

Il minor accumulo di serotonina non dipende neanche da un minor numero di granuli densi, in quanto il loro numero non differisce significativamente tra soggetti sani e malati. Anche la sonda fluorescente arancio di acridina, che entra all'interno dei granuli densi in risposta al gradiente di pH, viene accumulata solo leggermente meno nelle piastrine ET rispetto a quelle controllo. Abbiamo inoltre dimostrato che nei pazienti ET la quantità di serotonina, ATP e calcio rilasciabili in seguito a stimolazione piastrinica (determinati rispettivamente mediante dosaggio ELISA, luciferin/luciferasi e sonda fluorescente FURA) era circa la metà di quello dei soggetti sani.

Abbiamo inoltre esaminato il ruolo delle tirosin chinasi nei meccanismi di accumulo di serotonina nei soggetti con ET dato che recentemente abbiamo dimostrato che le chinasi Src modulano l`accumulo di serotonina (Zarpellon et al. 2008). Diversamente dai soggetti sani i soggetti con ET non mostrano una diminuzione dell accumulo di serotonina in presenza di inibitori delle chinasi Src. Non vi e` infine un effetto della chinasi JAK nella modulazione del transporto di serotonina nelle piastrine. In parallelo è stata esaminata anche l'attivazione piastrinica indotta da serotonina, che interagendo con il recettore 5-HT_{2a} agisce da agonista debole, ed è risultato che l'aumento del Ca^{2+} citosolico era significativamente maggiore nelle piastrine patologiche rispetto a quelle controllo, indicando una loro maggiore sensibilità al neurotrasmettitore che potrebbe, almeno in parte, rendere ragione dei fenomeni trombo/emorragici presenti in queste patologie.

I dati da noi ottenuti dunque suggeriscono che il ben noto difetto nell' accumulo e nel trasporto di serotonina delle piastrine dei soggetti con trombocitemia essenziale, possa dipendere da meccanismi che regolano il trasportatore VMAT2. Ulteriori studi dovranno essere effettuati per chiarire eventuali legami con il diminuito accumulo di ADP e Ca^{2+}, e per chiarire con esattezza quale o quali chinasi sono coinvolte nella disregolazione della funziona piastrinica nei soggetti trombocitemici essenziali.

Chapter 1

Platelets

Platelets are anucleated fragments of cytoplasm originating from megakaryocytes, haematopoietic cells residing in the bone marrow, and released into circulating blood to function as sentinels of the integrity of vascular system. Accordingly, platelets react to any type of vessel wall injury that alter the endothelial cell lining, whether accompanied or not by exposure of subendothelial matrix components. This "defense" mechanism is elicited whenever there is a deviation from normal condition of vasculature. The most common situation inducing a platelet response results from traumatic injures to tissue, where the continuity of the vascular tree is interrupted and blood begins to pour outside. Haemostasis is a complex set of regulated events leading to the arrest of post-traumatic haemorrhage and preventing death from exsanguination. Platelets cannot distinguish vessel damage caused by traumatic wounds from damage as a complication of pathologic vascular alterations. Under the latter circumstances, the beneficial defence role that prevents excessive blood loss may become a life-threatening disease mechanism. Indeed platelets may participate in the formation of occlusive thrombi that may become the cause of sudden death or serious pathological condition, such ischemic syndromes of heart and brain.

1.1 Platelets morphology

Platelets were discovered by G. Bizzozero in 1882 and "rediscovered" in the 1960s after many decades of oblivion. Interestingly enough, their role was initially more clearly associated with thrombosis than with haemostasis (de Gaetano, 2001). Platelets are the smallest corpuscular components of human blood: their mean diameter is <1.5-2.5 μm, from one-third to one-fourth that of erythrocytes. The physiological number varies from 150.000 to 300.000/mm³ blood.

Platelets are no true cells, as they are not provided with a nucleus. Their origin is the bone marrow, where megakaryocytes liberate platelets as the end product of protrusions of their membrane and cytoplasm.

The typical shape of resting platelets is discoid, upon activation they undergo a shape change to a spiny sphere with long, thin filopodia extending up to 5 μm out from platelet and ending in points that are as small as 0.1 μm in diameter.

Electron microscopy reveals that a resting platelet is divided into three zones

- Peripheral zone: responsible for adhesion and aggregation. It consists of glycocalix, cytoskeleton and platelet membrane.
- Sol-Gel zone: responsible for contraction and constitutes the support microtubule system. Contains the connecting system called the open canalicular system and the dense tubular system.
- Organelle zone: contains several different types of cytoplasmatic organelles such as dense body system, alpha granules, lysosomal granules, mitochondria and glycogen granules.

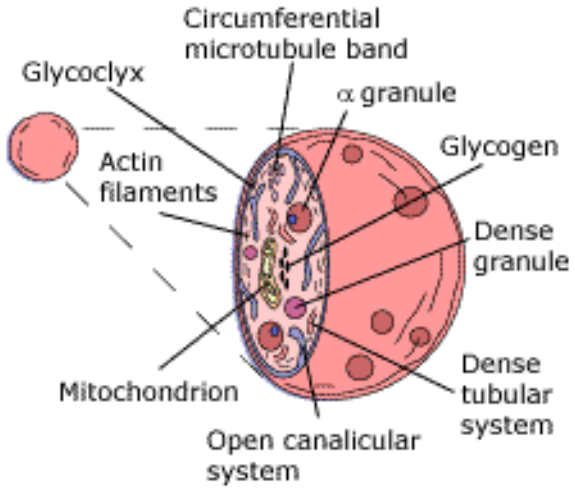

Figure 1. Platelet anatomical structure

Cartoon depicting all the essential features of a human platelet.

The surface of the platelet has a fuzzy coat, named glycocalix, extending 14 to 20 nm and which is composed of membrane glycoproteins (Gp), glycolipids, mucopolysaccharides and adsorbed plasma proteins.

The plasma membrane is a trilaminar unit composed of bilayer of phospholipids in which cholesterol, glycolipids, and glycoprotein are embedded. Approximately 57% of platelet phospholipids is contained in the plasma membrane where they are asymmetrically organized.

The negatively charged phospholipids such as phosphatidylserine (PS) and phosphatidylethanolamine (PE) are mainly sequestered in the inner (cytoplasmic) leaflet of the plasma membrane whereas the others, including sphingomyelin (SM) and phosphatidylcholine (PC), constitute the majority of the outer (exoplasmic) leaflet. This asymmetric distribution is under the control of an inward ATP-dependent aminophospholipid translocase (flippase) that actively pumps PS and PE from the outer to the inner leaflet. The negatively charged phospholipids, especially PS, are able to accelerate several steps in the coagulation sequence and so their presence in the inner leaflet of resting platelets, separated from the plasma coagulation factors, is thought to be a control mechanism for preventing inappropriate coagulation. During platelet activation induced by select agonists, the aminophospholipids may become exposed on the platelet surface or on the surface of microparticles (Ware and Coller, 1995).

Immediately below the plasma membrane, a network of short actin filaments makes up a membrane cytoskeleton that stabilizes the membrane's discoid shape and supports platelet spreading after adhesion. The membrane cytoskeleton is probably attached to the cytoplasmatic domains of transmembrane glycoproteins, including GPIb/IX, integrin $\alpha_{2b}\beta_1$ and perhaps integrin $\alpha_{2b}\beta_3$, via intermediate cytoskeletal proteins such as acting-binding protein and spectrin; thus it may play a role in moving certain receptors from surface to the interior of platelet and vice versa via the open canalicular system.

Microtubules and microfilaments are main components of platelet cytoskeleton and contribute to maintain the discoid shape of resting platelets. Microtubules are composed of polymers of M_r 111kDa, each composed of two proteins of M_r 55 kDa (α- and β-tubulin) that associate with high-molecular proteins (microtubule-associated proteins).

The platelet cytoplasm is filled with a three-dimensional network of actin filaments that perform the contractile functions of cytoskeleton. The organization of these filaments is regulated by their association with proteins such as α-actinin, tropomyosin, and actin-bindig protein. When platelets are activated, myosin associates with this cytoplasmic

actin filaments, generating the tension required for the centralization of granules. New filaments are formed by the polymerisation of monomeric actin and this new filaments induce the extension of filopodia (Authi et al., 1993).

The membrane system is composed by the dense tubular system (DTS) and the open canalicular system (OCS). The first is a closed-channel network of residual endoplasmatic reticulum characterized histocytochemically by the presence of peroxidase activity.

Contrary to organelles involved in the release reaction, the DTS is located near the membrane in the vicinity of microtubules and is the major site for prostanoid biosynthesis. This intracellular membrane organelle contains phospholipid-modifying enzymes that catabolize arachidonic acid towards thromboxane, namely cyclooxygenase and thromboxane (TX) synthetase activities.

The calcium stored in the DTS represents 30% of total platelet calcium content and is mobilized during platelet activation. The storage of calcium is controlled by a sophisticated machinery of ATPase pumps, termed SERCAs (sarcoplasmic endoplasmic reticulum calcium ATPase), located on DTS membranes, and tightly coupled with PMCAs (plasma membrane calcium ATPases). The calcium ATPases are controlled by the cytosolic cAMP level (Rendu and Bohn, 2001).

The surface-connected open canalicular system is an elaborate series of conduits that begins as indentation of plasma membrane and course throughout the interior of the platelet. OCS may serve several functions. It provides a mechanism for entry of external elements into the platelet interior. It also provides a potential route for release of granule contents to the outside, eliminating the need for granule fusion with plasma membrane itself.

Platelet mitochondria are depicted by the classical structure and contain the typical activities of the oxidative pathway of fatty acid metabolism, oxidative phosphorylation and respiratory control. The mitochondria contribute to platelet energy metabolism, act to maintain a sufficient platelet energy content and a tight coupling between metabolic energy and platelet aggregation and secretion.

Dense granules are the smallest platelet granules (mean diameter of 150 nm). Normal human platelets contain three to eight dense granules per platelet with a luminal pH of

about 6.1 maintained thanks to a proton-pumping ATPase. They are characterized by the presence of an intensely opaque dense core surrounded by a clear space and a single membrane.

Dense granules are so-called because they are both heavy and electron dense. They contain high concentrations of adenine nucleotides (65% of the total platelet content) with an ADP/ATP ratio of 1.5, inverse to that in the whole platelet. This pool of adenine nucleotides is metabolically inert and can be distinguished from the metabolic pool in that it is not labelled by incubation of platelets with radiolabelled phosphate.

Dense granules are the storage granules for serotonin (5-hydroxytryptamine), at a concentration of about 65 mM, and hence were originally called the 5-hydroxytryptamine organelles.

Serotonin is the major osmiophilic factor of dense granules and is not synthesised in platelets but is actively taken up from the plasma and accumulated in dense granules where it is likely complexed with ATP and potentially with calcium.

Dense granules also contain 70% of the total platelet content of bivalent cations, with calcium as the predominant ion in human platelets at a specific concentration over 100 times higher than that of the whole platelet. This pool of calcium is distinct from the DTS pool, and is not mobilized for platelet activation. Within the dense core, adenine nucleotides and pyrophosphate form tight complexes with calcium and serotonin held together by intermolecular forces. This heavy complex confers two specific properties to dense granules: i) the high amount of calcium is not in an ionized form and contributes to their high stability; ii) dense granules incorporate serotonin with a very high concentration gradient; indeed, the serotonin concentration within the dense core can be 1000 times higher than in the plasma.

Small GTP-binding proteins, ral and rab, are present in the dense granule membrane indicating that the dense granule is equipped with transducing proteins required for the release reaction (McNicol and Israels, 1999).

The most abundant granules in platelets, numbering < 50 to 80 per platelet, are α-granules. They are < 400 nm in diameter on cross-section with a single membrane. They have spherical or ovoid morphology, with different staining patterns depending on the intragranular constituent observed.

Two major compartments can be identified: a dark nucleoid containing proteoglycans, and an electron-luscent gray matrix. The latter can be subdivided into a nucleoid adjacent region, an intermediate zone often associated with plasmatic proteins, and a small peripheral zone characterized by the presence of tubular structures where the massive proteins are colocalized, including von Willebrand factor (vWF), and factor V.

The α-granule population has two major characteristics: i) the complex mechanism of packaging of the protein content by both synthesis and endocytosis; ii) the nature and functions of the stored proteins, which are large adhesive and healing proteins (Rendu and Bohn, 2001).

Two specific platelet proteins, β-thromboglobulin (βTG) and platelet factor 4 (PF4), are localized in the α−granule nucleoid together with proteoglycans; these proteins bind heparin with different affinity and both neutralize heparin's anticoagulant activity.

Another category of granules involved in the release reaction concerns lysosomes. Lysosomes contain a variety of digestive enzymes, such as glycosidases, proteases, cationic proteins with bactericidal activity, active under acidic conditions. The size of lysosomes is intermediate between dense granules and α-granules measuring 175–250 nm in diameter. Their release is induced by strong agonists of activation (Rendu and Bohn, 2001).

1.2 Platelet activation

Platelets get activated following vascular injury and subsequently lead to the formation of a platelet plug. This process involves shape change, secretion of granule contents, aggregation and generation of lipid mediators like thromboxane A2 (TXA2) and platelet activating factor (PAF).

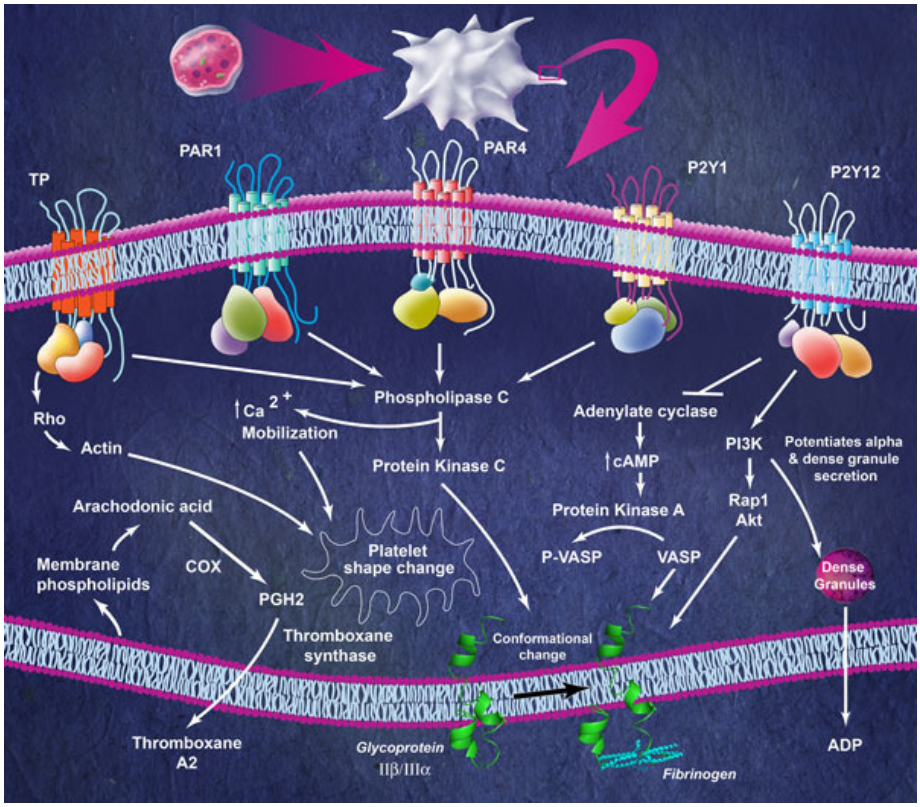

Figure 2. Platelets signalling.
Diagram illustrating the potential signal transduction pathways in platelet activation induced by various agonists

In general terms, the early platelet activation events include shape change and movement that are complex processes that depend on the cytoplasmic dynamics of the actin polymer. To spread the resting platelets must reorganize its cytoskeleton and assemble new actin filaments. Hence proteins that regulate actin architecture and dynamics control shape change. Platelet shape change follows a reproducible temporal sequence.The first event that is observed is that the discois shape is lost and it becomes roundesed or spheroid in form. Next fingerlike projections grow from the cell periphery

then the platelet flattens over surfaces and broad lamellae are extended. S the platelet flattens, granules and organelles are squeezed into the center of the cell resulting in a fried egg appearance. Finally a dynamic phase of memraben motility begins at various points along the lamellae membrane ruffles form and are retracted inward unique blunt filopods extend from the cell center and are rtotaed around the cell periphery.in the electron mmicroscope a dense netwrokf of 0.5 um long actin filaments is ofund to fill the lamellipidial spaces. These cortical networks derive from the assembl of new actin filaments which doubles the filament content of the cell.

The filament assembly reaction is so robust that latelets have a modified secretory process. During the docking step, the granules move under control of the rab GTPase protein, therefore the granular membrane receptors VAMPs 3 and 8 (v-SNARE) become in close opposition to the plasma membrane counter receptors syntaxins 2 or 4 (t-SNARE), bound to SNAP 23. Only then, these SNARE proteins associate at their N-terminal ends and subsequently form tight interactions via coil-coil domains forming an exocytotic core complex that facilitates the membrane fusion (Rendu and Bohn, 2001).

Fusion of membranes requires energy and is catalysed by specialized soluble accessory proteins that assemble at the fusion site to form a fusion complex. Indeed, the cytosolic proteins required for this fusion, N-ethylmaleimide-sensitive fusion protein (NSF), have ATPase activity and thus provide the energy required for the membrane fusion process

Specific lipid components, such as phosphatidic acid (PA) and PIP_2, have been shown to contribute to the membrane fusion event required for granule secretion in platelets. Moreover a set of chaperone proteins have been shown to bind and modulate the activity of the SNARE protein core to facilitate membrane fusion (Flaumenhaft, 2003).

Another pivotal event in the activation of platelets is the activation of one or more phospholipase C (PLC) isoforms yielding a rise in the cytosolic Ca^{2+} concentration and the activation of protein kinase C (PKC).

Platelets contain β and γ isoforms of this enzyme. The β forms are associated with heterotrimericG protein-linked receptors and can be activated by G_q, while the γ forms are regulated by tyrosine phosphorylation (Abrams, 2005).

PLCβ is primarily responsible for the rapid burst of phosphoinositide hydrolysis that occurs during platelet activation by agonists such as thrombin trough its receptors PAR1 and PAR4,ADP via P_2Y_1 receptor, and thromboxane A2.

Once activated, both PLCβ and PLCγ hydrolyze phosphatidylinositol 4,5-trisphosphate (PIP_2) and generate the second messengers sn-1,2-diacylglycerol (DAG) and inositol 1,4,5-trisphosphate (IP_3).

The lipid soluble DAG activates PKC and contributes to protein phosphorylation in serine/threonine residues, whereas the water-soluble IP_3 causes a cytosolic rise in Ca^{2+} by stimulating release of the intracellular ion from the dense tubular system (DTS) (Selheim et al.,2000).

Stimulation of G protein–coupled receptors leads also to the activation of PI3K that phosphorylates PIP_2 to generate the lipid second messenger phosphatidylinositol 3,4,5-triphosphate (PIP_3). A role for PIP_3 in platelets remains to be clearly identified, but it leads to the activation Akt, and in other cells types it was found to activate of both phosphatidylinositoldependent kinase 1 (PDK1), and exchange the factor for Rho family guanosine triphosphate phosphohydrolases (GTPases) (Lian et al., 2005).

In resting platelet cytosolic calcium concentration is about 100 nM while extracellular concentration of this bivalent ion is millimolar.

In basal condition the cytoplasmic calcium concentration represents the balance between passive calcium influx, active calcium extrusion across plasma membrane and active reuptake into intracellular storage compartments. In the plasmatic membrane, that has only a very limited permeability to calcium, there are two transport systems: the first one is a sodium-calcium antiporter that is closely dependent on Na^+/K^+ase pump and the second system is a Ca^{2+}ATPase pump regulated by calmodulin.

Stimulation of human platelets by agonists results in an elevation in $[Ca^{2+}]_c$ that consists in two components: Ca^{2+} release from the intracellular stores and activation of Ca^{2+} entry through plasma membrane channels.

Capacitative Ca^{2+} entry (CCE) is a major mechanism responsible for Ca^{2+} influx in human platelets; however, the mechanism by which the filling state of the Ca^{2+} stores is communicated to the plasma membrane is poorly understood. Current hypotheses fall into two main categories: indirect and direct (conformational) coupling. Recently, a

modification of the classical conformational coupling hypothesis has been presented in several non-excitable cells including human platelets. The de novo conformational coupling is proposed to be based on a reversible trafficking of portions of the Ca^{2+} stores (the dense tubular system (DTS)) towards the plasma membrane (PM) to facilitate de novo coupling between the IP3R and Ca^{2+} channels in the PM. In addition, an alternative mechanism for the activation of CCE has recently been reported in platelets [Rosado et al., 2004) regulated by the filling state of a Ca^{2+} pool located in lysosome-related (acidic) organelles (Lopez et al., 2005).

In contrast to other cells rise of cAMP levels turn off signaling in platelet, and an increase in cAMP synthesis is one of the main mechanisms by which endothelial cells prevent inappropriate platelet activation. PGI_2 and NO released from endothelial cells cause Gsa mediated increases in adenylyl cyclase activity (PGI_2) and inhibit the hydrolysis of cAMP by phosphodiesterases (NO).

Increased cytoplasmatic level of this nucleotide inhibits platelet function by several mechanism such as prevention of the agonists-induced elevation of cytosolic calcium and inhibition of PLC-mediated IP_3 and DAG production. Many, but not all, cAMP's actions are mediated by the enzyme cAMP-dependent protein kinase (PKA).

Adenylyl ciclase is inhibited by the platelet agonist ADP trough its interaction with $P2Y_{12}$ receptor that is coupled to the $G_{\alpha i2}$. Downstream of $G_{\alpha i2}$, the inhibition of cAMP production, although not sufficient to trigger platelet aggregation, has a facilitating effect on activation, at least by the inhibition of cAMP-dependent protein kinase (PKA). The activation of PKA leads to phosphorylation of multiple platelet proteins that are important in platelet aggregation, including the α chain of GPIb, actin-binding protein (filamin), myosin light chain, vasodilatator stimulated phospho-protein VASP, and Rap1B. VASP is an actin regulatory protein and a negative modulator of $\alpha_{IIb}\beta_3$ integrin activation (Gachet, 2005).

Platelets also contain guanylate ciclase, and activation of this enzyme produces an increase in cyclic GMP (cGMP). The roles of cGMP in regulating platelet activation have been controversial since the dawn of this field, because increases in platelet cGMP levels had been observed in response to either platelet agonists (thrombin, adenosine diphosphate, or collagen) or inhibitors (nitric oxide [NO] or NO donors).

The synthesis of thromboxane A_2 (TXA_2) from arachidonic acid and its passive diffusion out of platelets is a mechanism that amplifies platelet activation. Arachidonic acid generated by phospholipase A_2 mediated hydrolysis of membrane phospholipids. The activity of phospholipase A_2 is tightly controlled by the cytosolic Ca^{2+} changes that occur during platelet activation.

Once released from membrane phospholipids, arachidonic acid can be metabolized to eicosanoids (a family of prostaglandins) by cyclooxygenase-1 (COX-1) and finally to thromboxane A_2 by thromboxane synthase. Notably, aspirin inhibits platelet responses by acetylating and irreversibly inactivating COX-1.

Since platelets lack the ability to synthesize significant amounts of protein, inactivation of COX-1 by aspirin blocks TXA_2 synthesis until new platelets are formed. Once synthesized, the thromboxane A_2 can passively diffuse across the plasma membrane and activates other platelets through signaling pathways.

Late platelet activation events include the process of transforming integrin $\alpha_{IIb}\beta_3$ on the platelet surface into a competent receptor for fibrinogen. It is the final common pathway in platelet responses to most agonists, making it a frequent target for drug development.

Integrin $\alpha_{IIb}\beta_3$ is the most abundant surface-expressed integrin in platelets (approximately 80.000 receptors per cell), with an additional pool that can be recruited from internal membranes upon thrombin-induced platelet activation (Wagner et al. 1996; Faull et al.1994; Shattil et al. 1985). $\alpha_{IIb}\beta_3$ can bind several RGD ligands, including fibrinogen (Bennet et al. 1979), fibrin (Hantgan et al. 1988), von Willebrand factor (VWF) (Ruggeri et al. 1982), vitronectin (Thiagarajan et al. 1988), fibronectin (Ginsberg et al. 1983), and thrombospondin (Karczewski et al. 1989). Other ligands such as hantavirus may bind under pathological circumstances (Gavrilovskaya et al. 1999). While ligand recognition typically occurs through an RGD tract, in the case of fibrinogen, RGD tracts in the α- and γ-chains are not required, and interaction with $\alpha_{IIb}\beta_3$ is mediated by a dodecapeptide sequence at the γ-chain C-terminus (Hawiger et al. 1983). The first glimpses of purified $\alpha_{IIb}\beta_3$ complexes were obtained by electron microscopy of detergent-solubilized platelet membranes. in $\alpha_{IIb}\beta_3$, anatomically distinct regions within the subunits are recognizable: the α-chain contains a β-propeller, thigh, calf1, and calf2 domains, while the β-chain contains a βA (or β I-like) domain, followed

by hybrid, PSI (plexin–semaphorin–integrin), EGF-like, and β-tail domains. The large globular head domain observed by electron microscopy likely corresponds to the β-propeller and thigh domains in the α-chain, and the βA and hybrid domains in the β-chain, and the long tails correspond to the remainder of the extracellular portions of the molecule. One of the most striking features of the $\alpha_V\beta_3$ crystal structure is the 'bent knee' conformation observed for the molecule in the unliganded or liganded state. However, when physiological ligand or small molecule inhibitors were crystallized together with the αIIbβ3 headpiece, an open conformation was observed (Takagi et al. 2002), consistent with rotary shadowed images of liganded integrin and with mutational studies. Molecular modeling studies of the $\alpha_{IIb}\beta_3$ transmembrane domains indicate that α and β subunits associate as an α-helical coiled-coil structure (Adair et al. 2002), with a conserved glycophorin-A-like sequence motif of the α-chain present at the heterodimeric interface.

Engagement of the α_{IIb} and/or β_3 cytoplasmic tails by specific intracellular proteins is thought to promote regulation of $\alpha_{IIb}\beta_3$ affinity through transmission of long-range conformational changes to the extracellular portions of the integrin. The current "switchblade" model of integrin activation proposes that separation of the cytoplasmic and transmembrane domains causes knee extension of the bent, unactivated integrin and opening of the ectodomain. The intracellular protein talin may be a final common effector of this process because talin head domain engagement of the β3-tail induces nuclear magnetic resonance imaging spectral shifts consistent with α_{IIb} and β_3-tail separation.The well-known divalent cation requirement is explained in large part by the presence of three metal ion coordination sites in the β_3 A domain. These have been designated the MIDAS (metal-ion-dependent adhesion site), the ADMIDAS (adjacent to MIDAS), and the LIMBS (ligand-induced metal-binding site), the latter site occupied by a divalent cation only in the ligand-bound state (Adair et al. 2005). Studies of wildtype β_3 A domains and β_3 A domains with mutations in the metal coordination sites have established the cation specificity of each site and the importance of all three sites for optimal ligand binding (Pesho et al. 2006).

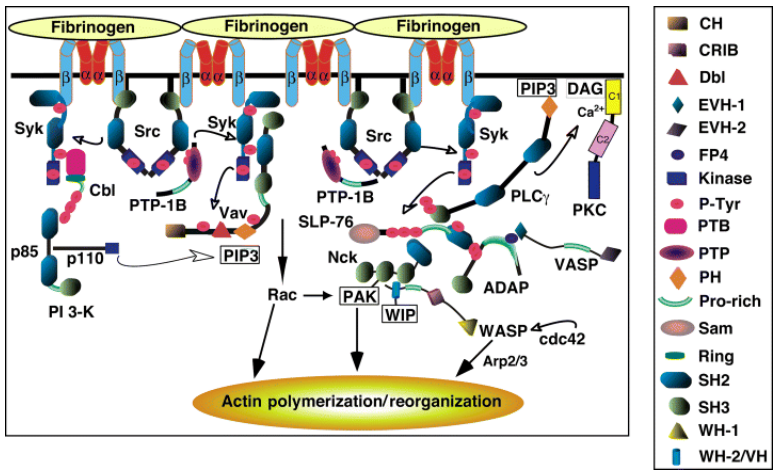

Fig. 3. Cartoon depicting portions of the signaling network linking $\alpha_{IIb}\beta_3$ to actin polymerization and reorganization. The insert provides a key to some of the modules or domains within the proteins that mediate or regulate protein functions and/or interactions. The figure is offered solely to provide a visual of early phases of outside-in signaling.

The $\alpha_{IIb}\beta_3$ is required for platelet aggregation, spreading on ECM, and clot retraction. Its biological importance is reflected by the absence of platelet aggregation and the bleeding diathesis in individuals with classical or variant Glanzmann thrombasthenia who lack or exhibit dysfunctional $\alpha_{IIb}\beta_3$ (Nurden et al. 2006; Weiss et al. 1986; Coller et al. 1995) and by the successful targeting of this integrin for therapeutic blockade in patients with acute coronary syndromes associated with a high risk for occlusive thrombi (Scarborough et al. 1999; Lefkovits et al. 1995; Bhatt et al. 2003). Platelet aggregates are formed by the cross-linking of $\alpha_{IIb}\beta_3$ on adjacent platelets by soluble fibrinogen at low shear rates (Bennet et al. 1979; Marguerie et al. 1979) or VWF at high shear rates (Savage et al. 1998; Mendolicchio et al. 2005). Interestingly, under conditions of extremely high shear stress, VWF binding to its alternate receptor, GPIb-V-IX, may be sufficient to support activation-independent platelet aggregation. Mice deficient in β_3 mirror the human defect and have been used as a model for thrombasthenia and, as expected, show absent platelet thrombus formation in a model of hemorrhagic vasculitis or thrombosis (Bergmeier et al. 2006). As in classical thrombasthenia in humans, the uptake of fibrinogen from plasma into α granules is impaired in these mice.In unstimulated platelets such as those in the normal circulation,

$\alpha_{IIb}\beta_3$ is in a low-affinity state and is unable to bind soluble ligands. In vitro, $\alpha_{IIb}\beta_3$ can become activated by platelet stimulation by one or more excitatory agonists or by activating antibodies (Mondoro et al. 1996; Tomiyama et al 1992), by manganese chloride (Smith et al. 1994), or by the binding of RGD ligands (Du XP et al. 1991). Soluble agonists such as adenosine diphosphate (ADP), thrombin, and thromboxane A2 (TxA2) initiate inside-out signaling through heptahelical G-protein-coupled receptors (Brass et al. 1997; Kauffestenstein et al. 2001), while immobilized agonists such as VWF or collagen initiate the process by interacting with GPIb-IX-V or collagen receptors GPVI and $\alpha_2\beta_1$, respectively. Positive signaling downstream of all these receptors is complicated and networked, variably involving several classes of signaling molecules and second messengers, including phospholipases, protein and lipid kinases and phosphatases, adapters, and second messengers, the latter including calcium, diacylglycerol, and phosphoinositides (Ozaki et al. 2005; Kasirer-Friede et Al. 2004). Alternatively, platelet activation can be dampened by factors that decrease the local concentration of platelet agonists (Marcus et al. 1997) or increase the platelet concentration of nitric oxide or cyclic adenosine monophosphate (Geiger et al. 2001; Siess et al 1993). However, as mentioned above, inside-out signals are thought to ultimately modulate $\alpha_{IIb}\beta_3$ affinity by regulating the interaction of specific proteins, such as talin, with integrin cytoplasmic tails (Shattil et al. 2004; Jackson et al. 2004; Watson et al 2005). Ligand binding to $\alpha_{IIb}\beta_3$ stimulates outside-in signaling to promote (i) firm platelet adhesion and spreading on ECMs (Savage et al 1998, Ruggeri et al ,1997), (ii) fibrin clot retraction (Schoenwaelder et all, 1997), and (iii) development of platelet procoagulant activity and microparticle generation in response to certain stimuli (e.g. collagen, thrombin, and C5b9) (Chang et al 1993). One of the first steps involves receptor oligomerization and a complex regulation by protein tyrosine kinases and phosphatases to activate c-Src and other Src family kinases as well as Syk (Arias–Salgado et al. 2005; Shattil et al. 2004). These initial reactions lead to the assembly of a larger integrin-based signaling complex made up of additional enzymes, adapter molecules, and substrates, including Src homology-2 (SH2)-domain-containing leukocyte-specific phosphoprotein of 76 kDa (SLP-76), Vav1, phospholipase Cγ (PLCγ), adhesion- and degranulation-promoting adapter protein (ADAP), Nck, and

cdc42, which promote actin polymerization and reorganization (De virgilio et al. 2004; Wonerow et al. 2003). In the absence of added agonists, ADP in small amounts released from storage granules is required as a costimulus for full platelet spreading (Goncalves et al. 2003). Bond disruption forces for fibrinogen– $\alpha_{IIb}\beta_3$ are relatively high (80–100 pN) (Litvinov et al. 2002), and bond avidity is enhanced during spreading. Although $\alpha_{IIb}\beta_3$ is required for the growth of stable thrombi (Bergmeier et al. 2006). The interaction between immobilized fibrinogen and $\alpha_{IIb}\beta_3$ promotes only minimal aggregation and thrombus formation ex vivo. Thus, other thrombogenic matrices such as VWF and collagen likely fulfill this role.

In fact, fibrinogen is not a major component of normal ECM, although it increases in atherosclerotic arteries. Activation of platelets with thrombin generates fibrin clots. Retraction of these clots is mediated by $\alpha_{IIb}\beta_3$ and requires integrin binding to fibrin, platelet tyrosine phosphorylation, and production of actin cables that couple indirectly to $\alpha_{IIb}\beta_3$ at the matrix contacts to generate force. The fibrinogen domain involved in clot retraction, differs from domains involved in adhesion and may similarly interact with regions in $\alpha_{IIb}\beta_3$ that do not interact with fibrinogen. Mutation of the two β_3 cytoplasmic tail tyrosines to phenylalanine in mouse platelets (diYF) disrupts outside-in signaling, including fibrin clot retraction. In addition, mice with deletions of extracellular proteins (TSSC6 and gas6), a transmembrane tetraspannin (CD-151), and intracellular proteins (PTP-1B) that have outside-in signaling defects also show defective clot retraction and indicate the complex network of protein–protein interactions required for this response (Arias-Salgado et al. 2005).

1.3 Interactions between platelets and the coagulation system

The classic cascade is composed of two basic parts, an intrinsic pathway and an extrinsic pathway - the intrinsic pathway occurring by physical chemical activation and the extrinsic pathway being activated by tissue factor released from damaged cells. Both pathways are thought to be activated simultaneously to initiate and sustain clot formation. At the same time, platelets are also activated.

The Intrinsic Pathway

This pathway begins with trauma to the blood vessel, exposure of collagen to blood in a damaged vascular wall. In response to these stimuli, two events occur. First, Factor XII (Hageman Factor) is converted from its inactive form (zymogen) to an active form Factor XIIa. Activated Factor XII is actually a protease which enzymatically activates Factor XI to Factor XIa.

This reaction requires the presence of high molecular weight kininogen and prekallekrein. Activated Factor XI is also a protease, but its function is to convert Factor IX to Factor IXa. Also a protease, Factor IXa then converts Factor X to Factor Xa. This activation of Factor X is also greatly accelerated by Factor VIIIa. Activated Factor X functions as a protease to converts the inactive molecule prothrombin to the active thrombin. This step requires the presence of Factor Va. Thrombin then cleaves fibrinogen to fibrin, which then polymerizes to form fibrin strands.

The Extrinsic Pathway

In this pathway, the initial step is a traumatized vascular wall or extravascular tissue. Non-vascular tissue cells contain an integral membrane protein called tissue factor. Damage to the vessel wall or extravascular tissue exposes the plasma to tissue factor. Factor VII is a circulating plasma protein that then binds to tissue factor, creating a complex. In doing so, Factor VII is activated to Factor VIIa. This complex, in the presence of Ca^{2+} and phospholipids, activates Factor X to Factor Xa. Once Factor Xa is generated, the remainder of the cascade is similar to the intrinsic pathway.

Although the concept of "intrinsic" and "extrinsic" pathways served for many years as a useful model for coagulation, more recent evidence has shown that the pathways are not, in fact, redundant but are highly interconnected. For example, the tissue factor/VIIa complex activates not only factor X but also factor IX of the intrinsic pathway. Furthermore, patients with severe factor VII deficiency may bleed even though the intrinsic pathway is intact. Likewise, the severe bleeding associated with deficiencies of factors VIII or IX would not be expected if the extrinsic pathway alone were sufficient to achieve normal hemostasis. Exposure of plasma to tissue factor initiates coagulation. Tissue factor is a non-enzymatic lipoprotein constitutively expressed on the surface of cells that are not normally in contact with plasma (e.g., fibroblasts and macrophages). Exposure of plasma to these cells initiates coagulation outside a broken blood vessel. Endothelial cells also express tissue factor when stimulated by endotoxin, tumor necrosis factor, or interleukin-1, and may be involved in thrombus formation under pathologic conditions. Tissue factor binds factor VIIa and accelerates factor X activation about 30,000-fold. Although factor VII is activated by its product, factor Xa, a trace amount of factor VIIa appears to be available in plasma at all times to interact with tissue factor. Factor VIIa also activates factor IX in the presence of tissue factor, providing a connection between the "extrinsic" and "intrinsic" pathways. Factors IXa and Xa assemble with their non-enzymatic protein cofactors (VIIIa and Va, respectively) on the surface of aggregated platelets. This leads to local generation of large amounts of Xa and thrombin (IIa), followed by conversion of fibrinogen to fibrin. Tissue factor pathway inhibitor (TFPI) is a 34-kDa protein associated with plasma lipoproteins and with the vascular endothelium. It binds to and inhibits factor Xa. The Xa-TFPI complex then interacts with VIIa/tissue factor and inhibits activation of factors X and IX. TFPI may prevent coagulation unless the VIIa/tissue factor initially present generates a sufficient amount of factor IXa to sustain factor X activation via the "intrinsic" pathway. Thus, VIIa/tissue factor may provide the initial stimulus to clot (in the form of relatively small amounts of IXa and Xa) and then be rapidly turned off, while IXa and VIIIa may be responsible for generating the larger amounts of Xa and thrombin required for clot formation.

Amplification and localization of coagulation reactions.

The catalytic nature of coagulation reactions allows tremendous amplification of the initial stimulus. Each VIIa/tissue factor complex can produce many Xa molecules, which subsequently produce an even greater amount of thrombin. Amplification also results from positive feedback reactions. These include activation of V, VIII, and possibly XI by thrombin, as well as activation of VII by Xa. Assembly of activation complexes on cell membranes normally serves to localize coagulation to sites of vessel injury. Membrane-associated reactions include :

(a) activation of X and IX by the VIIa/tissue factor complex on the surface of smooth muscle cells or other cells located beneath the vascular endothelium.
(b) activation of X by the IXa/VIIIa complex on the surface of platelets that have become activated at the site of injury.
(c) activation of prothrombin by the Xa/Va complex on the surface of activated platelets.

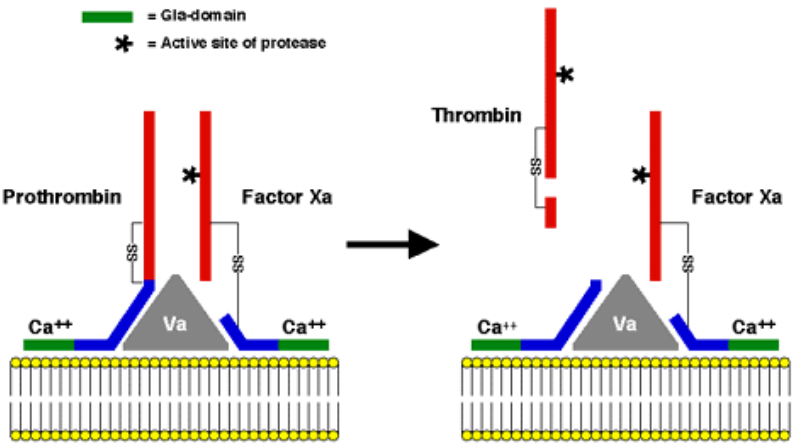

Fig. 4**. Prothrombin Activation Complex**

Human platelets provide an activated membrane surface for the assembly of FX-activating complex (Fig 4). Both the membranes of activated platelets and other cells, as well as phospholipid membranes of defined composition containing aminophospholipids, provide binding sites for the assembly of FIXa, FVIIIa and FX and

for the efficient activation of FX, which in solution is an extremely inefficient process. The study of platelet–coagulant protein interactions has resulted in the view that platelets have plasma membrane receptors for coagulation proteins thrombin (Dahlback et al. 1978; Tracy et a 1979), FXI (Greengard et al. 1986), FXIa (Sinha et al 1984), FIXa and FIX (Ahmad et al. 1989), FX and FII, and for FVIII and FVIIIa. It has been demonstrated that human FXa binds specifically and reversibly in the presence of calcium ions to high-affinity receptors on platelets and that FXa binding is closely correlated with enhanced rates of prothrombin activation(Kane et al. 1980; Tracy et al. 1979).

The functional consequence of the assembly of the prothrombinase complex on platelets is a 300.000-fold acceleration of the rate of prothrombin activation by Fxa (Miletich et al. 1978). The reversible, saturable, high-affinity binding of FXa to platelets depends on the presence of FVa, which has been suggested as the binding site for FXa, and coordinate binding studies of FXa and FVa to platelets indicate that a stoichiometric complex is bound.

According to the revised theory of blood coagulation, although activated endothelial cells and monocytes have been shown to support assembly of FX-activating and prothrombinase complexes, virtually all of the enzymatic reactions occur on the surface of platelet membrane receptors that colocalize the enzymes, the cofactors, and the substrates in a kinetically favorable complex, the assembly of which requires platelet activation. Circulating resting platelets do not bind components of the FX activation complex. Activation of platelets with ADP, while leading to many other functional outcomes, does not result, in exposure of binding sites for FX or FVIIIa or in assembly of a functional FX-activating complex. However, activation of platelets with strong agonists such as thrombin or collagen, results in the expression of binding sites for all the constituents of the FIXa-catalyzed FX-activating complex, namely the enzyme FIXa, the cofactor FVIIIa, and the substrate FX.

It has been established that a combination of thrombin and collagen promote assembly of the prothrombinase complex in a synergistic manner which is closely correlated with the exposure on platelet membranes of negatively charged aminophospholipids.

One step known to be required for platelet-supported FX activation is the exposure of aminophospholipids. Not only can artificial vesicles containing aminophospholipids above a threshold concentration promote FX activation with similar kinetics as activated platelets (Rawala-Sheikh et al 1990), but the calcium-dependent aminophospholipid binding protein Annexin V inhibits FX activation. Scott syndrome platelets with a genetic defect in aminophospholipid exposure following platelet activation show defective FVIIIa binding and FX activation.

The signaling events by which thrombin or collagen lead to platelet procoagulant activities are poorly understood. The activation of FX is a cell membrane mediated event that can occur either when tissue factor and FVIIa are exposed on the cell surface or when cell membrane binding sites are exposed for the components of the intrinsic FX-activating complex on platelets, endothelial cells or monocytes. The weight of evidence points to the platelet membrane as the normal physiological site of coagulation enzyme–cofactor–substrate assembly involved in the intrinsic pathway. Platelets have an essential role in the activation of FX by the intrinsic pathway and none whatsoever in the extrinsic pathway of FX activation, although more recent evidence suggests that platelets can acquire tissue factor from microparticles circulating in blood. Following the generation of FXa, similar interactions occur on the activated platelet surface resulting in the assembly of the prothrombin activating complex consisting of the enzyme (FXa), the cofactor (FVa), and the substrate (prothrombin). Over the past 20 years, a great deal has been learned about the assembly of the prothrombinase complex on human platelets. Although there are differences in some of the particular results of these studies, it is evident that FVa binds directly to platelets and provides a high-affinity binding site for FXa. The binding of human FVa to human platelets is not saturated at concentrations up to 12 nM where, in the presence of FXa and prothrombin, 3000 molecules are bound per cell (Kane et al. 1982). Nonetheless, the kinetic sequel of FVa binding, in terms of its ability to enhance the catalytic efficiency of FXa towards prothrombin, saturates either in the picamolar or the nanomolar. Both FIX and FIXa bind specifically and with high affinity to a discrete number of sites exposed on the activated platelet surface. Moreover, FIXa binds to an additional number of high-affinity, specific sites, which respond to the presence of FVIIIa with enhanced binding

affinity. FX also binds to a high-capacity, low-affinity platelet-binding site that is shared with prothrombin (Scandura et al. 1996), occupancy of which is closely coupled to rates of FX activation in the absence of FVIII. An inference to be drawn from these studies is that each of the components of the FX-activating complex binds to a separate and distinct receptor site on the activated platelet membrane and that the presence of the other two components significantly enhances the affinity and specificity of binding of any one component. Another inference to be drawn is that the platelet FX-activating complex may function in part by providing a large 'target area' for substrate binding and for 'funneling' the bound substrate from a high-capacity, low-affinity binding site to the low-capacity, high-affinity, highly specific enzyme–cofactor complex. Studies are needed to define the interaction between coagulation proteins and platelets because this is the area of hemostasis that is both critical to the maintenance of normal hemostasis and is pathogenetically important in human disease.

Chapter 2

An intriguing story : The binding of α-thrombin to platelets

2.1.1 Structure of the ligand α-thrombin

Human prothrombin, which circulates in the blood stream, is the precursor of human α-thrombin. It is a glycoprotein with 579 amino acid residues and has an N-terminal γ-carboxyglutamic acid (Gla)-rich domain, two kringle domains, a short activation peptide, and the thrombin/catalytic/serine proteinase domain. During the initiation and propagation phases of coagulation, the membrane-bound human prothrombin is activated and truncated by thrombin and FXa, mostly in the form of prothrombinase associated with cofactor Va, yielding the soluble active α-thrombin via the active membrane bound intermediate meizothrombin or the shorter but inactive prethrombin-2. The soluble active α-thrombin is released into the lumen of the blood vessel. Proteolytic activity is gained when the R15-I16 bond (chymotrypsinogen numbering) (Bode et al. 1989) is cleaved. The newly generated I16-V17 N-terminus can then insert into the interior of the molecule to form a salt bridge with the carboxylate of D194, the side chain of which has to rotate outside-in. This rotation is connected with an inside-out turn of the preceding 191 to 194 loop, opening the S1 specificity pocket (Schechter et al 1967) and formation of a functional oxyanion hole.

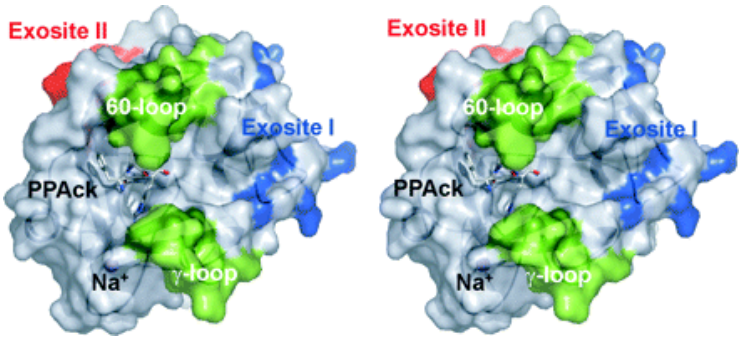

Figure 5. **Thrombin topography.** Stereo view of surface representations of thrombin, shown in the standard orientation (Protein DataBank entry 1PPB), bound to the active site inhibitor d-Phe-Pro-Arg-ck (PPAck). The figure (displayed with a transparent surface and underlying ribbon structure) shows positions of relevant specificity-determining sites: the 60- and γ-loops (green), residues that make up exosite I (blue), and residues in exosite II (red). The position of coordinated Na^+ is indicated.

The α-thrombin consists of a 36-residue A-chain and a 259-residue B-chain covalently linked by a disulfide bridge C1-C122. The B-chain is organized into two adjacent b-barrels, two helices, and some surface loops, similar to trypsin and the catalytic domains of related serine proteinases (Bode et al. 1989). The active-site residues S195, H57, and D102 are present at the junction between both barrels. The active-site cleft extends across both barrels perpendicular to this junction. The thrombin B-chain is 27 residues longer than the corresponding B-chain of chymotrypsin, giving rise to insertion loops located on the surface. Most of these insertion residues occur as extensive loops that border and shape the canyon-like active-site cleft, making it exceptionally deep and narrow, with the reactive S195 residue at its base. In particular, the 60 and the 149 insertion loops (named according to typical or central residues contained) block the access of many macromolecular substrates or inhibitors to the catalytic residues, which is a primary cause for the narrow specificity of α-thrombin. The boomerang shaped A-chain lies in a groove of the B-chain in the back of the molecule, opposite the active. This chain may contribute to the stability of the entire thrombin molecule. The thrombin structure has unique features that control specificity, such as loops and charged patches surrounding the pocket of the active site. A particularly striking feature of the thrombin molecule is its pronounced uneven charge distribution, resulting in localized highly positive and negative electrostatic fields on the thrombin surface (Bode et al. 1992). Three contiguous surface patches, two of positive and one of negative potential have received particular attention. The negatively charged region extends around the active site of thrombin, with D189 and E192 located at the bottom of and at the entrance to the S1 pocket, respectively. The first positively charged patch extends along the convex thrombin surface, where the active-site cleft levels off due to its interaction with fibrin(ogen), it had been designated as fibrin(ogen) secondary binding exosite or fibrinogen recognition exosite (Bode et al. 1992), but now it is referred to primarily as anion binding exosite I. The second positively charged surface patch, with an even stronger positive electrostatic field, (Bode et al. 1992) extends from the intermediate helix toward the C-terminus of thrombin. Due to its interaction with heparin, this positively charged patch has been designated heparin binding site or anion binding exosite II. These energetically unfavorable electrostatic patches, the generation of which

costs considerable extra free energy of folding, create strong electrostatic surface potentials used by the thrombin molecule to select and preorient substrates and inhibitors. Both exosites differentially influence the active site and mutually affect the binding properties of the opposite exosite (Fredenburgh et al. 1997).

Na^+ binding site and allosteric effects

Evidence that α-thrombin is regulated allosterically, independently of the conformational changes that occur during activation, was observed initially in the 1990`s. Sodium has been found to be an important allosteric modulator of α-thrombin (Wells et al. 1992). Kinetically, two allosteric states have been defined that are characterized by the absence and presence of a Na^+ ion, resulting in a slow and a fast form of α-thrombin, respectively (Ayala et al. 1994). The two forms exhibit different relative activities toward macromolecular substrates. The fast thrombin form cleaves fibrinogen and PARs more efficiently and displays procoagulant, prothrombotic, and prosignaling properties. The slow form preferentially cleaves protein C, exhibiting more anticoagulant properties.

α-Thrombin exosites

Two electropositive exosites, in near opposition on the α-thrombin surface, play crucial roles in the recognition of specific macromolecular substrates, effectors, and inhibitors, and their properties have been characterized by extensive crystallographic, mutagenetic, biophysic, and enzymologic studies. Exosite I, composed of insertion loops 30–40 and 70–80, mediates binding of fibrinogen, fibrin, PAR-1 and -4 substrate recognition, staphylocoagulase binding, and binding of the C-terminal 55–65 residue sequence of the thrombin-specific inhibitor, hirudin. Exosite II, a positively charged cluster of residues, mediates different interactions specifically, including heparin, a specific monoclonal antibody, and the fragment 2 domain of ProT(F2). A variety of inhibitors from snake venoms and the saliva of hematophagous organisms also bind to thrombin exosites.

Alanine scanning studies of thrombin exosite complexes provide a basis for interpreting the mechanisms involved in specific binding of structurally diverse protein substrates with strict specificities for exosite I or II. The structures illustrate a mechanism of specific ligand recognition in which the conformational flexibility of thrombin is necessary to accommodate diverse ligands with high specificity for each exosite. It is apparent that exosite I-specific ligands bind competitively through overlapping constellations of distinctly different residues critical to each interaction. The epitope for Y63-sulfated hirudin-(55–65) involves exosite I extensively (Priestle et al. 1993). Fibrinogen (Tsiang et al. 1995) and PAR-1 (Ayala et al. 2001) binding epitope to exosite I overlap with the hirudin peptide and include many of the same residues. The extensive overlap in exosite I epitopes accounts for competitive binding of the hirudin peptide, fibrinogen, and PAR-1. Rapid-reaction kinetic studies of hirudin and hirudin-(54–65) binding to thrombin support electrostatic steering of anionic exosite I ligands, such as the peptide, which mediates initial weak encounter complex formation, followed by establishing direct ionic interactions, and final conformational rearrangement of the exosite and ligand by engagement of hydrophobic interactions (Myles et al. 2001). Thermodynamic studies of thrombin–hirudin interactions also support significant changes in the 70–80 loop of exosite I and structural ordering of the peptide on complex formation (Malkowski et al 1997). It has been suggested that all exosite I ligands follow a similar model, in which complementary asymmetric electrostatic fields enhance the rate of complex formation (Myles e al 2001). In agreement with this idea, analysis of the ionic strength dependence of the kinetics of fibrinogen cleavage by thrombin similarly supports diffusion-controlled electrostatic steering that facilitates initial formation of the transition state (Vindigni et al. 1996). Exosite II interactions are stabilized mainly by electrostatic interactions, whereas exosite I interactions involve a greater contribution from hydrophobic interactions (Huntington et al. 2005). Exosite II-specific interactions with heparin (Carter et al. 2005) and ProT F2 overlap to some extent, but with only one common residue. As part of the GpIb-IX-V platelet receptor complex, GpIbα acts as a thrombin cofactor, producing a 5- to 7-fold enhancement in PAR-1 activation and 6- to tenfold acceleration of GpV cleavage, resulting in platelet activation, and a five thousand fold enhancement

of FXI activation (Adams et al. 2006). Two divergent crystal structures of GpIbα–thrombin complexes showed two thrombin molecules bound, one through exosite I and the other exosite II (Dumas et al. 2003; Celikel et al. 2003), which continued the controversy concerning the mode of thrombin binding. Mutagenesis studies with eight alanine substitutions of exosite II residues and two charge reversal mutants demonstrated decreased thrombin affinity (De Cristofaro et al. 2001), indicating exosite II binding, whereas more limited exosite I mutagenesis showed no effect on GpIba binding (Yun et al. 2003). Binding of individual ligands to each exosite is typically accompanied by changes in tripeptide substrate specificity, and distinct fluorescence spectral changes reporting each binary interaction with thrombin active site-specifically labeled with tripeptide chloromethyl ketone-tethered fluorescence probes (Panizzi et al. 2006). It had been suggested that exosite I and II binding was subject to extremely negative thermodynamic linkage, such that simultaneous interactions with both exosites was prevented allosterically (Fredenburgh et al. 1997). An evaluation of linkage between binding of the exosite I ligands, fibrinogen, and hirudin peptide, and exosite II binding of a monoclonal antibody and F2 demonstrated no detectable inter-exosite linkage (Verhamme et al. 2002). These studies concluded instead that binding of ligands to each exosite is linked to changes in the environment of the catalytic site. Ternary complexes formed with non-interacting ligands for both exosites produce additive or non-additive fluorescence changes, reporting changes in the active site environment (Hogg et all, 1996). These studies illustrate the sensitive linkage between the thrombin active site and exosite binding.

Thrombomodulin interacts with exosite I residues that also overlap those involving the hirudin peptide, fibrinogen, and PAR-1 binding, and with exosite II via its chondroitin sulfate moiety. Factor V and FVIII substrate recognition are mediated primarily by a distinct group of exosite I residues, which are subsets of those involving the hirudin peptide. The epitopes overlap, but a smaller of residues contributes to FVIII activation. Three important exosite II residues are involved in FV activation, while mutation of only one residue in exosite II has significant effects on FVIII activation. The differences between these interactions explain the primary involvement of exosite I and the secondary role of exosite II in FV and VIII activation.

2.1.2 Thrombin receptors in human and mice platelets

Human platelets express PAR1 and PAR4. While activation of either receptor can trigger secretion and aggregation (Vu et al. 1991; Xu et al 1998; Kahn et al. 1999), PAR1 is likely the more important. Antibodies to the thrombin interaction site in PAR1 blocked platelet activation at low concentrations of thrombin (Hung et al. 1992). Similar results were obtained with a PAR1 antagonist (Bernatowicz et al. 1996). By contrast, antibodies to the thrombin cleavage site in PAR4 by themselves had no effect on activation of human platelets by thrombin, but when PAR4 antibodies were combined with PAR1 blockade, platelet activation was markedly inhibited even when high concentrations of thrombin were used (Kahn et al. 1999). These results suggest that PAR1 mediates activation of human platelets at low thrombin concentrations and that, in the absence of PAR1 function, PAR4 can mediate platelet activation but only at high thrombin concentrations.If PAR1 is sufficient for human platelet activation at low concentrations of thrombin, what does PAR4 contribute? It is possible that PAR4 simply provides some redundancy in an important system. It is also possible that PAR4, which lacks a thrombin-binding hirudin-like sequence, contributes responsiveness to proteases other than thrombin. In this regard, platelet activation by cathepsin G (Selak et al. 1988), a granzyme released by activated neutrophils, is mediated by PAR4 (Sambrano et al. 2000); whether this phenomenon is important in vivo is unknown. An additional possibility is that qualitative differences in PAR1 vs. PAR4 signaling make important contributions to platelet function. For example, PAR4 is shutoff more slowly than PAR1, and the tempo of thrombin-triggered increases in cytoplasmic calcium in human platelets appears to represent the sum of contributions from both receptors [Shapiro et al. 2000; Covic et al. 2000). Differences in G protein coupling may also exist between PAR1 and PAR4 (at least for the human isoforms). Like PAR1, PAR4 activates Gq and probably G12/13 signaling (Offermanns et al. 1994), but unlike PAR1, PAR4 does not appear to couple to Gi in fibroblasts (Faruqi et al. 2000). The importance of such differences for platelet function is unknown.In addition to interacting with PARs, thrombin also binds to GpIbα on the surface of human platelets (Okamura et al. 1978). GpIbα is part of a multifunctional protein complex that also

binds VWF and P-selectin (Andrews et al. 1999). Platelets from patients with Bernard–Soulier syndrome lack surface GpIbα and show decreased thrombin responsiveness, but such platelets are also structurally abnormal (Ware et al. 1990; De Marco et al. 1990-1991). However, antibodies that block thrombin binding to GpIbα attenuate platelet activation by thrombin and decrease PAR1 cleavage (De Marco et al. 1994; De Candia et al. 2001). These and other observations support the model that GpIbα may serve as a cofactor that localizes thrombin to the platelet surface to support thrombin cleavage of PARs, analogous to the interaction between PAR3 and PAR4 reported in mouse platelets described below. Attempts to directly demonstrate such cofactor activity by co-expressing the GPIb complex with PARs have been unsuccessful (Nakanishi-Matsui et al. 2000), but the significance of such negative results is, of course, uncertain. Studies in mouse platelets have also suggested a connection between the GPIb complex and thrombin signaling, but the exact nature of that connection remains unclear.

While human platelets utilize PAR1 and PAR4 to respond to thrombin, mouse platelets utilize PAR3 and PAR4 (Kahn et al. 1998). PAR1 agonists that are fully active on human and mouse PAR1 in heterologous expression systems (Connoly et al. 1996) activate human but not mouse platelets, and knockout of PAR1 had no effect on thrombin signaling in mouse platelets but did ablate thrombin signaling in mouse fibroblasts (Connoly et al. 1996). It was these observations that triggered a search for other thrombin receptors in mouse platelets and led to identification of PAR3. Expression of human PAR3 cDNA in COS cells or Xenopus oocytes conferred phosphoinositide hydrolysis in response to low concentrations of thrombin, and in situ hybridization using a mouse PAR3 probe detected PAR3 mRNA in mouse megakaryocytes. Thus mouse PAR3 appeared to be a good candidate for the 'missing' mouse platelet thrombin receptor, and indeed, knockout mouse studies revealed that PAR3 was necessary for activation of mouse platelets at low but not high concentrations of thrombin. Responses of PAR3-deficient mouse platelets to high concentrations of thrombin were attributable to PAR4 (Kahn et al , 1998). At face value, these data conjured a dual receptor model analogous to that described for human platelets with PAR3 simply substituting for PAR1 as the 'high affinity' thrombin

receptor in mouse platelets. However, subsequent characterization of the mouse homologue of PAR3 presented a paradox. Despite strong evidence that PAR3 was necessary for mouse platelet responses to low concentrations of thrombin, expression of mouse PAR3 cDNA in heterologous expression systems failed to confer thrombin signaling. The resolution of this paradox provided several interesting lessons. While expression of mouse PAR3 in COS cells did not by itself confer thrombin signaling, co-expression of mouse PAR3 with mouse PAR4 reliably enhanced cleavage of the latter and signaling at low concentrations of thrombin compared with that seen when mouse PAR4 was expressed alone. When tethered to the plasma membrane, the N-terminal exodomain of mouse PAR3 was sufficient to promote PAR4 cleavage and signaling, and the thrombin-interacting sequences within this domain were necessary. Although an appealing model, no evidence was found for formation of PAR3-PAR4 heterodimers. Thus, it appears that mouse PAR3 does not by itself mediate transmembrane signaling but instead functions as a cofactor that localizes thrombin to the surface of the mouse platelet to promote cleavage and activation of mouse PAR4 at low thrombin concentrations, a curious example of an interaction between G protein-coupled receptors in which one 'receptor' acts as an accessory protein that aids ligation of the other. This model predicts that, in contrast to the case in human platelets, activation of mouse platelets by thrombin should be PAR4-dependent. Platelets from PAR4-deficient ($Par4^{-/-}$) mice are indeed unresponsive to even micromolar concentrations of thrombin despite the presence of PAR3 .

Perhaps surprisingly, a similar cofactor relationship between hPAR1 and hPAR4 or between GpIbα and hPAR1 or hPAR4 could not be detected when these molecules were co-expressed in same systems in which the mPAR3-mPAR4 interaction was readily demonstrated (Nakanishi-Matsui et al. 2000). It is certainly possible that such negative results were because of differences in absolute expression levels or the stoichiometry of the various components achieved in these systems vs. platelets or to other technical issues. Interestingly, mouse platelets that lack GPV, part of the GPIb complex, have been reported to show enhanced responsiveness to thrombin (Ramakrishnan et al. 2001) and to become responsive to active site-inhibited thrombin preparations. Thus, as in

human platelets, there is evidence that the GPIb complex contributes to thrombin responses in mouse platelets. However, the apparently absolute lack of thrombin responses in Par4$^{-/-}$ mouse platelets (Hamilton et al. 2004) suggests that the GPIb complex is not sufficient to mediate platelet activation by thrombin, and the observation that responses to high concentrations of active-site inhibited thrombin preparations were also ablated in Par4$^{-/-}$ platelets (Sambrano et al 2001) suggests that such responses may have been caused by active protease(s) in these preparations. The notion that GPIb plays a cofactor role or interacts with PAR signaling in other ways remains appealing. Studies of platelets from mutant mice in which the thrombin-binding site of GpIbα is selectively disrupted will be of interest, and in this context we generate a mutant mouse that holds the Y279F mutation.

2.1.3. Thrombin signalling via PAR receptors

In common with several other helipthical receptors, PAR1 has been shown to couple to multiple heterotrimeric G-proteins . In a number of early studies, two main signaling events were characterized that were assumed to involve receptor G-protein coupling. The first event involves the inhibition of cAMP through interactions with inhibitory G-protein of the Gi class (Hung et al., 1992; Kanthou et al., 1996).

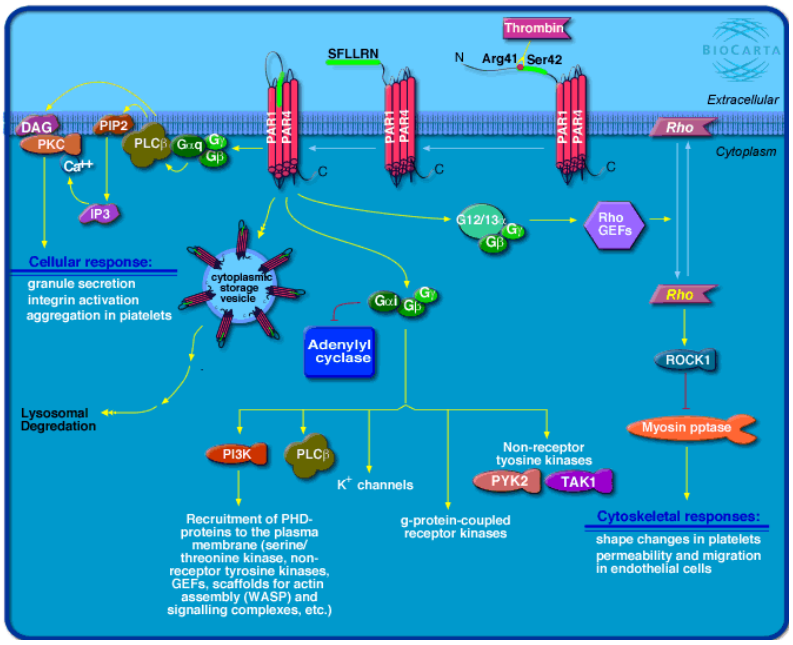

Fig 6. Thrombin signaling and protease-activated receptors

Signalling events triggered by PAR receptors.

The second event is stimulation of phospholipase C (PLC)-catalyzed hydrolysis of polyphosphoinositides, resulting in the formation of InsP3, mobilization of intracellular Ca^{2+}, and generation of diacylglycerol, the endogenous activator of protein kinase C (PKC) (Babich et al., 1990; Hung et al., 1992). Thrombin also stimulates the rapid hydrolysis of other phospholipids, implying roles for PLD, PLA2 and phosphatidylcholine-specific PLC in the initial generation of lipid activators of protein kinase C isoforms. The recent identification of multiple G-protein subunits and their corresponding effector enzymes allowed examination of these transduction

mechanisms. Microinjection of antibodies directed against $G_{q/11}$ into CCL-39 cells inhibited PAR-1 mediated Ca^{2+} mobilization (Baffy et al. 1994), whereas the same antibodies abrogated GTPase activity in thrombin-stimulated platelet membranes (Benka et al. 1995). Furthermore, in platelets derived from transgenic mice lacking Gq, thrombin-stimulated phosphoinositide hydrolysis was abrogated (Offermanns et al. 1997). A direct interaction between PAR1 and $G_{q/11}$ and G_{12} has been recently demonstrated by immunoprecipitation of PAR1 with G_{12} and $G_{q/11}$ in thrombin-stimulated human neuroblastoma SH-EP cells (Ogino et al. 1996), clearly indicating interaction of PAR-1 with these two G-protein subunits. In a number of cell systems, pertussis toxin (PTX)-mediated ADP ribosylation of G_i/G_o α-subunits also reduced thrombin-stimulated InsP3 formation and Ca^{2+}, indicating the potential for coupling of PAR1 to G_i/G_o subunits (Babich et al. 1990; Brass et al. 1991). Antibodies to G_o also reduced PAR1-mediated responses (Baffy et al. 1994), suggesting that this subunit contributes to PLC activation. However, Go expression is cell-specific, and it is likely that another pertussis sensitive G-protein, possibly G_{i2}, may also be involved. At present, it remains unclear for thrombin receptor systems whether βγsubunits derived from G_{12} or G_o are able to activate other isoforms of PLC-β, such as PLC-β_2 or PLC-β_3. PAR1 is also linked to other second messenger systems via pertussis-sensitive G-proteins. Thrombin-mediated inhibition of adenylyl cyclase has been demonstrated to involve a direct interaction of the receptor with G_{i2} (Hung et al. 1992; Swift et al. 2000). Stimulation of other phospholipase activity, such as PLD and PLA_2 has also been shown to be sensitive to PTX in some cell types (Banga et al., 1988; Suzuki et al., 1996). However, evidence supporting a direct interaction between the receptor and a G-protein α-subunit in a manner analogous to $G_{q/11}$/PLC-β_1 is minimal. One study has shown that expression of a mutant G_{12} protein can specifically inhibit arachidonic acid release in response to thrombin (Winitz et al., 1994) through a mechanism that does not involve intermediates known to regulate PLA2 activity. In general. regulation of these phospholipases following PAR1 activation is likely to be downstream of initial activation of PLC_β isoforms and, indeed, in cells where $PLC_{\beta 1}$ is poorly expressed, thrombin stimulation of PLD and $cPLA_2$ is diminished (Fee et al., 1994).

2.1.4 Structure of the receptor complex GpIb-V-IX

The GPIb-V–IX complex is constitutively expressed on the platelet plasma membrane in about 20.000 copies per platelet. It is composed of four transmembrane subunits: GpIbα, disulphide-linked to GPIb$_\beta$, and the noncovalently associated GPIX and GPV, in the ratio of 2:2:2:1. Each subunit of the complex belongs to the leucine-rich repeat proteins superfamily, as it contains one or more leucine-rich repeats (LLRs) of approximately 24 amino acids, flanked by conserved N- and C-terminal disulphide loop structures. Recently, it has been demonstrated that a subset of GPIb-V–IX is constitutively associated with the lipid rafts in unstimulated platelets and that additional copies of the receptor are further recruited to these microdomains upon stimulation with VWF.

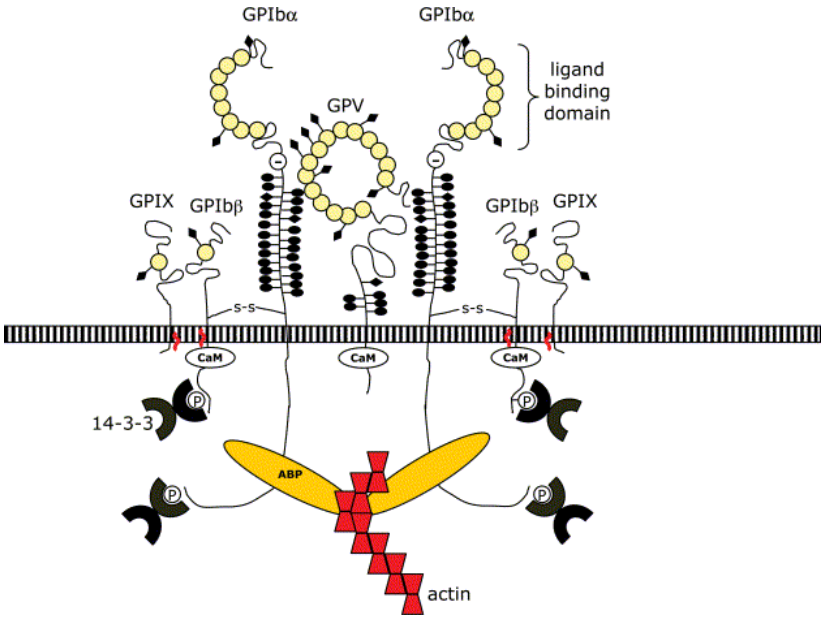

Fig. 7. Structure of GPIb-V–IX. Platelet GPIb-V–IX is composed by four different transmembrane polypetides: GpIbα, GPIbβ, GPIX, and GPV. GpIbα is disulphide-linked to GPIbβ, which, in turn, is noncovalently associated with GPIX. A single GPV molecule interacts noncovalently with two adjacent GPIbIX complexes to form the complete receptor. Each member of the complex contains one or multiple leucine-rich repeats (yellow circle) in the extracellular domain. Carbohydrate moieties are represented as black line (diamonds on stalks represent N-linked oligosaccharides, while circles are O-linked oligosaccharides). Many extracellular ligands interact with GPIb-V–IX by binding to a domain on the N-terminal region of GpIbα. The short cytoplasmic domains of GPIbβ and GPIX contain acylated cysteine residues (drawing in red) that represent additional sites for membrane anchorage. The figure shows the phosphorylation sites on GpIbα and GPIbβ. The C-terminal serine of GpIbα is constitutively phosphorylated, while serine phosphorylation of GPIbβ is promoted by the PKA. The cytoplasmic domains of the single subunits interact with a number of proteins, including the cytoskeletal actin-binding protein (ABP), calmodulin (CaM), and the 14-3-3 protein.

GpIbα (610 residues) has an apparent molecular mass of 135 kDa and represents the largest subunit of the complex. Different structural and functional domains can be recognised in the GpIbα subunit. An N-terminal domain (residues 1–282), delimited by two conserved disulphide loop structures, is composed by eight LRRs and contains the binding sites for many GPIb-V–IX ligands. It is then followed by a region (residues 283–302) enriched in negatively charged residues, including aspartic and glutamic acids as well as three sulfated tyrosines (Dong et al. 1994), which is connected to a single transmembrane region (residues 486–514) by a long and highly glycosylated mucin-like macroglycopeptide domain (residues 303–485). The cytoplasmic tail of GpIbα is composed by 96 amino acids (residues 515–610) (Lopez et al. 1987). The integrity of the tandem LRRs of GpIbα is essential for normal processing and function of GPIb-V–IX (Ulsemere et al. 2000). LRRs 2, 3, and 4 of GpIbα are critical for VWF binding and platelet adhesion (Shen et al. 2002) and mutations within the LRRs 2, 5, 6, and 7 of GpIbα have been found associated with the bleeding disorder Bernard–Soulier syndrome (Whisstock et al. 2002). The region enriched in negatively charged residues is also quite important for interaction with extracellular ligands. In particular, mutation of the three sulfated tyrosine residues (Y276, Y278, Y279) results in a strong reduction of VWF and thrombin binding (Marchese et al. 1995). The macroglycopeptide is highly polymorphic and contains predominantly O-linked sialylated oligosaccharides, on the average, every three or four amino acids (Korrel et al. 1984). The cytoplasmic tail of GpIbα contains binding sites for intracellular signalling molecules, such as 14-3-3ζ (Du et al 1996), and for proteins of the platelet cytoskeleton, such as actin-binding protein (Andrews et al. 1992). The binding of GpIbα to actin-binding protein involves residues 557–575 and links the whole receptor to the submembranous actin filament network. This interaction is important for the regulation of VWF-induced platelet adhesion and activation (Feng et al. 2003).

GPIbβ (25 kDa, 181 residues) has a single LRR with conserved flanking sequences in the extracellular sequence. It is covalently linked to GpIbα through a disulphide bridge involving a cysteine proximal to the transmembrane region (Lopez et al. 1988). GPIbβ also interacts noncovalently with GPIX through residues 15–32 (Kenny et al. 2002).

The cytoplasmic tail of GPIbβ is 34 amino acids in length and contains a serine residue (Ser166) which is phosphorylated by cAMP-dependent protein kinase (PKA) (Wardell et al. 1989). The cytoplasmic domain of GPIbβ has been found to interact with calmodulin and with 14-3-3ζ (Calverley et al. 1998) and contains cysteines that can be palmitoylated.

GPIX (22 kDa, 160 residues) has only a single LRR with conserved flanking sequences, like GPIbβ (Hickey et al. 1989). Its cytoplasmic tail is very short, as it consists of just 5 amino acids. Like GPIbβ, GPIX is palmitoylated on cysteine residues in the cytoplasmic domain, proximal to the plasma membrane. However, the analysis of guinea pig megakaryocytes has suggested that GPIX may be predominantly myristoylated rather than palmitoylated. These modifications may provide an additional mechanism for anchoring the entire complex to the platelet membrane, and they may contribute to its localisation within the lipid rafts .

GPV (82 kDa, 544 residues) is composed of an extracellular domain with 15 LRRs, a single transmembrane domain, and a cytoplasmic tail of 16 amino acids (Lanza et al. 1993). GPV links adiacent GPIbIX complexes through direct interaction with GpIbα (Li et al. 1995). The cytoplasmic tail of GPV (residues 529–544) associates with calmodulin and 14-3-3ζ in resting platelets (Andrews et al. 2001). GPV has been shown to play a role in strengthening the interaction of GPIb-V–IX with VWF under high shear conditions. Moreover, GPV has been demonstrated to bind collagen and to form a high-affinity binding site for thrombin (Moog et al. 2001; Dong et al. 1997).

Intracellular interactors of GPIb-V–IX

The short cytoplasmic domains of the different subunits of GPIb-V–IX are not associated to GTP-binding proteins and do not possess intrinsic enzymatic activities. However, GPIb-V–IX interacts constitutively with a number of intracellular proteins, including actin-binding protein, 14-3-3ζ , and calmodulin (Andrews et al. 2001). These interactions may regulate different GPIb-V–IX-dependent cellular events, such as platelet rolling, adhesion, cytoskeleton reorganisation, and transmembrane signalling

(Englund et al. 2001).The cytoplasmic tail of the GpIbα subunit contains a binding site for actin-binding protein within the residues 557–575.

Actin-binding protein directly interacts with actin filaments, and thus it anchors the entire receptor to the membrane skeleton. Studies performed in CHO cells transfected with mutant GpIbα subunit lacking the binding domain for actin-binding protein demonstrated that this interaction is critical for maintaining adhesion on a VWF matrix at high shear stress and to facilitate platelet rolling on VWF. In addition, the interaction of GPIb-V–IX with actin-binding protein has been demonstrated to play a role in cell activation and aggregation (Christodoulides et al. 2001). For instance, using a synthetic peptide able to block actin-binding protein–GpIbα interaction in a CHO cells reconstituted model, were observed a dose-dependent inhibition of VWF-induced aggregation in response to both ristocetin and shear stress and a diminution of shear-dependent protein tyrosine phosphorylation.The 14-3-3 proteins are 30-kDa ubiquitous proteins that regulate the activity of several signalling molecules and control different physiological processes such as mitogenesis, cell cycling, and apoptosis. A wide variety of proteins have been demonstrated to associate with 14-3-3, including Raf-1 kinase, protein kinase C (PKC), and PI-3K. The 14-3-3 isoform most commonly involved in signalling transduction pathway is 14-3-3ζ. It is usually expressed as a dimer, and thus it may bind simultaneously two cytoplasmic proteins to assemble a sovramolecular complex. GPIb-V–IX binds to 14-3-3ζ through both GPIb and GPV. The major binding site for 14-3-3ζ on GpIbα is composed by the four C-terminal amino acids, and interaction is favoured by the phosphorylation of Ser609. The analysis of overlapping peptides revealed an additional binding site for 14-3-3ζ located in the central region of GpIbα (residues 570–590). The 14-3-3ζ interaction with GPIbβ occurs through binding to residues 160–175 and requires the phosphorylation of Ser166 by PKA. It has recently been demonstrated that the PKA-mediated phosphorylation of GPIbβ at Ser166 negatively regulates VWF binding to GPIbIX. Mutated S166A GPIbβ, and truncated forms of GPIbβ lacking Ser166 showed enhanced VWF binding. Altogether, these findings suggest that the interaction of 14-3-3ζ with the cytoplasmic domain of GPIbβ may be important in the negative regulation of GPIbIX binding to immobilised VWF under flow. The binding of 14-3-3ζ to GPIb subunits shows some kind of cooperativity

because the deletion of the GpIbα binding domain eliminates 14-3-3ζ binding to GPIbβ, and conversely, the enhanced binding of 14-3-3ζ to GPIbβ results in a similar enhanced binding to GpIbα. The 14-3-3ζ protein also binds to GPV by interaction with residues 529–544 in the cytoplasmic tail. 14-3-3ζ may participate in the GPIb-V–IX-induced platelet activation by organising a signalling complex, which includes PI-3K and pp60src.In resting platelets, calmodulin has been found to be constitutively associated with GPIb-V–IX, through interaction with residues 149–167 in the cytoplasmic tail of GPIbβ, and residues 529–544 in the cytoplasmic tail of GPV (Andrews et al. 2001). Upon platelet stimulation with thrombin, calmodulin dissociates from the receptor and relocates to the cytoskeleton [23]. Although the physiological role of calmodulin association with GPIb-V–IX is unknown, this interaction may potentially regulate different aspects of receptor function and signaling. GP Ib-IX-V is attached to actin binding protein using a binding site within the cytoplasmic tail of GP Iba an interaction that may indirectly couple GPIb-IX-V to the myriad of cytoskeletal-associated signaling molecules. These include phosphatidylinositol (PI)3-kinase, src-related tyrosine kinases (pp60src, pp60fyn,pp62yes, pp54/58lyn, and pp72syk), focal adhesion kinase pp125fak, p21ras GTPase-activating protein (GAP), and tyrosine phosphatases such as PTP-1B and SHPTP1. GP Ib-IX-V interacts directly with 14-3-3 z through additional sites on GP Ibα and GP Ibβ, and possibly GP V. Clearly, an important focus of current research is to define the signaling pathway(s) linking engagement of GP Ib-IX-V to the Ca^{2+}-dependent activation of $\alpha_{IIb}\beta_3$. Although precise pathways remain obscure, some signaling molecules that might be involved are 14-3-3 protein that has the capacity to simultaneously bind to two or more ligands, and as such potentially links GP Ib-IX-V with other signaling proteins like raf-1, PKC, and/or PI3-kinase, to regulate at least some of the signaling events downstream of the receptor. Association of 14-3-3 with PI3-kinase would enable linkage of GP Ib-IX-V to pp60src and pp60fyn, known to be activated and redistributed to the cytoskeleton following vWF binding to platelets. PKC-dependent phosphorylation of pleckstrin (p47) is also induced by vWF and 50-kDa alboaggregin binding to GP Iba. Overall, definition of interactive sites on GP Ib-IX-V and 14-3-3 z suggests that 14-3-3 protein may be involved in the assembly/regulation of GP Ib-IX-V–related signaling and cytoskeletal complexes.

2.2 Aim of the Study

Adhesion of blood platelets to damaged vessel walls and aggregation of platelets at sites of injury are regulated by Gp Ib-IX-V, a complex composed of four transmembrane subunits: GpIbα, GpIbß, GpIX, and GpV. The GpIbα subunit binds the plasma glycoprotein von Willebrand factor (vWF), a multimeric ligand that together with GpIbα regulates adhesion of platelets to the subendothelium. Although a major function of GpIbα is to adhere to vWF at sites of injury, GpIbα is also a receptor for α-thrombin, an allosteric serine protease released from damaged tissue that is essential for hemostasis and platelet activation. Thrombin binding studies have identified sites of high, moderate, and low affinity on human platelets, and GpIbα receptors have been shown to account for high-affinity binding (dissociation constant Kd ~100 nM). Binding of thrombin to GpIbα is essential for initiation of platelet procoagulant activity, and exposure to <1 nM thrombin is sufficient to induce aggregation and activation. In pathological states, extensive platelet aggregation can overcome the normal mechanisms that limit the size of the hemostatic plug and lead to thrombosis, the precipitating factor in most cases of life-threatening acute coronary occlusion. Thrombin-mediated platelet activation requires a complex set of interactions involving multiple substrates and receptors. Recent studies suggest that this process involves not only hydrolysis of protease-activated G protein–coupled receptors (PARs), but also signaling responses through the GpIb-IX-V complex that follow GpV cleavage by α-thrombin, or an α-thrombin/GpIb–dependent pathway that does not require hydrolysis of substrate.

Although all these extensive biochemical and functional data indicate that GpIbα is a thrombin receptor, the precise nature of GpIbα-thrombin interactions is controversial. For example various studies suggest that exosite II on thrombin interacts with GpIbα, whereas few others implicate exosite I in GpIbα interaction. Moreover three Tyr residues in the anionic region of GpIbα are subject to post translational sulfation (sTyr), and sulfation is necessary for optimal binding to α-thrombin in vitro (Marchese et al. 1995).

Recently two differents crystal structure of GpIbα-α thrombin complex were obtained, with major differences in the way the two protein interacts. This raises bigger questions than those answered.

Aim of this study carried out at the Scripps Research institute (La Jolla, CA) in the laboratory directed by prof. Z.M. Ruggeri, was to shed light into the dynamics of interactions between GpIbα and thrombin using several techniques. We assessed the role of sulfated tyrosines using the wild type GpIbα protein at different degrees of sulfation, as much as single point mutation of GpIbα tyrosine residues, with different experimental approaches : in static condition, monitoring the ability of any different mutant to form a stable complex that can be isolated with size exclusion chromatography ; in flow conditions, using SPR technique trying to determine kinetic parameters of the interaction between the two proteins; with an ex vivo approach, assessing the binding of thrombin to human and mice platelets, having the possibility to study the effect of the Y279F mutation in an ex vivo model.

All this data bring us a step closer to understanding the physiological role and mode of interactions of these two pivotal players of the complex mechanism of haemostasis and thrombosis.

2.3 Results

Altough is well known that thrombin induce platelets aggregation via the PARs, GpIbα represents the major binding site for this protease in platelet membranes. The role of the binding of α-thrombin to GpIbα is far from having been complitely elucidated.

We espressed then the N-terminal part of GpIbα (aa 1-290) ($GpIb_{\alpha}N$) that bears all the necessary aa for the binding of α-thrombin. In the purification process four distinct peaks could be identified that contained GP $Ib_{\alpha}N$ with essentially identical characteristics when analyzed by SDS-PAGE.

The peaks were arbitrary named : Pk 1, Pk 2, Pk 3 and Pk 4.

These peaks were treated then with Abalonis sulfatase to discriminate a potential role for the sulfation in the etereogenity of GP $Ib_{\alpha}N$.

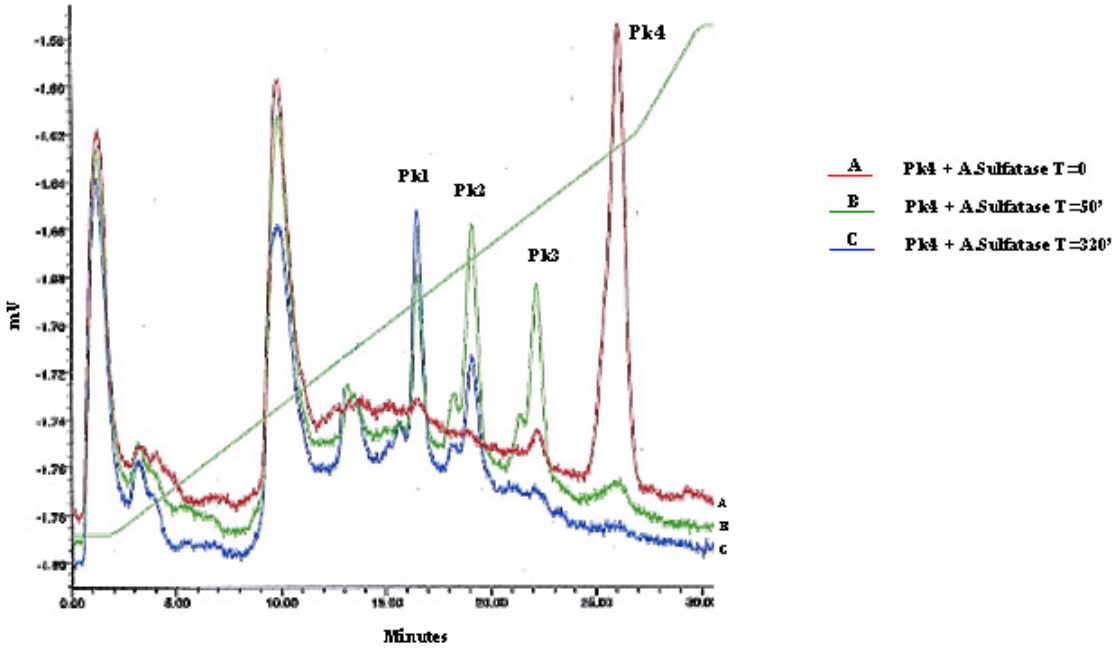

Figure 8. Pk 4 digestion with Abalonis Sulfatase

Cromatographic profile (ion exchange) of: A) Pk 4 alone or after digestion with A. Sulfatase for B) 50 min or C) 320 min. The chromatographic run was performed as detailed in Matherial and methods.

Indeed, as shown in figure 8, treatment of Pk 4 with sulfatase, shifted the isoelectric point of the protein to less charged values. The digestion of Pk 4 indeed made evident that the peaks we called Pk 3, Pk 2 and Pk 1, represent the different degree of sulfation, since after 320 min of digestion, the most abundant peak 1, the unsulfated protein.

Three tyrosine residues on GpIb$_\alpha$ are known to be sulfated, namely Y276, 278 and 279. This was a direct evidence that the four peaks isolated represent GpIb$_\alpha$ with different degree of sulfation. Since Pk 3 represent the more abundant expressed peak, we started testing the ability of Pk 3 to bind and form a stable complex with α-thrombin.

We mixed Gp IbN Pk 3 with α-thrombin at 37°C for 30 min, the mixture was then loaded on a gel-filtration column, and fractions were analized for the presence of the complex.

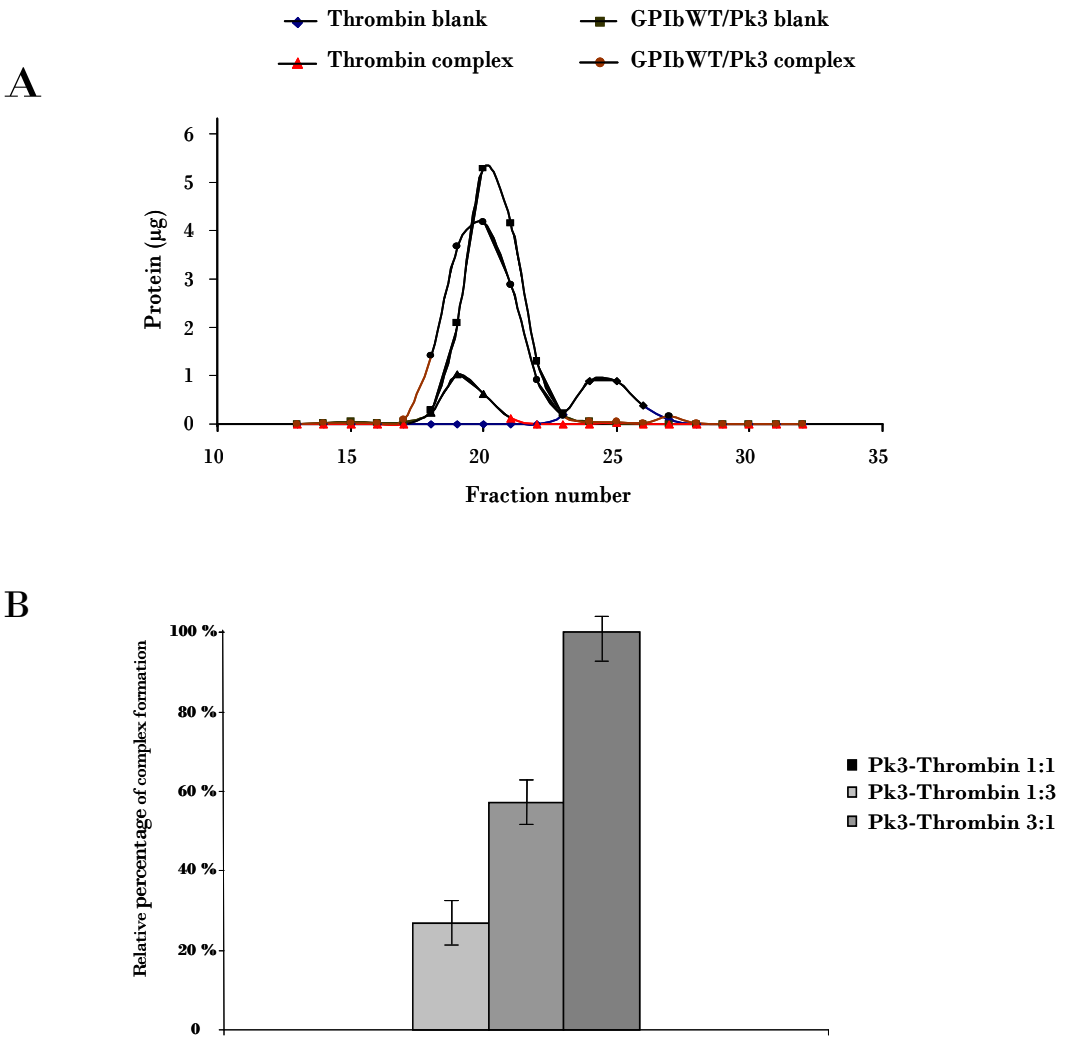

Figure 9. Thrombin binding to GPIbN

Panel a) Cromatographic profile of thrombin (♦) and GPIbN(■) alone and their relative shift (▲thrombin) (● GPIbN) in elution time when complexed. Complex formation was performed as detailed in matherial and methods. Panel B) Relative percentage of complex formation for the different stoichometric ratio, 1:1 or the excess of both proteins. Values are means of 3 experiments performed in triplicate with S.E. indicated by vertical bars.

As shown in fig 9 Pk 3 form a stable complex with α-thrombin as highlitghted by the shift in the thrombin and GpIbN elution peaks (Panel A). The stability of complex is dependent on the stochiometric ratio of the two proteins since for a defined amount of α-thrombin added, more complex is formed when the two proteins are mixed in excess of $GPIb_{\alpha}N$, suggesting a stoichiometry of the complex different from that of 1:1 ratio (Panel B).

We then analyzed the ability of the other peaks, to form stable complexes with α-thrombin.

As shown in fig. 10, Pk 4 is the protein that allow the formation of the most stable complex. The Pk 3 and Pk 2 retains the ability to create complex altough the lower the sulfation the lower is the amount of complex generated, indeed Pk 1 mixed with α-thrombin generated a negligible amount of complex.

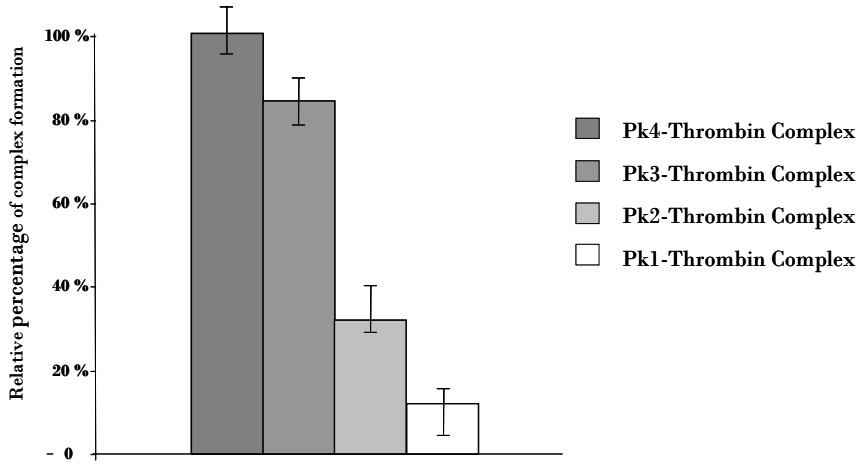

Figure 10. Thrombin binding to GPIbN

Relative percentage of complex formation for the different sulfated form of GPIbN. Complex formation and separation was performed as detailed in matherial and methods. Values are means of three experiments performed in triplicate with S.E. indicated by vertical bars.

Although analyses of the complexes formed by GPIbN peaks assign an essential role to tyrosine sulfation in the complex formation, this approach does not give enough information about the role of the single tyrosines involved in this process. To adress this issue, we generate therefore single mutants of the three tyrosine, namely Y276F, Y278F, and Y279F. Any of these mutants showed eterogenity in ion exchange chromatography, indeed all the mutants presented a Pk 3, Pk 2 and a Pk 1. All these mutants were subjected

to A. sulfatase treatment showing the same behaviour of the wild tipe protein, conferming that the different peaks represent different sulfation level (data not shown).

We then tested the Pk 3 of these mutants for the ability to form stable complexes with α-thrombin.

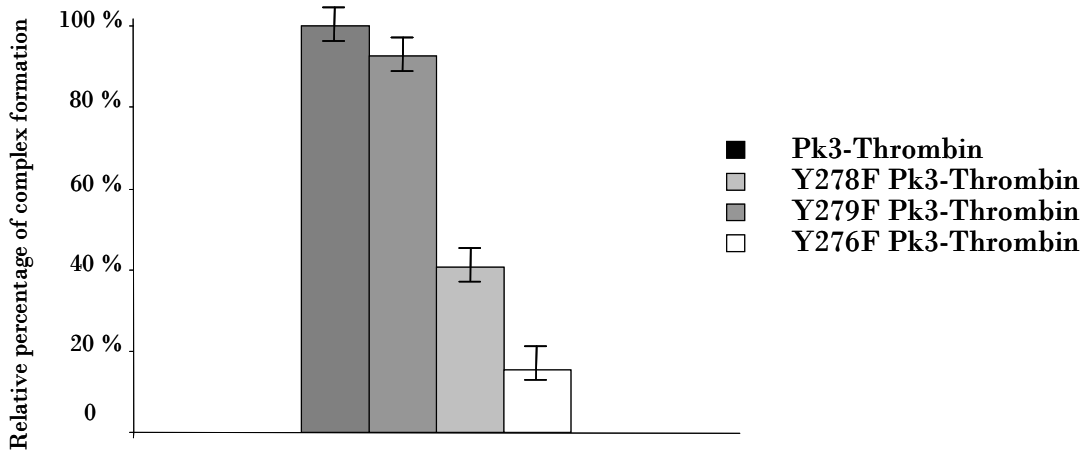

Figure 11. Thrombin binding to GPIbN

Relative percentage of complex formation for the different mutated forms of GPIbN. Complex formation and separation was performed as detailed in matherial and methods. Values are means of three experiments performed in triplicate with S.E. indicated by vertical bars.

As shown in Fig 11, Y278F Pk 3 mutant didn't show remarkable difference from the wild tipe protein, suggesting a non functional role for this tyrosine. The mutant Y279F strongly inhibit the complex formation (60%), suggesting the formation of an unstable complex, whereas Y276F shows the major degree of inhibition (82%) of the complex formation.

SPR analysis of thrombin binding to GP1bN.

We have then analyzed the binding of α-thrombin to recombinant GpIbN fragments using the SPR technology that allows to monitor the reactions in real time, giving the possibility to deduce kinetic parameters. All the esperiments were performed with PPACK-thrombin, a catalytic inactive thrombin, to avoid autoproteolitic digestion. Preliminary experiments were done to assure that α-thrombin and PPACK-thrombin showed the same experimental behaviour.

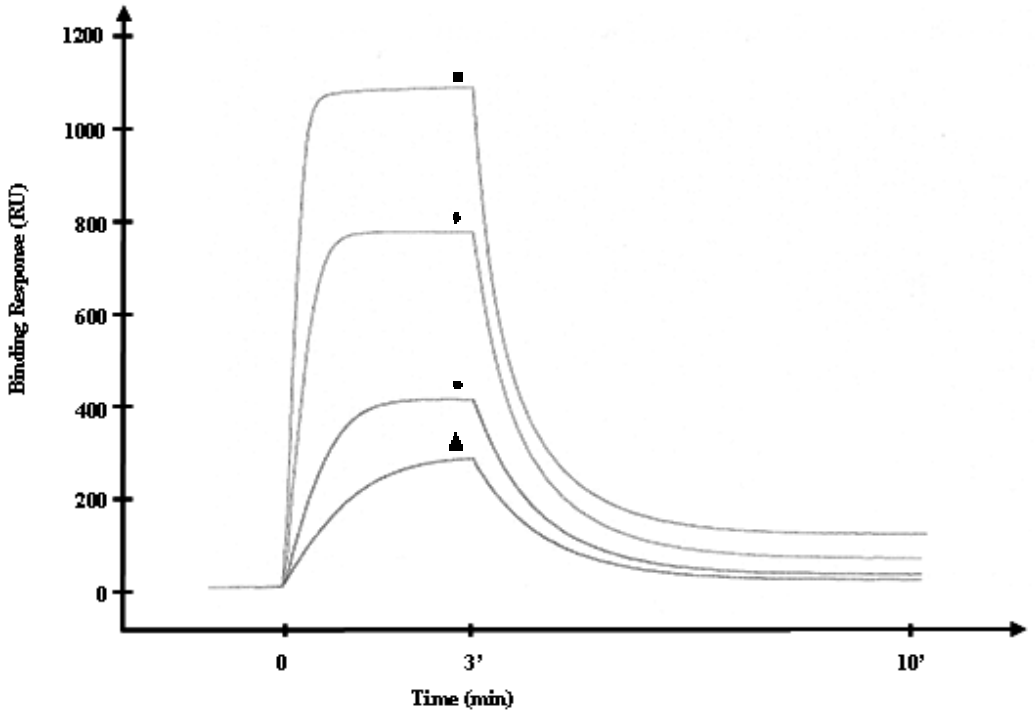

GPIbN PK4 (24℃)

Model	Heterogeneous Ligand-Parallel reaction						
Kon_1 ($m^{-1}s^{-1}$)	$Koff_1$ (s^{-1})	Kon_2 ($m^{-1}s^{-1}$)	$Koff_2$ (s^{-1})	Kd_1 (nM)	Kd_2 (nM)	$Rmax_1$ (RU)	$Rmax_2$ (RU)
$1.38\ e^5$	$7.21e^{-5}$	$9.4e^5$	$1.84e^{-2}$	522	19.57	2730	540

Figure 12. Binding of thrombin to GpIbN Pk 4 at 24C.

The receptor was captured by the LJP3 Ab immobilized at the chip surface until a density of 2000 RU was reached. Thrombin at different concentrations was then injected and flowed over at 40 µl/min. For the sake of clarity here are shown only 6.25 nM (▲) 12 nM (●) 50 nM (♦) and 100 nM (■).

Analysis of sensorgrams was made using the BIAevolution software V3.0 (GE Healthcare Uppsala, Sweden). Altough all the analyses had a χ^2 below the 5% (the χ^2 represent the discrepancy between the theorical and the experimental data), given the complexity of the reactions involved in the binding of α-thrombin to GPIbα, the kinetic parameters deduced has to be considered as preliminary results.

For GpIbN Pk 4, the model that fitted better the experimental data is the one called heterogeneous ligand (parallel reactions).

This model describes an interaction between one analyte molecule and two independent ligands, or two sequential interactions between a molecule of analyte and two different ligand molecules. The equations for these model are described in the material and methods section.

At 24° C the kinetic parameters for the association of GpIbN Pk 4 to α-thrombin are the following: a first low affinity site with a Kd = 522 nM, a $K_{on} = 1.38 \times 10^5\ m^{-1}s^{-1}$, and a $k_{off} = 7.21 \times 10^{-2}\ s^{-1}$, and an high affinity site with a Kd = 19.57 nM a $K_{on} = 9.4 \times 10^5\ m^{-1}s^{-1}$, and a $k_{off} = 1.84 \times 10^{-2}\ s^{-1}$.

In SPR experiments the R_{max} value it's an index of the maximum amount of molecules that can bind at that specific site.

The low affinity site is the one that involves the most part of thrombin molecules with a $R_{max} = 2730$ while the high affinity site has an $R_{max} = 541$.

Interestingly in our experimental conditions, after seven minutes (the time we followed the dissociation of the complex) not all the α-thrombin bound was dissociated from the surface.

Since previous reports indicated an temperature influence for the α-thrombin binding to platelets, hence we monitored the binding of GpIbN Pk 4 at 4° C.

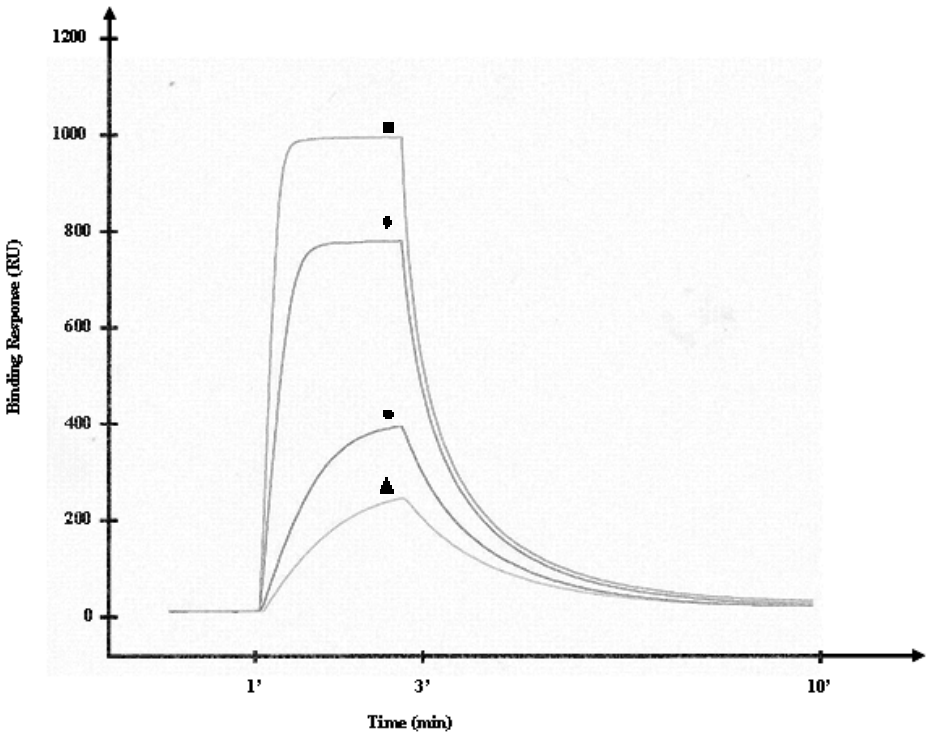

GPIbN PK4 (4℃)

Model **Heterogeneous Ligand-Parallel reaction**

Kon_1 ($m^{-1}s^{-1}$)	$Koff_1$ (s^{-1})	Kon_2 ($m^{-1}s^{-1}$)	$Koff_2$ (s^{-1})	Kd_1 (nM)	Kd_2 (nM)	$Rmax_1$ (RU)	$Rmax_2$ (RU)
8.81 e^5	6.76e^{-3}	3.41e^5	3.43e^{-2}	7.67	101.5	458	1330

Figure 13. Binding of thrombin to GPIbN Pk 4 at 4°C.

The receptor was captured by the LJP3 Ab immobilized to the chip surface until a density of 2000 RU was reached. Thrombin at different concentrations was then injected and flowed over at 40 µl/min. For the sake of clarity here are shown only 6.25 nM (▲) 12 nM (●) 50 nM (♦) and 100 nM (■).

As shown in figure 13 at this temperature the affinity of α-thrombin for GpIbN increases since the Kd of the high affinity site is 7.67 nM with a $K_{on} = 8.81 \times 10^5$ $m^{-1}s^{-1}$, and a $k_{off} = 6.76 \times 10^{-3}$ s^{-1} while the low affinity site got a Kd =101.5 nM with a $K_{on} = 3.41 \times 10^5$ $m^{-1}s^{-1}$, and a $k_{off} = 3.43 \times 10^{-2}$ s^{-1}. The low affinity site is the one that

involves the majority of thrombin molecules with an R_{max} = 1330 while the high affinity site has an R_{max} = 458. Interestingly at 4°C no α-thrombin left bound at the surface after 7 min. Since the correct stoichiometry of the thrombin-GpIbN Pk 4 complex is far from clear, we monitored the complex formation in the presence of a low density of GpIbN Pk 4.

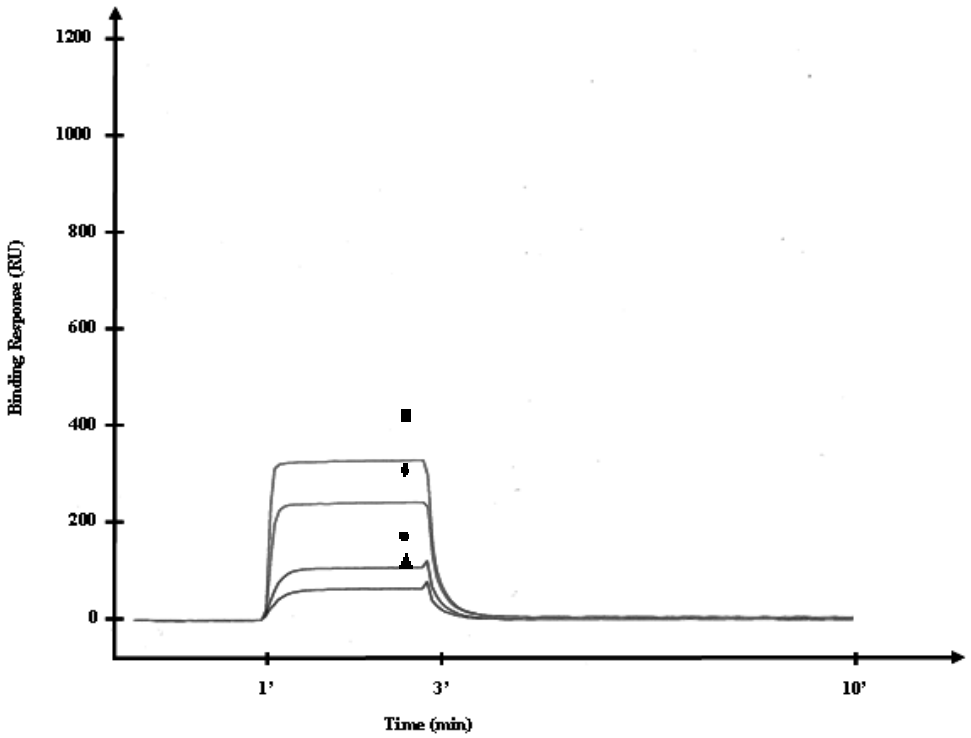

GPIbN PK4 (4℃ – low density)

Model	**Heterogeneous Ligand-Parallel reaction**						
***Kon*$_1$ (m^{-1}s^{-1})**	***Koff*$_1$ (s^{-1})**	***Kon*$_2$ (m^{-1}s^{-1})**	***Koff*$_2$ (s^{-1})**	***Kd*$_1$ (nM)**	***Kd*$_2$ (μM)**	***Rmax*$_1$ (RU)**	***Rmax*$_2$ (RU)**
6.48 e^5	7.26e^{-2}	3.08e^1	1.33e^{-4}	112	43	459	8

Figure 14. Binding of thrombin to GPIbN Pk 4 at low density.

The receptor was captured by the LJP3 ab immobilized to the chip surface until a density of 600 RU was reached. Thrombin at different concentrations was then injected and flowed over at 40 μl/min. For the sake of clarity here are shown only 6.25 nM (▲) 12 nM (●) 50 nM (♦) and 100 nM (■).

Interestingly when the amount of GpIbN Pk 4 is reduced to a low density of receptor, the affinity constants for the two binding site are respectively Kd = 112 nM with a $K_{on} = 6.48 \times 10^5$ $m^{-1}s^{-1}$, and a $k_{off} = 7.26 \times 10^{-2}$ s^{-1}, with an R_{max} =459 ; the second site

has a Kd = 43 µM with a K_{on} = 3.08 $m^{-1}s^{-1}$, and a $k_{off} = 1.33 \times 10^{-4}$ s^{-1}, with a R_{max} = 8. In the presence of a low amount of GpIbN the high affinity binding did not likely occur, while the site with µmolar affinity is like to be an experimental artifact. This is in agreement with data shown concerning the complex formation in static conditions, where the amount of complex formed correlates with the amount of GPIbN in the reaction mixture.

Pk 3 and Pk 2 and Pk 1, represent intermediates degree of sulfation, we then generated sensogram for each one of these proteins.

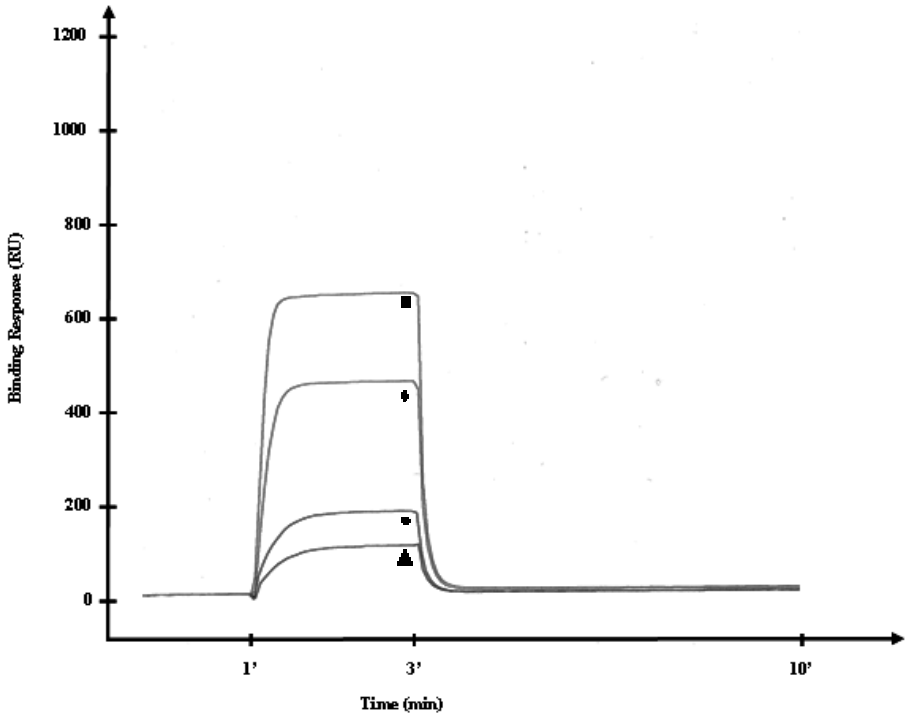

GPIbN PK3 (4°C)

Model	Heterogeneous Ligand-Parallel reaction						
Kon_1 ($m^{-1}s^{-1}$)	$Koff_1$ (s^{-1})	Kon_2 ($m^{-1}s^{-1}$)	$Koff_2$ (s^{-1})	Kd_1 (nM)	Kd_2 (µM)	$Rmax_1$ (RU)	$Rmax_2$ (RU)
3.1 e^5	1.82e^{-3}	4.57e5	1.44e^{-1}	5.8	315	33	1560

Figure 15. Binding of thrombin to GPIbN Pk 3 at 4°C.

The receptor was captured by the LJP3 Ab immobilized to the chip surface until a density of 2000 RU was reached. Thrombin at different concentrations was then injected and flowed over at 40 µl/min. For the sake of clarity here are shown only 6.25 nM (▲) 12 nM (●) 50 nM (♦) and 100 nM (■).

The kinetic analysis of the thrombin binding to Pk 3 at 4°C and at high density of receptor shows that the high affinity binding site has a Kd = 5.8 nM with a $K_{on} = 3.1 \times 10^5$ $m^{-1}s^{-1}$ and a $k_{off} = 1.82 \times 10^{-3}$ s^{-1}, but the Rmax = 33 is really low suggesting that only few molecules interact with this site. Instead the second site, the low affinity one, binds the majority of the molecules with a Rmax =1560 and a Kd = 315 nM, $K_{on} = 4.57 \times 10^5$ $m^{-1}s^{-1}$, and a $k_{off} = 1.44 \times 10^{-1}$ s^{-1}, but with an affinity lower than that exibited by Pk 4 under the same experimental conditions (Kd = 101 nM).

We therefore examined if also for Pk 3 there was a correlation with the density of the receptor.

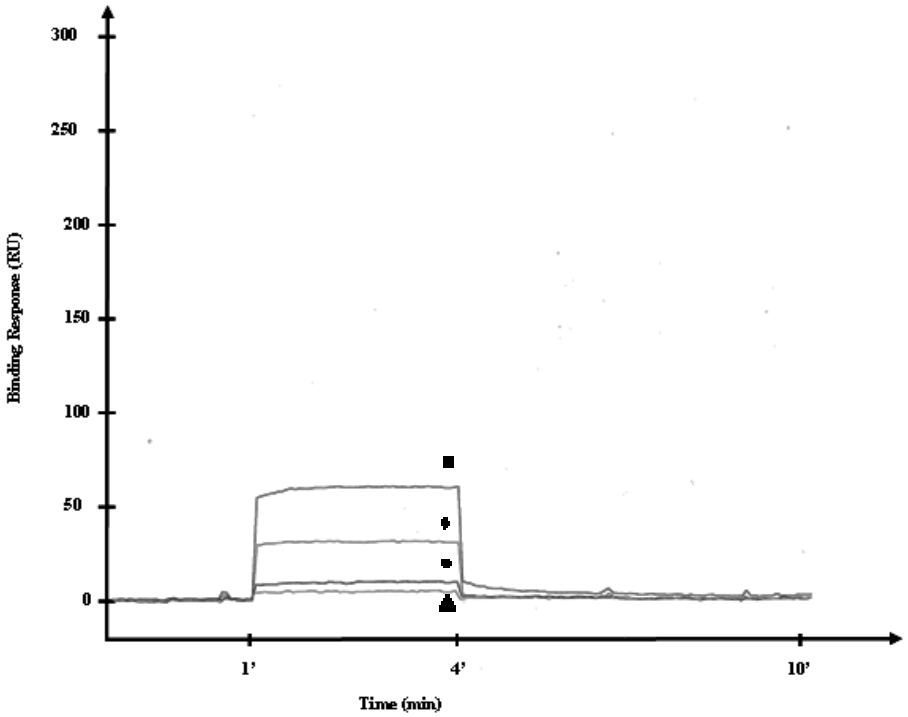

GPIbN PK3 (4°C – low density)

Model	**Langmuir Binding**		
***Kon*$_1$ ($m^{-1}s^{-1}$)**	***Koff*$_1$ (s^{-1})**	*Kd*$_1$ (nM)	***Rmax*$_2$ (RU)**
2.87 e^3	**1.96e^{-3}**	679	2451

Figure 16. Binding of thrombin to GPIbN Pk 3 low density.

The receptor was captured by the LJP3 Ab immobilized to the chip surface until a density of 600 RU was reached. Thrombin at different concentrations was then injected and flowed over at 40 µl/min. For the sake of clarity here are shown only 6.25 nM (▲) 12 nM (●) 50 nM (♦) and 100 nM (■).

As shown in fig 16 also the binding of GpIbN Pk 3 is influenced by the density of the receptor : interestingly the best fitting model for GpIbN Pk 3 at low density is a Langmuir binding (1:1 interaction). Thrombin binds GpIbN Pk 3 with a Kd = 679 nM and $K_{on} = 2.87 \times 10^3$ $m^{-1}s^{-1}$, $K_{off} = 1.96 \times 10^{-3}$ s^{-1}. Thus the lack of a sulfotyrosine modifies the interaction mechanism between the two molecules and lowers the affinity of GpIbN for thrombin by five times in comparison of Pk 4 under the same experimental conditions (Kd = 679 nM vs 112 nM).

Pk 2 represents the molecule of GPIbN with only a sulfated tyrosine, we hence studied the binding of thrombin to this molecule.

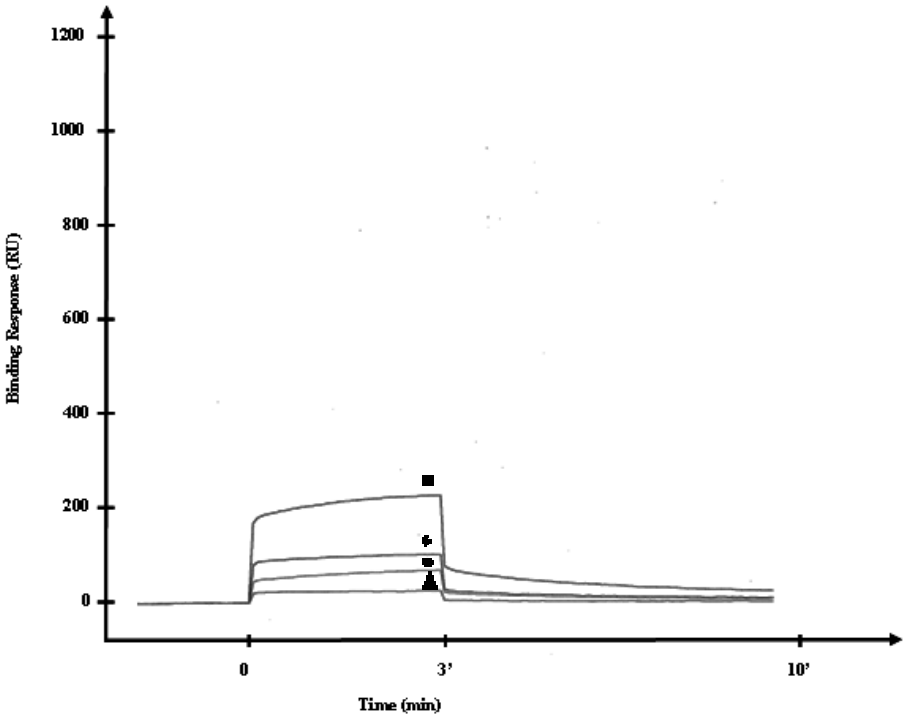

GPIbN PK2 (4°C)

Model	**Heterogeneous Ligand – Parallel reaction**

Kon_1 ($m^{-1}s^{-1}$)	$Koff_1$ (s^{-1})	Kon_2 ($m^{-1}s^{-1}$)	$Koff_2$ (s^{-1})	Kd_1 (nM)	Kd_2 (µM)	$Rmax_1$ (RU)	$Rmax_2$ (RU)
1.3 e^6	6.76e^{-1}	1.26e^4	3.21e^{-3}	524	254	68	791

Figure 17. Binding of thrombin to GPIbN Pk 2 at 4°C.

The receptor was captured by the LJP3 ab immobilized to the chip surface until a density of 2000 RU was reached. Thrombin at different concentrations was then injected and flowed over at 40 µl/min. For the sake of clarity here are shown only 6.25 nM (▲) 12 nM (●) 50 nM (♦) and 100 nM (■).

The best fitting model for GPIbN Pk 2 is the heterogeneous ligand (parallel reactions) model. The first site has a Kd = 524 nM with a $K_{on} = 1.3 \times 10^{6}$ $m^{-1}s^{-1}$, and a $k_{off} = 6.76 \times 10^{-1}$ s^{-1} with an $R_{max} = 68$, whereas the second site has a Kd = 254 nM with a $K_{on} = 1.26 \times 10^{4}$ $m^{-1}s^{-1}$, and a $k_{off} = 3.21 \times 10^{-3}$ s^{-1}, with an R_{max} =791.

Last we generated the sensorgram of the interaction between Pk 1 and α-thrombin.

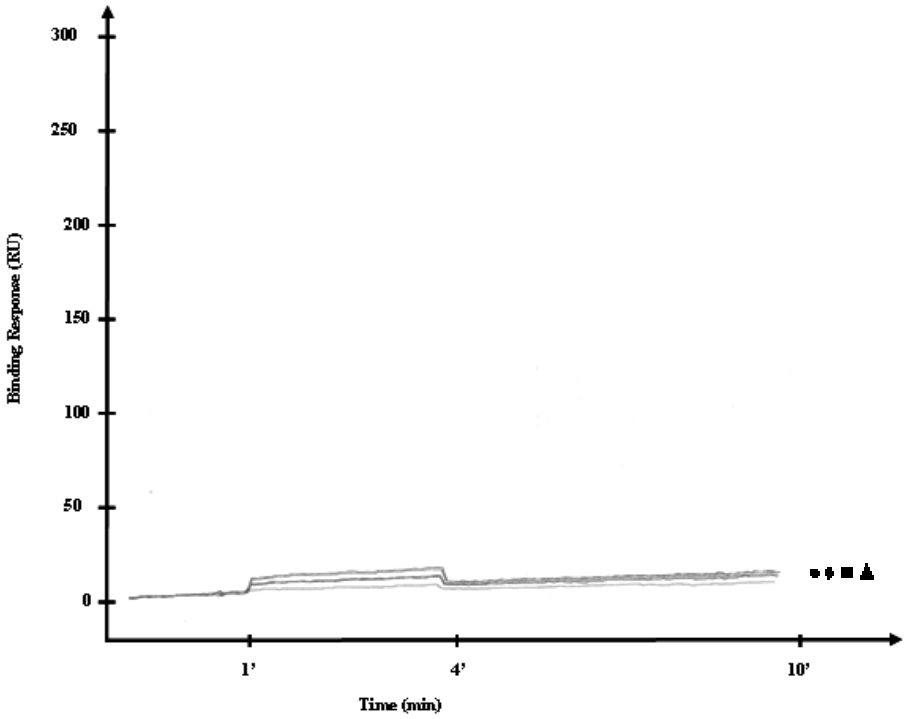

GPIbN PK1 (4 ℃)

No Significant Kinetics Parameters

Figure 18. Binding of thrombin to GPIbN Pk 1 at 4C.

The receptor was captured by the LJP3 ab immobilized to the chip surface until a density of 2000 RU was reached. Thrombin at different concentrations was then injected and flowed over at 40 µl/min. For the sake of clarity here are shown only 6.25 nM (▲) 12 nM (●) 50 nM (♦) and 100 nM (■).

The interaction between GpIbN Pk 1 and α-thrombin, by means of the Biacore Evaluation software did not give us any significant and reliable kinetic data, thus we concluded that no remarkable binding of α-thrombin to GpIbN is possible in the absence of sulfated tyrosines.

To adress more specifically the specific role of any of the residues, we employed site-directed mutagenesis to generate mutants Y276F, Y278F and Y279F of GPIbN.

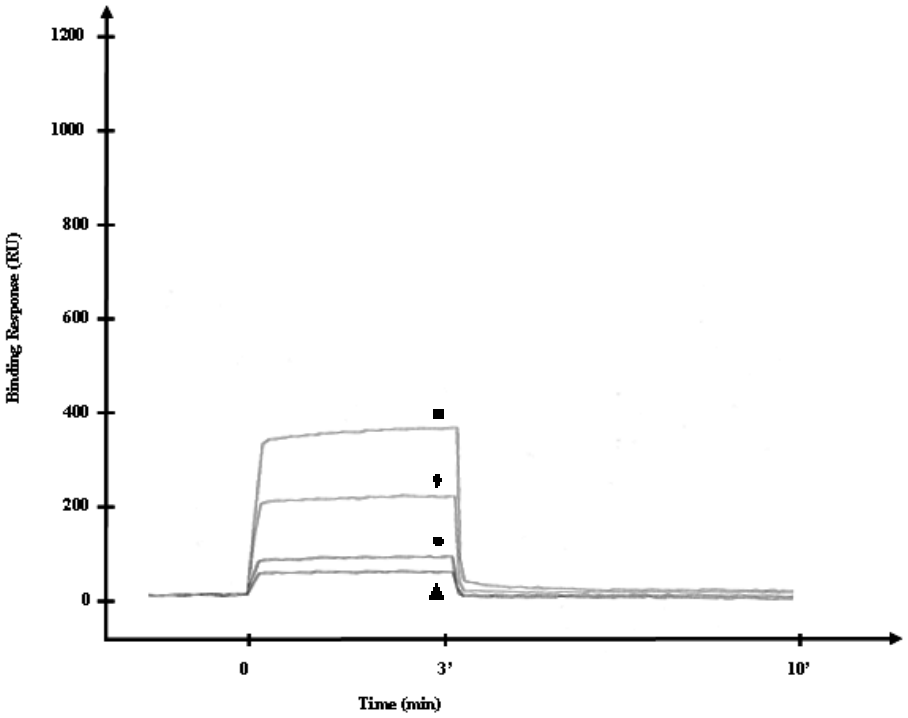

GPIbN Y279F PK3 (4°C)

Model	**Bivalent Analyte**					
Kon_1 ($m^{-1}s^{-1}$)	$Koff_1$ (s^{-1})	Kon_2 ($m^{-1}s^{-1}$)	$Koff_2$ (s^{-1})	Kd_1 (nM)	Kd_2 (µM)	$Rmax_1$ (RU)
$2.45\ e^5$	$9.9e^{-2}$	$2.69e^1$	$1.46e^{-6}$	412.5	542.7	672

Figure 19. Binding of thrombin to GPIbN Y1279F Pk 3 at 4C.

The receptor was captured by the LJP3 ab immobilized to the chip surface until a density of 2000 RU was reached. Thrombin at different concentrations was then injected and flowed over at 40 µl/min. For the sake of clarity here are shown only 6.25 nM (▲) 12 nM (●) 50 nM (♦) and 100 nM (■).

As shown in fig. 19 the mutation Y279F fitted a model of interaction different from the previous ones. This model, called bivalent analyte, describes the binding of a bivalent analyte to immobilized ligand, where one analyte molecule can bind to one or two ligand molecules. The binding to the first ligand molecule is described by a single set of rate constants, so that the two sites on the analyte are equivalent in the first binding step.

The binding to the second ligand molecule is described by a second set of rate constants, allowing the model to take cooperative effect into account. If the two sets of rate constants are the same, there are no cooperative effects and the increased affinity resulting from bivalent binding is frequently referred to as avidity. The first site has a Kd = 412.5 nM with a $K_{on} = 2.45 \times 10^5$ $m^{-1}s^{-1}$, and a $k_{off} = 9.9 \times 10^{-2}$ s^{-1} and a second one with a Kd = 542.7 nM and a $K_{on} = 2.69 \times 10^1$ $m^{-1}s^{-1}$, and a $k_{off} = 1.46 \times 10^{-6}$ s^{-1}, the global R_{max} is 672.

We also tried to generate a sensogram of the binding of α-thrombin with a low density of Y279F Pk 3 but we did not obtain significant kinetic parameters.

Then we have examined the sensograms generated by the mutant Y278F and Y276F.

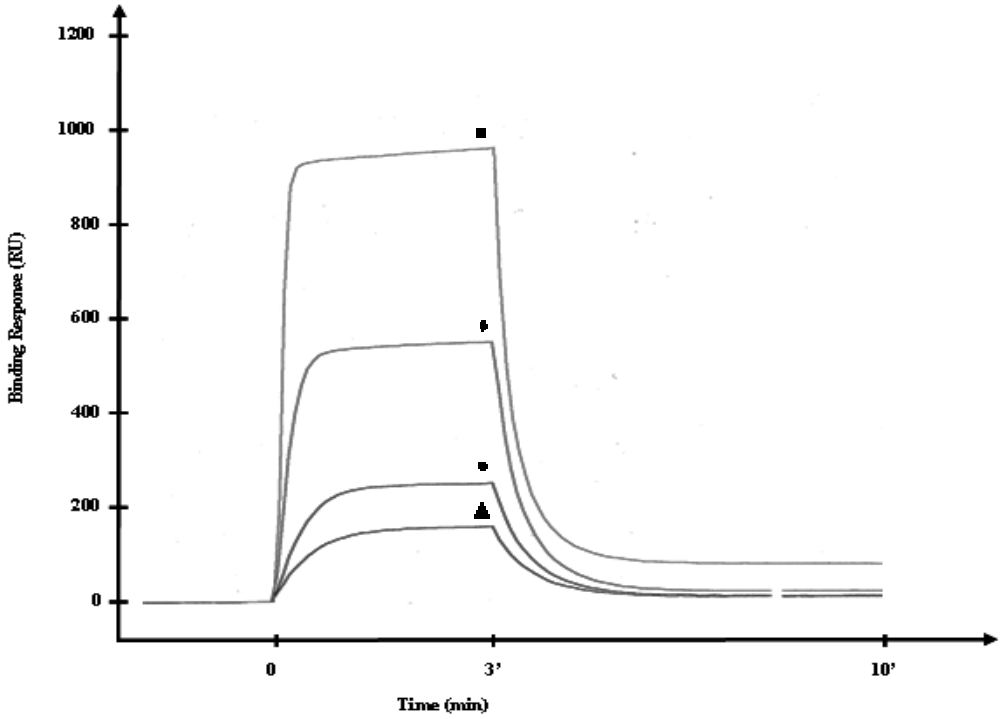

GPIbN Y278F PK3 (4℃)

Model	**Bivalent Analyte**					
Kon_1 ($m^{-1}s^{-1}$)	$Koff_1$ (s^{-1})	Kon_2 ($m^{-1}s^{-1}$)	$Koff_2$ (s^{-1})	Kd_1 (nM)	Kd_2 (μM)	$Rmax_1$ (RU)
$3.79\ e^5$	$3.91e^{-2}$	$1.33e^1$	$1.48e^{-5}$	103.8	11	643.3

Figure 20. Binding of thrombin to GPIbN Y278F Pk 3 at 4°C.

The receptor was captured by the LJP3 ab immobilized to the chip surface until a density of 2000 RU was reached. Thrombin at different concentrations was then injected and flowed over at 40 μl/min. For the sake of clarity here are shown only 6.25 nM (▲) 12 nM (●) 50 nM (♦) and 100 nM (■).

Mutation Y278F fitted, as previously shown for Y279F, a bivalent analyte model displaying two interaction sites, one with a Kd of 103.8 nM, a $K_{on} = 3.79 \times 10^{5}$ $m^{-1}s^{-1}$, and a $k_{off} = 3.91 \times 10^{-2}$ s^{-1}, the second one with a Kd of 11.08 µM, a $K_{on} = 1.33 \times 10^{1}$ $m^{-1}s^{-1}$, and a $k_{off} = 1.48 \times 10^{-5}$ s^{-1}. The global R_{max} was 643,3.

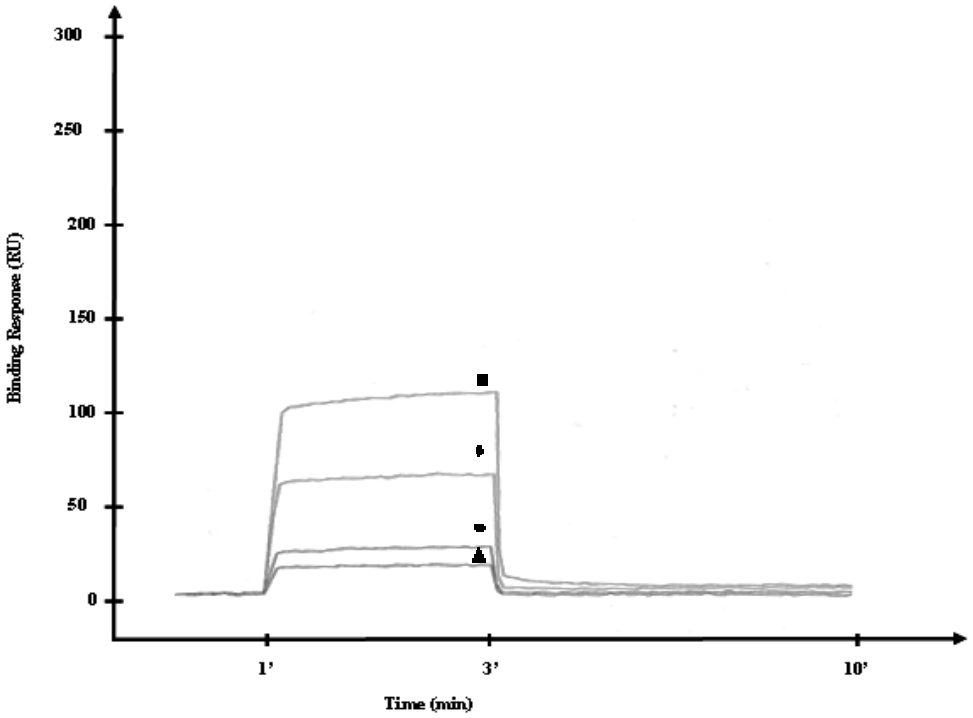

GPIbN Y276F PK3 (4°C)

No significant kinetic parameters

Figure 21. Binding of thrombin to GPIbN Y276F Pk 3 at 4°C.

The receptor was captured by the LJP3 ab immobilized to the chip surface until a density of 2000 RU was reached. Thrombin at different concentrations was then injected and flowed over at 40 µl/min. For the sake of clarity here are shown only 6.25 nM (▲) 12 nM (●) 50 nM (♦) and 100 nM (■).

We then examined the role of the mutation Y276F on the binding of thrombin to GpIbN. As shown in fig. 21 this mutation abolished almost completely the binding of thrombin to GPIbN, indeed we did not obtain significant kinetic parameters, suggesting a fundamental role for this residue.

We also produced a M3 mutants where all the three tyrosines where mutated to phenylalanine to determine the aspecific binding.

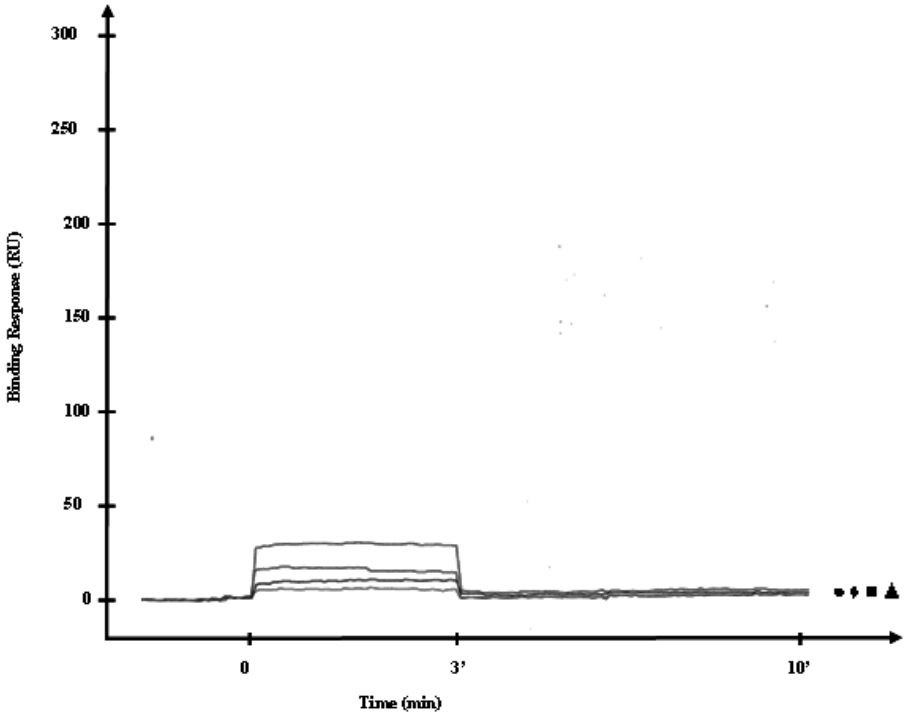

GPIbN M3 (4°C)

No significant kinetic parameters

Figure 22. Binding of thrombin to GPIbN M3 at 4° C.

The receptor was captured by the LJP3 ab immobilized to the chip surface until a density of 2000 RU was reached. Thrombin at different concentrations was then injected and flowed over at 40 µl/min. For the sake of clarity here are shown only 6.25 nM (▲) 12 nM (●) 50 nM (♦) and 100 nM (■).

As expected M3 mutant was unable to bind a significative amount of α-thrombin, and the fitting software didn't generate any statistically significant kinetic constants.

Up to date is well recognized that Exosite II plays an essential role in the binding of α-thrombin to GPIbN. Altough several studies on Exosite I showed no important roles for it, is still argueable if the latter play a role in α-thrombin binding to GpIbα.

To adress this issue, we monitored the binding of α-thrombin in the presence of hirudin and heparin, well known inhibitors of Exosite I and II respectively.

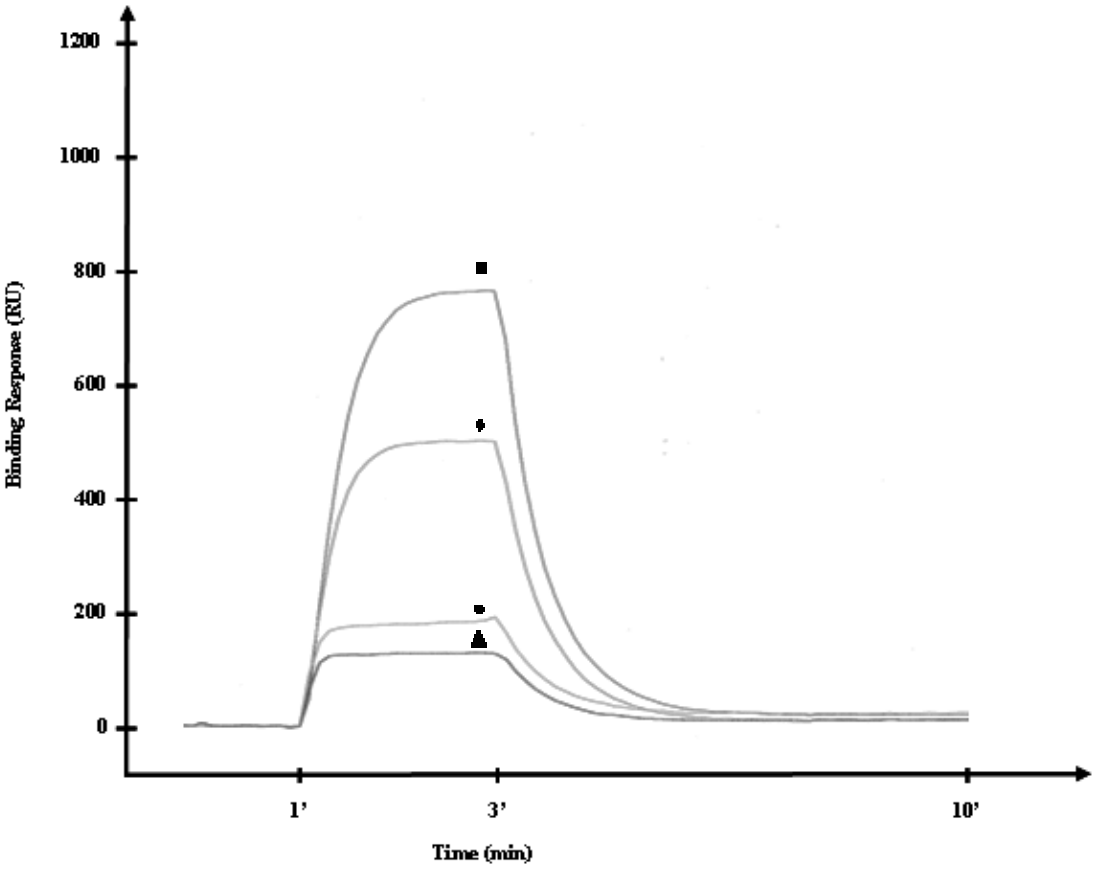

Figure 23. Binding of thrombin to GPIbN Pk 4 at 4°C in the presence of exosites inhibitors.

Thrombin (50 nM) was injected at 40 µl/min over a CM5 chip where GPIbN Pk 4 was bound via LJP3 Ab. Binding was monitored in the presence of vehicle (■), hirugen 25 µM (♦), heparin 0.5 U/ml (●) or both (▲).

The results shown on fig. 23 clearly suggest that in the presence of hirugen (25 µM) and heparin (0.5 U/ml) the level of maximum binding is lowered, to a major degree when the two inhibitors were used together, hence demonstrating that both exosites should be available for strong and long lasting interactions. To note, in a collateral experiment, we found that while high concentration of heparin completely abolished the binding of thrombin, hirugen even at millimolar concentration range never completely abolished it.

FACS analysis of α-thrombin binding to human and murine platelets.

While experiments with purified proteins were designed to determining the kinetic parameters of α-thrombin binding to GpIbN, we thought interesting also to evaluate the binding of α-thrombin to GpIbα present to platelet membranes. We used cytofluorimetry since this technique allows the analysis of the events that occur to the single platelets.

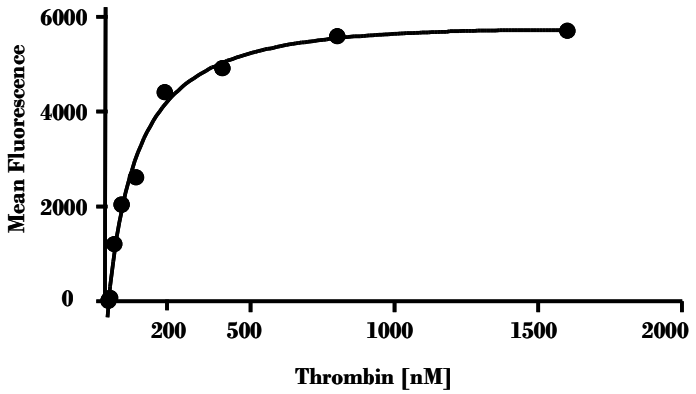

Figure 23. Binding of α-thrombin to human platelets.
Washed platelets (33.000/µl) were incubated with biotin-PPACKthrombin for 25 min at room temperature, subsequently streptavidin-PE (1.5ng/µl) was added for 5 min and platelets were analyzed with a FACS cytofluorimeter as detailed in matherial and methods section.

We found that human platelets bind thrombin with a Kd of 104 nM, while the estimate number of receptors is 17279, an amount in agreement with the density of GpIbα on human platelets. To rule out the hypothesis that the thrombin was bound to receptors others than GpIbα, we carried out the same experiment in the presence of 1b10 Ab, an antibody that has been shown to bind GpIb at the same epitope used by thrombin. In these conditions no significant amount of thrombin was bound to platelets, supporting the idea of GpIb as the major receptor for thrombin on platelets.
We next investigated the role of tirosine sulfation in mutant mice carrying the Y279F mutation. We compared the binding of thrombin of mutant mice, wild type mice (C57BL6) and mice having the human GpIbα called TKK-mice. We also evaluated the binding of thrombin to mice platelets that lacks the amino terminal part of GpIbα, substituted by the extracellular part of IL4 receptor. This has been done to have an

estimate to the specific binding of thrombin to receptors others than GpIbα and the aspecific bond.

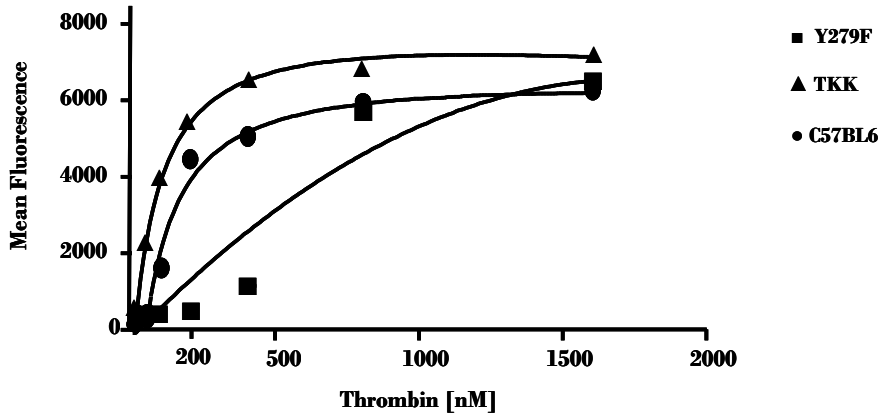

Figure 24. Binding of α-thrombin to mice platelets.

We compared washed platelets (33.000/µl) from TKK(▲), C57BL6(●) and Y279F (■). Platelets were incubated with biotin-PPACK-α-thrombin for 25 min at room temperature, subsequently streptavidin-PE (1.5ng/µl) was added for 5 min and platelets were analyzed with a FACS cytofluorimeter as detailed in matherial and methods section.

As figure 24 shows TKK mice bound the maximum amount of thrombin (as expected since TKK mice express human GpIbα). Binding analysis fit with a Kd of 114 nM, comparable with the one with found for human platelets, while the number of receptors on the surface is 21321.

For the BL6 mouse, the GpIbα binding site for α-thrombin has an affinity Kd of 178 nM with a number of GpIbα molecules at the platelets surface of 19478.

We then evaluated the binding of α-thrombin to the Y279F mutant mice platelets. As shown in fig. 24, Y279F platelets generally binds a deeply lower amount of thrombin, except at the higher concentration of thrombin tested, for whom the binding is comparable to wild tipe mice. No available fitting was significant for these platelets.

The binding of IL4 mice that lacks GpIbα while having the extracellular fragment of IL4 receptor, was subtracted from the above mentioned analysies as negative control for our experiments (data not shown).

2.4 Discussion

The first report about thrombin binding to GpIbα go back to 1978, when Okamura et al. discovered that purified glycocalin is an inhibitor of α-thrombin binding to platelets.
Since then several research groups tried to elucidate how α-thrombin binds to GpIbα especially focusing on the physiological role of this interaction.
In 30 years a lots of discover has been made in this field, for example now its well known that GpIbα has three tyrosine residues that can be sulfated in vitro (Dong et al. 1994),namely residues 276,278 and 279. Moreover the sulfation of these residues has been proved having a deep impact for the binding of α-thrombin to the recombinant receptor (Marchese et al. 1995).
This work specifically address the role of sulfation of the tyrosine residues in the GpIb molecule, using different experimental approach. We studied the full sulfated GpIbα (Pk 4), the GpIbα sulfated in two tyrosines (Pk 3) or one (Pk 2) or not sulfated (Pk 1). We have also generated single point mutation (tyrosine→phenylalanine) for each of these three residues. We have then studied the binding of α-thrombin to whole human platelets and, for the first time to murine platelets lacking tyrosine 279. We confirmed, using a gel-filtration approach that sulfation of tyrosines is a *condicio sine qua non* for the binding of α-thrombin to GpIbα : indeed Pk 1, mixed with α-thrombin to generate a complex, and applied to a size exclusion column (SEC), does not induce the formation of stable complex, proved by the absence of a shift in α-thrombin retention time. Differently, Pk 2 was able to form a complex altough in a minimum amount (Fig 10), while Pk 3 formed a stable complex as indicated by the clear shift in thrombin retention time. We then evaluated the complex formation of Pk 4, the fully sulfated form of GpIbα, that is supposed to represent also the level of GpIb sulfation present on platelets. The protein Pk 4 was the one that formed the maximum amount of complex, thus indicating that all the three tyrosines are necessary for the stronger and long lasting complex to form.
We next investigated if the complex formation was influenced by the ratio of the proteins. Interestingly we found that in the presence of an excess of GpIbα (3:1) basically all the α-thrombin molecules are engaged in the complex with GpIbα, while

no significant difference were founded between the normal ratio (1:1) and the excess of thrombin (1:3) (Fig. 9). This likely reflect a binding mechanism different from a one to one interaction. This general behaviour of GpIbα-thrombin complex formation was confirmed also by data generated with the SPR technology. This powerful technique allowed us to obtain kinetic parameters from the interaction of the two molecules. For Pk 4 we found that at 24° C α-thrombin is likely to binds GpIbα at two different site with affinity range within 10^{-7}-10^{-8} M. Since influence of temperature on the binding of α-thrombin to GpIbα has been previously reported (De Marco et al. 1999), we monitored the interaction at 4°C. At this temperature the affinity of thrombin for GpIb becomes stronger and more notably while at 24° C we were not able to completely dissociate α-thrombin from the GPIbα surface, sensograms generated at 4° C showed complete dissociation of the analyte. We thus decided to conduct all the experiments at 4°C, with the rationale to generate sensograms to be fitted in a more robust way. All this data were generated using an amount of GpIbα comparable to the one present on platelets surface. To evaluate the role of receptor density, we allow the binding to occur at a low level of GpIbα : in this situation the two affinity constant found suggest that in the presence of low level of receptor is likely to occur the binding of thrombin only at the low affinity site (10^{-7} M), while the 10^{-6} M affinity site are unlikely to have a real significance given the neglectible number of interactions, indicated by the Rmax level.

Interestingly the maximum level of thrombin bound at any given concentration is greatly reduced at low receptor density. All together this data are in agreement with the cromatographic ones, and suggest that the interaction involves two different site on two different molecule of GpIbα. This data also suggest that the interaction with the highest affinity is unlikely to happen if under a certain density of GpIbα, suggesting a two step mechanism of interaction.

We studied then the interaction of GpIbα Pk 3. The fitted data generated for this protein suggest the presence of two binding site. Also for GpIbα Pk 3 we tested the effect of the receptor density, and in agreement with data obtained with Pk 4 we found that in this condition the interactions is likely to happen to only one site.

We then analyzed the interaction of GpIbα Pk 2 with α-thrombin, founding again a two site interaction with Kd in the 10^{-8}M range. When GpIbα Pk 1 was analyzed we were

unable to generate any kinetic parameter, this in agreement with the chromatographic data where GpIbα Pk 1 was unable to generate the complex. We also generated and analzyed a triple mutants (M3) of the s-tyrosines and as expected it wasn't able to significantly bind α-thrombin (Fig 22).

To assess the influence of each single residue that can be potentially sulfated on GpIbα, we generate single mutants of this tyrosines: namely Y276F, Y278F and Y279F. All these mutants presented a Pk 3, Pk 2 and Pk 1 form, with two one or no S-tyrosine respectively. With the SEC assay, the mutation Y276F completely abolished the complex formation, this was confermed also with the SPR technique where we were not able to generate any fittable kinetics data. When we analized mutant Y279F Pk 3 with SEC we were able to separate approximately 40% of the amount of complex in comparison to the wild type protein (Fig 11) ; interestingly analized with SPR technique the mutant Y279F bind α-thrombin with a fitting model that involve the presence of two site on the thrombin molecule, with Kd in the 10^{-8}M range. Since the affinity of the two site is slightly different, is likely that the binding is mediated by just one site, while the other reflect an avidity effect.

While the mutation Y278F does not affect the formation of the complex in comparison to the wild type protein in SEC experiments, using SPR technique we found that Y278F Pk 3 bind to α-thrombin with two interaction site, with affinity in the 10^{-6} and 10^{-8}M, with the site that has a 10^{-6} M Kd is unlikely to represent a realistic interactions.

An another interesting question not fully explained, that represent an hot topic in thrombin research, is which one of the two exosites really mediate the binding to platelets via GpIbα. We adress this issue monitoring the binding of α-thrombin to GpIbα with SPR technique in the presence of two well known inhibitors of Exosite I and Exosiste II, hirugen and heparin respectively.

We found that both inhibitors affects the way the two proteins interacts, suggesting that both exosites are necessary for a fully strength complex. To note, while high concentration of hirudin completely blocked the interaction, concentration up to mM of hirugen never completely abolished the binding of thrombin. One could be tempted to speculate that α-thrombin binds two different GpIbα molecules, in a way that involves sequentially the two exosites.

To prove this theory others experiments need to be done, expecially focusing on the mutated GpIbα.

We therefore examinated the binding of α-thrombin to whole human platelets, using a cytofluorimetric approach. In our experiments thrombin bound to human platelets with a Kd of 104 nM, while we estimated the number of GpIbα molecules present at the platelets surface to be around 17000 unit. We then evaluated the affinity of α-thrombin for mice platelets that express the human GpIbα (TKK) and platelets that express the mutation Y279F in the human GpIbα sequence. We found that the ability of Y279F mice to bind platelets was greatly impaired, altough at concentration of α-thrombin close to mM, the two mice showed the same binding behaviour. This could suggest that in the absence of Y279, the site with the higher affinity is unavailable. The binding of α-thrombin to BL6 mice was lower than TKK mice, a consequence probably of the sequence differences in the mouse and human GpIbα. It might be worth to note, this is the first ex vivo evidence for a determinant role of the Y279F on the binding of α-thrombin to platelets.

In conclusion, our studies suggest the existence on platelet GpIbα of two binding sites for α-thrombin. One of these it is likely to mediate contacts with the functionally relevant anion-binding exosite I, while the other is mediated by exosite II. Moreover our experiments suggests that these two sites are probably located in two different GpIbα molecules, and the bind to the second site mediated by Exosite I can be relevant only after the binding to the first mediated by exosite II.

Chapter 3 : Serotonin, platelets and CMPDs : a fleeting connection

3.1.1 Serotonin

Serotonin is a monoamine neurotransmitter synthesized in serotonergic neurons in the central nervous system (CNS) and enterochromaffin cells in the gastrointestinal tract of animals including humans. Serotonin is also found in many mushrooms and plants, including fruits and vegetables. It was initially identified as a vasoconstrictor substance in blood serum – hence serotonin, a serum agent affecting vascular tone. This agent was later chemically identified as 5-hydroxytryptamine (5-HT) (Rapport et al. 1948), and as the broad range of physiological roles was elucidated, 5-HT became the preferred name in the pharmacological field.

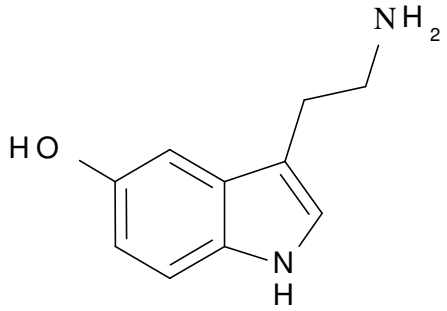

Figure 26. Serotonin structure

In the central nervous system, serotonin is believed to play an important role as a neurotransmitter, in the regulation of anger, aggression, body temperature, mood, sleep, vomiting, sexuality, and appetite. In addition, serotonin is also a peripheral signal mediator. For instance, serotonin is found extensively in the human gastrointestinal tract (about 90%), and the major storage place is constituted by platelets in the blood stream.In the body, serotonin is synthesized from the amino acid tryptophan by a short metabolic pathway consisting of two enzymes: tryptophan hydroxylase (TPH) and

amino acid decarboxylase (DDC). The TPH mediated reaction is the rate limiting step in the pathway. TPH has been shown to exist in two forms; TPH1, found in several tissues and TPH2, which is a brain specific isoform. There is evidence that genetic polymorphisms in both these subtypes influence susceptibility to anxiety and depression. There is also evidence that ovarian hormones can affect the expression of TPH in various species, suggesting a possible mechanism for postpartum depression and premenstrual stress syndrome.

Serotonin taken orally does not pass into the serotonergic pathways of the CNS because it does not cross the blood-brain barrier. However, tryptophan and its metabolite 5-hydroxytryptophan (5-HTP), from which serotonin is synthesized, can and do cross the blood-brain barrier. These agents are available as dietary supplements and may be effective serotonergic agents.

One product of serotonin breakdown is 5-Hydroxyindoleacetic acid (5 HIAA) which is excreted in the urine. Serotonin and 5 HIAA are sometimes produced in excess amounts by certain tumors or cancers, and levels of these substances may be measured in the urine to test for these tumors

Serotonin biological effects

Serotonin produces its effects through a variety of membrane-bound receptors. 5-HT and its receptors are found both in the central and peripheral nervous systems, as well as in a number of non-neuronal tissues in the gut, cardiovascular system and blood. In evolutionary terms, 5-HT is one of the oldest neurotransmitters and has been implicated in the aetiology of numerous disease states, including depression, anxiety, social phobia, schizophrenia, and obsessive–compulsive and panic disorders; in addition to migraine, hypertension, pulmonary hypertension, eating disorders, vomiting and, more recently, irritable bowel syndrome (IBS).

With the exception of the 5-HT_3 receptor, which is a ligand-gated ion channel, 5-HT receptors belong to the G-protein-coupled receptor (GPCR) superfamily and, with at least 14 distinct members, represent one of the most complex families of neurotransmitter receptors. Furthermore, peptide or lipid receptor modulators have been

reported, such as 5-HT moduline (Leu–Ser–Ala–Leu (LSAL), a putative product of a chromogranin), which demonstrates selectivity for the 5-HT_{1B} and 5-HT_{1D} receptors, or oleamide, which acts on several 5-HT receptors (including 5-$HT_{2A/2C}$ and 5-HT_7).

5-HT exerts several actions on blood vessels too. Arteries and veins are contracted by serotonin for a direct action on smooth muscular cells, mediated by 5-HT_{2A} receptors. Serotonin can mediate vasodilatation too with different mechanism mediated by 5-HT_1: it can act on endotelhial cells, stimulating the production of NO, a relaxing molecule or inhibiting the secretion of noradhrenaline.

Serotonin determines relaxation of arterioles and at the same time contractions of venules, with the net effect of an increase in capillary pressure.

5-HT its a weak agonist for platelets that induces aggregation and release of more serotonin that can interact with endothelial cells with a vasodilatatory effect, while in disease as atherosclerosis it determines vasocostriction.

5-HT_{2a} receptors

The 5-HT_{2A} receptor is known primarily to couple to the $G_{\alpha q}$ signal transduction pathway. Upon receptor stimulation with agonist, $G_{\alpha q}$ and $\beta\gamma$ subunits dissociate to initiate downstream effector pathways. $G_{\alpha q}$ stimulates phospholipase C (PLC) activity, which subsequently promotes the release of diacylglycerol (DAG) and inositol triphosphate (IP3), which in turn elicit protein kinase C (PKC) activity and cytosolic Ca^{2+} concentration increase. There are many additional signal cascade step that include the formation of arachidonic acid through PLA_2 activity, activation of PLD, Rho/RhoK, and ERK pathway activation initiated by agonist stimulation of the receptor. Serotonin concentrations lower than 2 μM induce just a weak amount of intracellular [Ca^{2+}], acting as a costimulus rather than a proper agonist, while at concentration higher than 10 μM induces per sè aggregation.

Several different drugs act as agonist or antagonist of 5-HT_{2a} receptor. Ketanserin, though capable of blocking 5-HT induces platelet adhesion, however it does not mediate its well known antihypertensive action through 5-HT_2 receptor family, but through its high affinity for alpha adrenergic receptors. It also display a high affinity for

H_1 histaminergic receptors. Compounds chemically related to ketanserin such as ritanserin are more selective 5-HT_{2A} receptor antagonists with low affinity for alpha-adrenergic receptors. However, ritanserin, like most other 5-HT_{2A} receptor antagonists, also potently inhibits 5-HT_{2C} receptors.

Serotonin and platelets

Uptake of serotonin into platelets consists of two steps :

- The first is the uptake of the 5-HT from the extracellular space into the cytoplasm and is mediated by the SERT;
- The second consists in the accumulation of serotonin into dense granules, a process mediated by the vesicular monoamine transporter VMAT2.

The mechanisms used by these two transporters to regulate their activity and the uptake of serotonin are not yet fully understood. While SERT transporter is known to be regulated by several mechanisms as phosphorylation, few works were focused on the regulation of the VMAT2 transporter in platelets. Evidence are rising that VMAT2 might be regulated by vesicle associated trimeric G-proteins (Brunk et al. 2006).

3.1.2 SERT transporter

Action mechanism of SERT

The serotonin transporter (SERT) selectively transports 5-hydroxytryptamine (5-HT) into platelets together with Na+ and Cl− and, at the same time, transports a K^+ ion out of the cell. SERT is a member of the SLC6 gene family designated as the neurotransmitter sodium symporter (NSS) family. Included in this family are many other transporters responsible for reuptake of small neurotransmitters, including glycine, γ-aminobutyric acid (GABA), dopamine (DA), and norepinephrine (NE) across the plasma membrane. The neurotransmitter transporters are plasma membrane proteins that take up extracellular neurotransmitters and thereby terminate the transmitters' action at extracellular receptor sites. They represent the first step in the process of transmitter recycling. These plasma membrane neurotransmitter transporters use transmembrane ion gradients of Na+, Cl− and K+ and an internal negative membrane potential for transport of their substrate neurotransmitters (Rudnick, 2002; Rudnick & Clark, 1993). SERT is of interest also as a drug target. A variety of compounds that are used to treat clinical depression, including fluoxetine (Prozac), sertraline (Zoloft), paroxetine (Paxil) and citalopram (Celexa), are inhibitors of SERT. In addition to drugs that specifically target SERT, this transporter is also affected by cocaine and amphetamines, psychostimulant drugs that are widely abused. Cocaine acts as a simple inhibitor of SERT and also of the closely related neurotransmitter-sodium simporters (NSS) for NE and DA (NET and DAT, respectively) (Gu, Wall & Rudnick, 1994).

A generalized mechanism for transport is based on the well-known alternate access model (Jardetzky, 1966; Tanford, 1983). In this model, transporters are believed to function by alternately exposing a substrate binding site to the cytoplasmic and extracellular faces of the plasma membrane. The model allows solutes to be transported from one side of the membrane to the other, but more importantly, it provides a mechanism for a transmembrane concentration difference of one solute to be utilized as a driving force to generate a concentration difference for another solute. The two main mechanisms for this process, named symport and antiport by Mitchell (1963), couple the movement of two solutes moving in the same direction across the membrane or in

opposite directions, respectively. In more complex transport systems, more than two solutes would be coupled by symport, in which case all solutes would need to bind before interconversion. Symport and antiport can occur as part of the same mechanism if more than one solute molecules move across the membrane together in exchange for one or more solute molecules moving in the opposite direction. In these cases, both symport and antiport rules apply. SERT catalyzes a complex reaction incorporating both symport and antiport. In 5-HT transport, SERT binds Na^+, Cl^- and 5-HT^+ in a 1:1:1 stoichiometry and only then undergoes a conformational change that occludes the binding site from the extracellular medium and exposes it to the cytoplasm (Nelson & Rudnick, 1979). Dissociation of Na^+, Cl^- and 5-HT^+ allows the transporter to return to its original conformation, but only after binding a cytoplasmic K^+ ion and releasing it to the extracellular medium (Fig. 27). The overall stoichiometry of this process is a 1:1:1:1 electroneutral exchange of K^+ with Na^+, Cl^- and 5-HT^+ (Rudnick & Nelson, 1978; Talvenheimo et al., 1983; Rudnick, 1998).

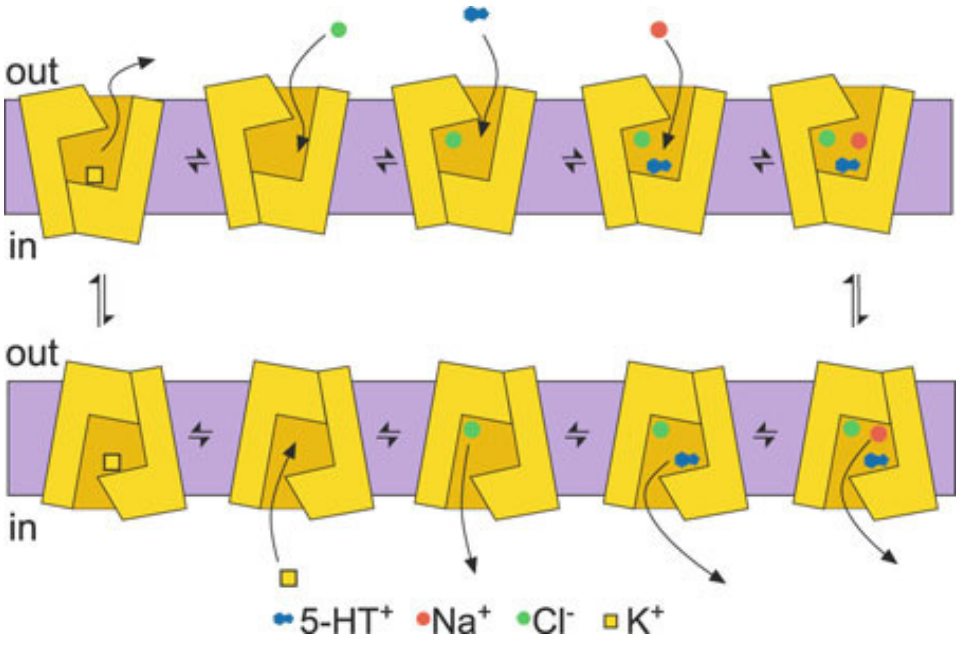

Fig. 27 **Possible mechanism of serotonin transport.** Transport of 5-HT together with Na^+ and Cl^- ions requires binding of each solute to the transporter. These binding events are depicted in the three steps on the upper right of the figure. Only after all three solutes are bound, is the transporter able to undergo a series of conformational changes that close off access to the extracellular medium and expose the binding site to the cytoplasm. This conformational change is depicted on the right side of the figure. After dissociation of 5-HT, Na^+ and Cl^- on the cytoplasmic side of the plasma membrane, as shown by the three rightmost steps in the lower part of the figure, a cytoplasmic K^+ ion is able to bind (lower left). Once K^+ has bound, SERT is able to undergo another series of conformational changes that close off access to the cytoplasm and expose the binding site to the extracellular medium. Dissociation of K^+ to the medium completes the cycle.

TOPOLOGY

In the mammalian transporters, glycosylation sites in the second extracellular loop (EL2, between TM3 and TM4) indicated that EL2 is extracellular (Tate & Blakely, 1994). For SERT, many residues predicted by the initial topological predictions to lie in hydrophilic loops were demonstrated to be accessible from the appropriate side of the membrane (Chen, Liu-Chen & Rudnick, 1998; Androutsellis-Theotokis & Rudnick, 2002), indicating a 12-TM structure with NH2- and COOH-termini in the cytoplasm. These studies extensively utilized cysteine scanning mutagenesis of internal and external loops and transmembrane domains. Figure 28 shows a summary of some of the results for SERT superimposed on a topology diagram generated from the crystal structure of LeuT and using an alignment of the NSS family (Beuming et al., 2006). The highlighted positions, where various studies demonstrated chemical reactivity with hydrophilic reagents, indicate that many of these residues are in regions predicted by the structure to be exposed to solvent (Androutsellis-Theotokis & Rudnick, 2002; Henry et al., 2003; Mitchell et al., 2004; Sato et al., 2004).

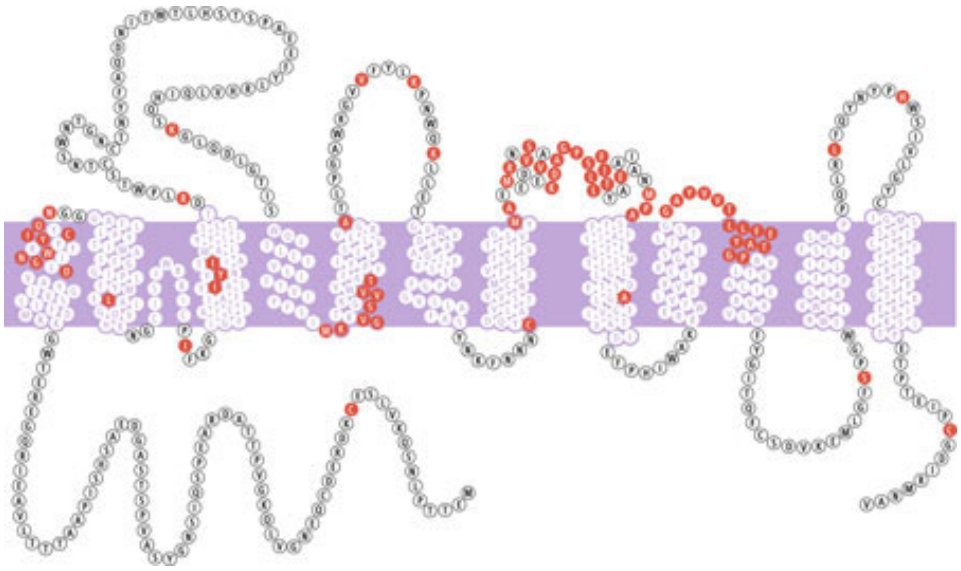

Fig. 28 Topology diagram of SERT.

The sequence of SERT was aligned with that of LeuTAa and presented as a topology diagram, using the beginnings and ends of each helix from the LeuT structure. Shaded residues are those where mutation to cysteine or lysine was found to introduce reactivity toward hydrophilic reagents. Not all positions were tested, and positions where reactivity was not detected are not marked.

The observation that residues predicted by the structure to be buried were nonetheless accessible in SERT suggests that these residues become exposed in other conformations of the protein.

In the proposed mechanism for SERT-mediated 5-HT transport, at least two important conformational changes are required, as deduced from a variety of approaches (Rudnick, 2002). The first of these occurs when 5-HT, Na^+ and Cl^- are bound to the extracellular form of the protein (upper part of Fig. 27). This conformational change occludes the bound substrates from the extracellular medium and exposes them to the cytoplasm. After the bound solutes dissociate to the cytoplasm and a cytoplasmic K^+ ion binds to SERT, the second major conformational change converts SERT from the cytoplasmic to the extracellular form (the lower part of Fig. 27), releasing K^+ to the medium. The requirement for specific ligand binding is crucial for the stoichiometric coupling of 5-HT, Na^+, Cl^- and K^+ (Rudnick, 1998). There may also be additional. intermediate conformational changes that lead to occluded forms of SERT.

Mechanisms of monoamine transporter regulation

Post translational modifications such as glycosylation and phosphorylation regulate monoamine transporter function and expression levels (Aughan et al. 1997; Ramamoorthy et al. 1998). In addition, variations in monoamine transporter gene sequences known as polymorphisms may also alter transporter expression levels, activity, and/or regulation. Recent studies demonstrate that the activity and expression of monoamine transporters are regulated by phosphorylation and dephosphorylation of the transporter proteins. Thus, monoamine transporters are dynamically regulated by intracellular and extracellular regulation of phosphorylation state, which in turn should have a significant impact on the duration and concentration of monoamines present in the synaptic cleft.

Altered transporter surface expression and intrinsic activity

Among various stimuli that acutely regulate monoamine transporters, the majority regulate transport function by altering the transporter surface expression. In a variety of preparations, including synaptosomes and cell lines, application of PKC activator phorbol 12-myristate 13-acetate selectively reduces the transport capacity (Vmax) for transport of DA, NE, and 5-HT (Jayanthi et al. 2004; Apparsundaram et al. 1998). The most consistent finding is that activators of PKC or the agents that maintain phosphorylation state such as phosphatase inhibitors rapidly reduce amine transport capacity. The major kinetic alterations typically observed in acute modulation paradigms are changes in Vmax, with little or no significant change in substrate affinity (Km). The reduction in Vmax values suggests silencing of plasma membrane resident amine transport protein or changing cell surface expression levels by regulating endocytosis or recycling or plasma membrane insertion of transporter proteins. Recent studies provided evidence for lipid raft localization and raft-mediated internalization of SERT (Samuvel et al. 2005). The presence of SERT in lipid rafts suggests that signaling machinery specific to lipid rafts may be linked to PKC-mediated transporter downregulation. Raft-associated sorting has been proposed to underlie several cellular processes including signal transduction, protein sorting, and membrane trafficking (Chamberlain et al 2002). Receptors, several channel proteins, many components of G protein coupled receptor (GPCR), adenylyl cyclase, Akt1, PLC, activated PKC, PP2Ac, non receptor tyrosine kinases, and other signaling molecules such as syntaxin 1A, α-synuclein, have been shown to be associated with lipid rafts (Simons et al. 2000). The localization of receptors such as NK1R that regulate monoamine transporter function and potential transporter-interacting proteins (syntaxin 1A, PP2Ac, PKC), as well as transporters in lipid raft microdomains, raises the possibility that lipid rafts may act as morphological “conveyers” of signal transduction by placing various signal transduction molecules near the transporter molecule. For example, transporter-interacting proteins may “guide” the transporter to lipid rafts and phosphorylation of a “motif/site” within the transporter may act as a “signal” for fostering protein-protein interactions and redistribution. Thus, protein redistribution from plasma membrane

microdomains may be one of the several mechanisms by which synaptic plasticity and neurotransmitter homeostasis are maintained (Parton et al. 2003).

Altered transporter phosphorylation

SERT is phosphorylated in response to PKC activation. SERT can also be phosphorylated following PKA activation and PP2A inhibition. The PKC-dependent phosphorylation shows a close temporal correlation with reduction in transport capacity (Ramamoorthy et al. 1999). SERT substrates and antagonists influence PKC-dependent SERT phosphorylation and surface redistribution (Ramamoorthy et al. 1999). Recent studies indicate that while PKC activation increases SERT basal phosphorylation, p38 MAPK inhibition decreases SERT basal phosphorylation indicating a role for p38 MAPK-induced phosphorylation in constitutive SERT expression (Samuvel et al. 2005). It has also been reported that activators of cGMP-dependent protein kinases, and the tyrosine kinase inhibitors genistein and 2,5-hydroxycinnamate (Hahn et al. 2003) cause a decrease of the 5-HT transport in human platelets and other cellular types expressing SERT. Recently our lab provided evidences for a role of tyrosine kinases on the modulation of SERT activity in platelets (Zarpellon et al. 2008).

3.1.3 VMAT transporter

Transport of monoamines like serotonin, catecholamines, or histamin into the secretory vesicles of a variety of cells is mediated by vesicular monoamine transporters (VMATs)(Liu et al. 1992). In mammals two closely related transporters, VMAT1 and VMAT2, are known (Liu et al. 1992, Erickson et al. 1989). These two subtypes differ in their substrate specificity, pharmacological properties, and tissue distribution (Peter et al. 1994). Both transporters represent proteins with 12 predicted transmembrane domains of different vesicle types like large dense core vesicles, small synaptic vesicles (SSVs), and synaptic-like microvesicles (Erickson et al. 1989). In contrast to the transporters of the plasma membrane, which mainly use the Na+ gradient across the plasma membrane to drive transport, activity of vesicular transporters relies on the

proton electrochemical gradient (ΔμH+) generated by a vacuolar H+-ATPase (Kanner et al. 1987). VMAT is the target of important drugs, as reserpine, an antihypertenisve drug.

The predicted molecular structure of VMAT2 comprises 12 putative transmembrane domains (TMDs) with both N- and C- termini in the cytoplasm and a large, hydrophobic, N-glycosylated loop between TMDs 1 and 2 facing the vesicle lumen (Yelin et al. 2002). Structural biology studies have identified important residues that may contribute to ligand binding and monoamine transport, for istance aspartate 33, which contains a negative charge, in TMD1 and serines 180 to 182 in TMD3 of VMAT2 play a critical role in substrate recognition, presumably by interacting with the protonated amino group of the ligand and hydroxyl groups on the catechol or indole ring, respectively (Merickel et al. 1995).

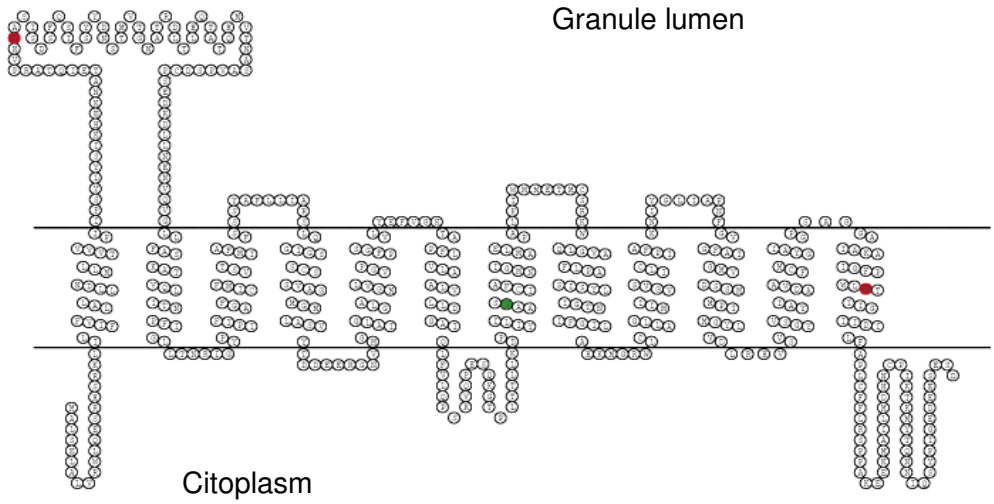

Fig. 29 VMAT structure

Serotonin efflux from platelets

Under physiological condition platelet activation induces the release of the serotonin stored in the dense granules. Also alcalinization of dense granules with permeable amine, ionofors and inhibitors of vacuolar H^+-ATPase induces 5-HT efflux dissipating the protonic gradient, the driving force of serotonin uptake.

Is still not clear how serotonin leaves the platelet cytoplasm to get into the extracellular compartment. Rudnick and Wall (1992) showed that serotonin efflux induced by PCA is a SERT-mediated process, since it was blocked by imipramine whereas (Scholze et al. 2000; Turetta et al. 2002) excluded a role for SERT in the efflux of serotonin since they found 5-HT release in the presence of imipramine and also when the release was induced by monensin. The discrepancies could have been raised by the different experimental conditions used.

3.2.1 Chronic myeloproliferative diseases

Chronic myeloproliferative disorders (CMPD) represent clonal proliferations of a pathological haematopoietic stem cell (HSC) and affect all or a subset of the haematopoietic lineages, resulting in a mono-, bi- or trilinear proliferation of megakaryocytic, erythroid and granulocytic precursor cells. CMPD encompass chronic myeloid leukaemia (CML), polycythaemia vera (PV), essential thrombocythaemia (ET) and chronic idiopathic myelofibrosis (CIMF)(Jaffe et al. 2001). Recognized at an early date (Heuck et al. 1879), the CMPD were grouped together as a closely related set of haematologic disorders by Dameshek (Dameshek et al. 1950 and 1951) but the pathogenesis remained a mystery. Despite overlap in clinical presentation, there are distinct morphological features which enable subtyping of CMPD in most instances. CMPD entities are characterized by altered bone marrow histology with a mono- to trilinear sustained proliferation and cellular atypia, the latter predominantly affecting megakaryocytes. Facultative changes are marrow fibrosis, blast increase and cytogenetic abnormalities. Clinical criteria used for subtyping CMPDS comprise enhanced blood cell counts, anaemia and organomegaly of the liver and spleen induced by extramedullary haematopoiesis. Complications may be caused by thrombotic events, haemorrhagic diatheses and constitutional weakness, and major inauspicious prognostic factors are blastic transformation into acute myeloid leukaemia (AML), severe myelofibrosis, portal hypertension and infection.

Typical bone marrow histology in PV displays prominent proliferation of all haematopoietic cell lineages with increase in erythropoiesis as well as granulopoiesis and almost complete erasure of fatty tissue. In early stages, the hypercellularity may not be as prominent with a considerable amount of preserved fat cells and a predominant megakaryocytic proliferation. In these cases discrimination from ET may pose a severe problem which can only be resolved by follow-up observation (Thiele et al. 2005).

A milestone was achieved with the most recently discovered 1849G 1 T mutation in exon 12 of the Janus tyrosine kinase (JAK) 2 gene (James et al. 2005) . This hot spot point mutation is located on chromosome 9p and leads to a gain of function due to a defective valine-to-phenylalanine exchange at the amino acid position 617 (V617F) of the autoinhibitory JH2 pseudokinase domain of JAK2. Thus the mutated JAK2 V617F tyrosine kinase is constitutively activated and conveys erythropoietin (EPO) hypersensitivity and growth factor independence to transfected cell lines. After antecedent irradiation, transplantation of JAK2 V617F transfected cells was sufficient to mimic human PV (Lacout et al. 2006) and its evolution towards myelofibrosis (Werning et al. 2006) in murine in vivo models. Interestingly, already in 1997 a gain of function point mutation of the Drosophila melanogaster JH2 homologue was linked to a leukemia-like aberrant hematopoiesis (Luo et al. 1997) and in 1999 an unsuccessful systematic search for a putative alteration in the JH2 domain of JAK2 was performed in patients suffering from myelodysplastic syndromes (MDS), CML, AML and acute lymphoblastic leukaemia, but not Ph–CMPD (Cools et al. 1999).

The gain of function mutation in JAK2 V617F affects the JAK/STAT cellular signal transduction pathway. Via cytokine-mediated receptor stimulation, signal transducers and activators of transcription (STAT) are activated through JAK-mediated tyrosine phosphorylation. This leads to STAT dimerization, nuclear translocation and regulation of target gene expression by several downstream effectors. The aberrant JAK2 V617F/STAT5 signal cascade is hypersensitive to EPO (Levine et al. 2005), thrombopoietin (TPO), interleukin-3 (Jones et al. 2005) and granulocyte colony-stimulating factor (G-CSF) (Kralovics et al. 2005) .

3.2.2 Characteristics of platelets in CMPDs

Patients with essential thrombocythemia (ET) and polycythemia vera (PV), have shortened platelet survival. increased β-thromboglobulin, platelet factor 4, and thrombomodulin levels, and increased urinary thromboxane B2 excretion. These symptoms are all reversible by inhibition of platelet cyclooxygenase 1 with aspirin, and are therefore indicative of platelet activation and platelet-mediated thrombotic processes. The thrombotic tendency persists as long as platelet counts are above the upper limit of normal (400×10^9/L). Despite strong evidence of in vivo platelet activation, the ex vivo platelet function tests are impaired. Platelet dysfunction in ET and PV typically is characterized by a missing second-wave adrenaline aggregation, an increased adenosine diphosphate aggregation threshold, and reduced secretion products, but a normal arachidonic acid or collagen-induced aggregation. The proposed concept is that platelets in thrombocythemia (ET and PV) are hypersensitive. Due to the existing high shear stress in the microvasculature, platelets spontaneously activate, secrete their products, form aggregates mediated by von Willebrand factor (vWF) that transiently plug the microcirculation, deaggregate, and then recirculate as exhausted defective platelets with secondary storage pool disease on ex vivo analysis. At increasing platelet counts from below to above 1000×10^9/L, the thrombotic condition changes into an overt spontaneous bleeding tendency as a result of a functional vWF deficiency that is caused by proteolysis of large vWF multimers. This is consistent with acquired type 2 von Willebrand syndrome (AvWS). AvWS is reversible by reduction of the platelet count to normal. The acquired JAK2 V617F gain of function mutation is the cause of trilinear myeloproliferative disease with the sequential occurrence of ET and PV. Heterozygous JAK2 V617F mutation with slightly increased kinase activity is enough for the induction of spontaneous megakaryopoiesis and erythropoiesis, and an increase of hypersensitive platelets is the cause of aspirin-sensitive, platelet-mediated microvascular ischemic and thrombotic complications in ET and early PV mimicking ET. Homozygous JAK2 mutation with pronounced increase of kinase activity is associated with pronounced trilinear megakaryocyte, erythroid, and granulocytic myeloproliferation, with the most frequent clinical picture of classical PV complicated

by major thrombosis, in addition to the platelet-mediated microvascular thrombotic syndrome of thrombocythemia.

Several studies have suggested the existence of an in vivo platelet hyperactivation in ET and PV (Bellucci et al. 2000). First, peripheral blood smear examination or ultrastructural studies brought evidence for the presence of activated platelets, with pseudopodia, centralized granules, and constituting platelet clumps and aggregates. Platelet aggregation tests may find a spontaneous platelet aggregation, and a decreased aggregation following stimulation reflects a secondary storage pool defect because an increase in platelet secretion products was reported by many teams regarding β-thromboglobulin (β-TG), platelet factor 4 (PF4), or thrombospondin (Bellucci et al. 2000). Compared with asymptomatic ET patients, symptomatic ET and PV patients, complicated by microvascular ischemic or thrombotic events, have shortened platelet survival. increased levels of platelet activation markers β-TG and PF4, increased urinary thromboxane B2 (TXB2) excretion, and increased thrombomodulin (TM) levels, reflecting endothelial cell activation (Van Genderen et al. 1999).

Unequivocal evidence for in vivo platelet activation in ET and PV patients is provided by the demonstration of increased urinary excretion of platelet-derived TXB2 in two studies (Landolfi et al. 1992 ; Rocca and al. 1995).

In vivo platelet activation, as measured by increased platelet expression of CD62p (P-selectin) and CD63 antigens, was observed in a recent study in ET and PV patients; in vivo platelet activation was associated with an increase in plasma vascular cell adhesion molecule-1, suggesting endothelial cell activation (Karakantza et al. 2004). All of these experimental data are consistent with a primary role for spontaneous platelet activation and vWF-mediated platelet aggregation and ongoing thrombosis in the end-arterial circulation in ET and PV patients.

Examination of the peripheral blood smear in ET and PV usually reveals abnormal platelet morphology, with many large and giant forms and platelet aggregates, which are not characteristic of normal platelets seen in reactive thrombocytosis (RT)(Michiels et al. 1996). In contrast to mature megakaryocytes of normal size and morphology in RT, the bone marrow histopathology in ET and PV typically shows increases and clustering of large and giant megakaryocytes with mature cytoplasm and hyperploid

nuclei (Michiels et al. 1985). Despite the strong evidence of in vivo platelet activation, ex vivo platelet function tests are impaired in asymptomatic and symptomatic ET and PV patients with either thrombotic or bleeding complications (Rao, 2004). Quantitative platelet function test results that characteristically differentiate ET/PV from RT and controls are missing second-wave adrenaline aggregation, increased adenosine diphosphate (ADP) aggregation threshold, and reduced secretion products during a normal arachidonic acid or collagen-induced aggregation (Cesar et al. 2005). Platelets in thrombocythemia are characterized by an acquired storage pool disease, and have downregulated adrenergic and glycoprotein (GP)Ib and $\alpha_{IIb}\beta_3$ integrin (Finazzi et al. 1996). It has to be emphasized that platelets from ET patients show a normal response to arachidonic acid but a decreased response to ADP, epinephrine, and collagen. They fail to release serotonin in response to various stimuli.

3.3 Aim of the study

An increase platelet number due to an increased megakaryocyte production is present in essential thrombocythemia (ET) and in other chronic myeloproliferative disorders (MPDs), such as primary thrombocythemia (PT), which are clonal diseases that could be associated with bleeding and/or thromboembolic complications.

In spite of the number of studies regarding the platelet function alteration in CMPDs none of the available biological assay-markers are completely reliable and usable for the pathology diagnosis nor have been recognized to be prognostic for hemostatic or thrombo/hemorrhagic complications in these patients.

The most relevant impaired function of platelets from CMPDs patients is considered an acquired storage pool disease (Pareti et al. 1981; Fabris et al. 1982) that seems, at least, to be suitable for distinguishing between thrombocytosis in MPD and the more common reactive/secondary thrombocytosis (Fabris et al. 1981) which are commoner then PT. In particular, a reduction of ADP and ATP dense granules content is associated with decreased platelet serotonin (5-HT) in myeloproliferative disorders (Pareti et al. 1982; Fabris et al. 1982), but the mechanism(s) underlying this reduced content remains undefined. Possible proposed mechanisms include altered amine uptake, storage and decreased in the dense granules (Caranobe et al. 1984; Cortellazzo et al 1985; Jackson et al. 1992). However whether this storage pool disease is due to an altered platelet production or to a exhaustion of platelets which continue to circulate is still a matter of debate. The aims of the present study are the following:

1) to determine the sub-cellular distribution of the neurotransmitter

2) to evaluate 5-HT transport in platelets either untreated or pre-incubated with reserpine, a known inhibitor of serotonin transport inside the dense granules

3) to establish whether the decreased accumulation of serotonin in pathological platelets was due to a decreased number of dense granules

4) to investigate the efficiency of the dense granules to accumulate basic amines;

5) to determine the amounts of ATP and Ca^{2+} contained in the dense granules

6) to evaluate the role of tyrosine kinases in the tranport of serotonin in platelets of MPDs subjects.

7) to analyze the serotonin-induced platelet activation (cytosolic [Ca^{2+}] increase).

3.4 Results

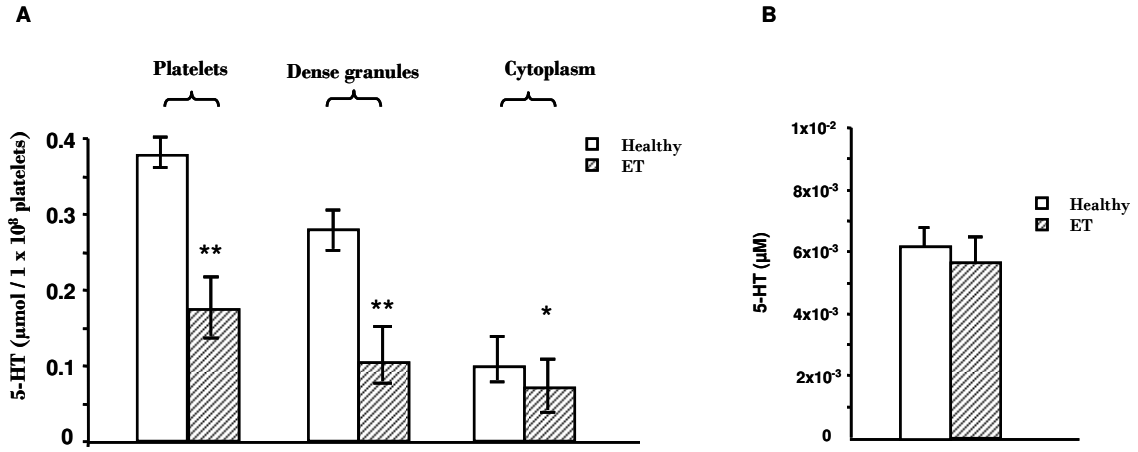

Fig. 30 Serotonin content in human platelets and plasma from healthy subjects and essential thrombocythemic (ET) patients.
A) Platelets were hypotonically treated or stimulated with thrombin (0.5 U/ml) as described in the Design and Methods section. The amount of serotonin was determined by an ELISA method. The 5-HT cytoplasmatic levels were obtained by differences between total and thrombin-induced secreted amount of serotonin. B): Plasma from healty subjects and ET patients. Values are means, with S.D., indicated by vertical bars, of 15 determinations performed in duplicate on different specimen. Statistical significance of differences *p<0.05, **p<0.001

A total of 103 patients were enrolled in this study but only those treated with the cytoreducitve agent hydroxyurea, who however constitute the majority of patients (74), were considered for the following analyses. Fig. 30 reports the concentration of 5-HT in whole platelets, dense granules, cytoplasm and blood plasma, and shows a significant decrease in the serotonin level of whole pathological platelets compared to that of healthy subjects (0.39 µmol vs 0.19 µmol /1 x 10^8 platelets). The diminution of the 5-HT content was more marked in the dense granules (0.27 µmol vs 0.09 µmol /1 x 10^8 platelets) than in cytoplasm (0.12 µmol vs 0.10 µmol /1 x 10^8 platelets). By contrast no significative differences were found between control and patient plasma.

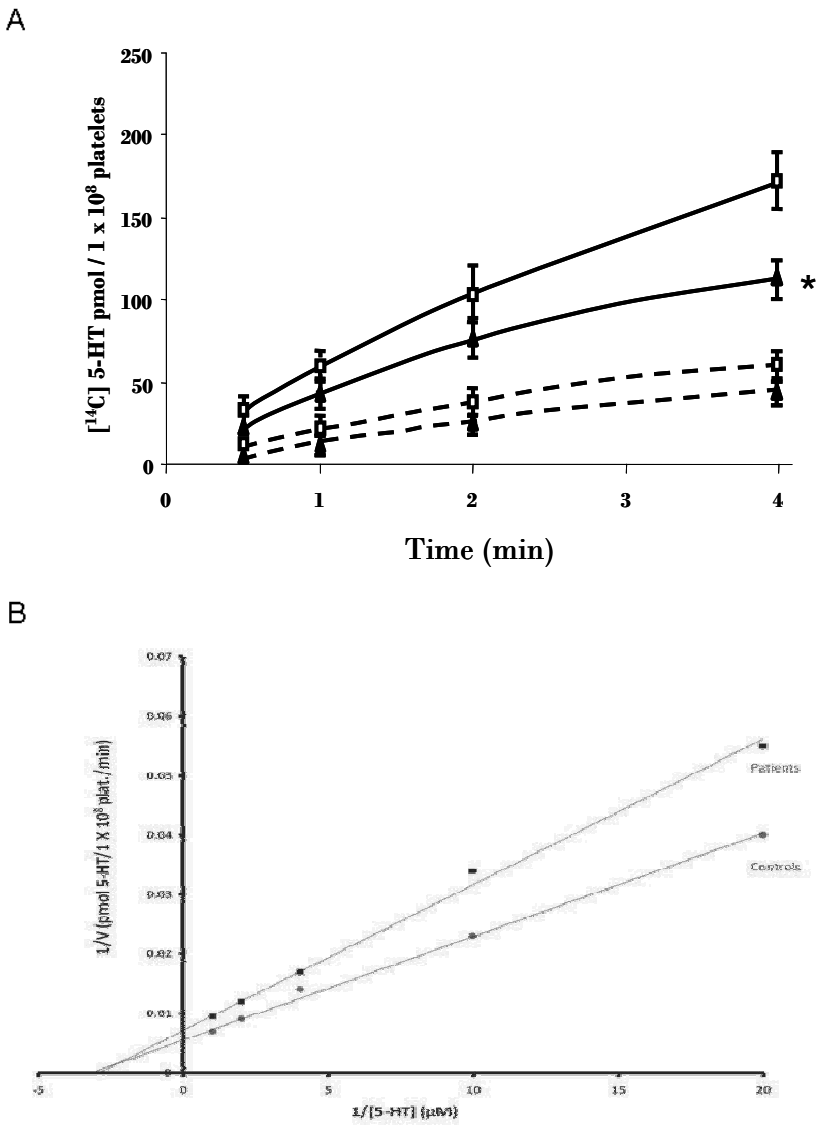

Fig. 31. Serotonin transport in platelets from controls and thrombocythemic patients.

Panel A: Time courses of 5-HT accumulation in control (°) and pathological (▲) platelets, untreated (continuous line), or pre-incubated with reserpine (dotted line); Statistcal significance of differences *p<0.01. Panel B: Double reciprocal plots of serotonin transport in control and pathological (non resepine treated) platelets. Values are means of twelve experiments performed in triplicate with S.D. indicated by vertical bars.

The amount of serotonin accumulated in platelets untreated from thrombocythemic patients was remarkably lower than that transported in platelets from controls. In contrast, no significant difference was found in the 5-HT accumulation in the platelets pre-incubated with reserpine from both patients and healthy controls (Fig. 31A).

In figure 31B is reported the double reciprocal plot of serotonin transport. Under the experimental conditions used, an apparent Km of 0.24 and 0.27 μM and a Vmax of 61 and 39 pmol/10^8 platelets/min were calculated for control and thrombocythemic platelets, respectively, indicating that platelets of trhombocythemic patients have a reduced serotonin uptake rate, but without an appreciably difference of its affinity towards the plasma membrane transporter.

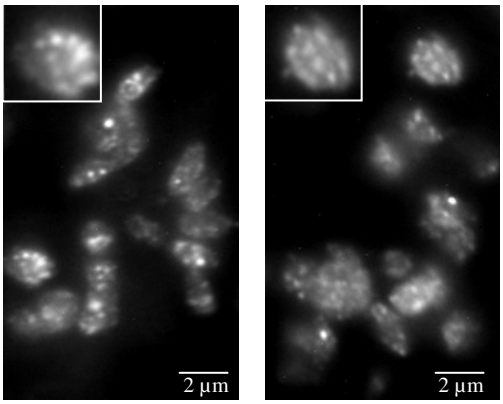

Fig. 32. Immuno-detection of serotonin-containing platelet dense granules by fluorescence microscopy.
The images are representative of twelve different specimen from control and patient donors. Platelet preparation and fluorescence microscopy analysis were performed as detailed under the Methods section.

Since the differences in the uptake of serotonin, could be due to different granule number we measured it with an immunofluorescence assay as described in material and methods. Accurate analyses of the obtained microscopic fluorescent images indicated only a slight non significative decrease in the number of dense granules present in the ET platelets compared to that of controls (Fig. 32).

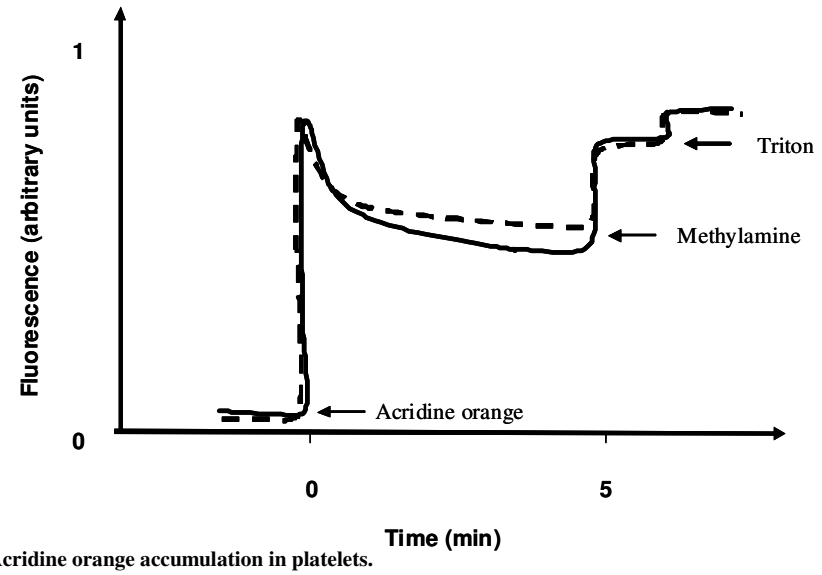

Fig. 33. Acridine orange accumulation in platelets.
At the arrow 2 µM acridine orange was added to suspensions of platelets from healthy subjects or ET patients. Traces are representative of twelve different determinations performed in duplicate.

We therefore monitored the uptale of acridine orange, a basic fluorescent probe that accumulates into the dense granules driven by the intra-granular acid pH. The amount of acridine orange taken up by platelets, measured as fluorescence decrease, was slightly lower in ET platelets than in controls (Fig. 33) suggesting that the decreased 5-HT uptake observed in thrombocythemic was only in part due to a less potential capacity of dense granules to accumulate amines.

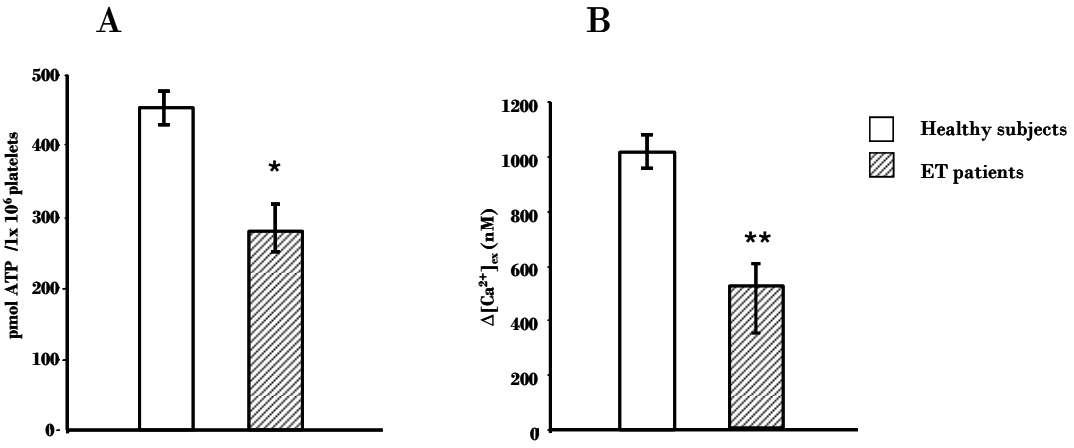

Fig. 34. Thrombin-induced secretion from control and ET platelets.
Platelets (200 x 10^6/ml) were stimulated with a-thrombin (50 mU/ml) and secretion was monitored by the mean of luciferin luciferase assay for ATP (Panel A), and with FURA acid as probe for calcium release (Panel B), as detailed in matherial and methods. The data are means of 32 different specimen. Statistcal significance of differences *p<0.01; **P<0.001

The amount of ATP and Ca^{2+} secreted by platelets of ET after thrombin stimulation were remarkably lower than that secreted by platelets from healthy subjects. To note while the difference between ATP levels is around the 40%, calcium levels are lowered by 55%.

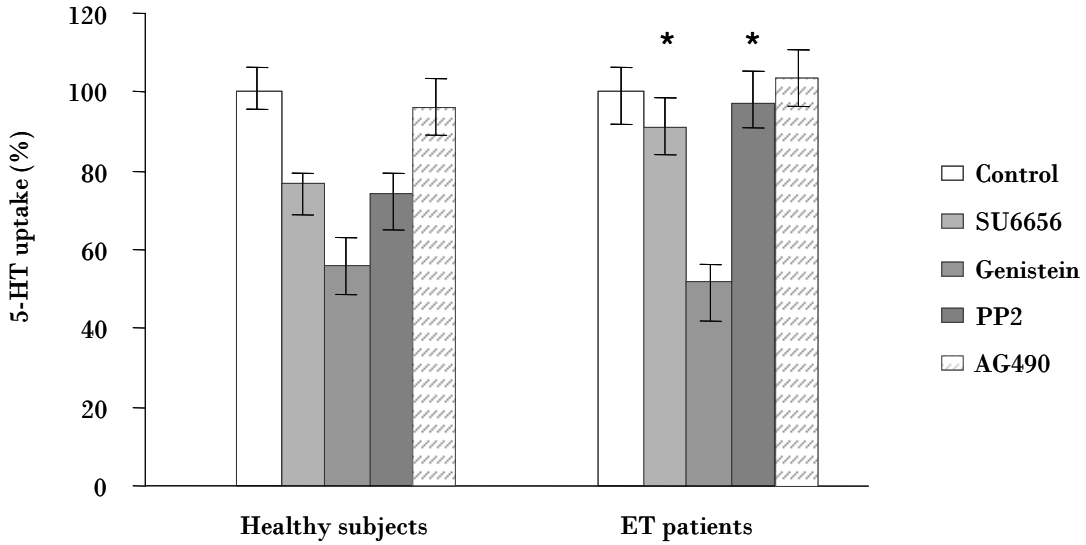

Fig. 35. Effect of tyrosine kinase inhibitors on 5-HT uptake

Effect of PP2 (5 μM, 10 min), SU6556 (10 μM, 10 min), genistein (100 μM, 10 min) and AG490 (10 μM), on [^{14}C]5–HT accumulation after 1 min incubation with 0.5 μM neurotransmitter in platelets from controls and patients. Data are means + S.D. of telve determinations carried out in duplicate with different samples. Statistcal significance of the different effect of SU6656 and PP2 on healthy subjets *vs* Et patients:*p<0.01.

Accumulating evidences suggest that both the SERT and the VMAT trasnporter are tightly regulated by differents mechanism within which the phosphorylation play a major role. We previously reported that platelet serotonin uptake is inhibited by various tyrosine-kinase inhibitors (Zarpellon et al. 2008). Here we show that both SU6556 and PP2, rather specific inhibitors of the Src-kinase family (Bain et al. 2003), inhibited more strongly the [^{14}C]5-HT uptake in the platelets from healthy subjects compared to those from ET patients. Since the mutation V617F in the pseudokinase domain of JAK2 is an hallmark of MPDs, we also evaluated the ability of AG490, inhibitors of JAK kinases to modulate the uptake of serotonin. In our experiments the AG490 didn't show any significant activity on the mechanism of serotonin accumulation.

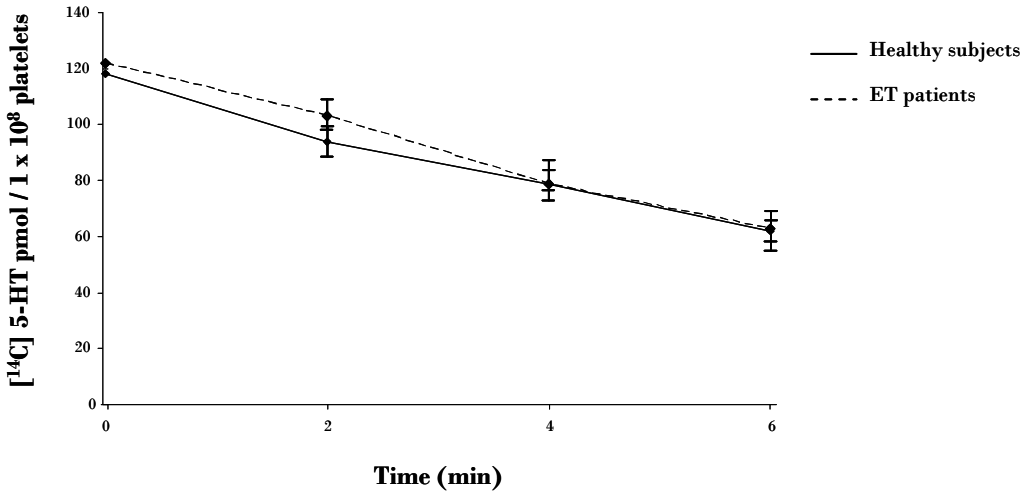

Fig. 36. Serotonin efflux from platelets induced by monensin.

Reserpine-treated platelets were loaded with [^{14}C]5-HT as described in the material and methods section; and then exposed to monensin (0.15 μM). Values are means of six experiments with S.D. indicated by vertical bars.

Next we investigated whether the different concentration of 5-HT in ET platelets was consequent to a different efficiency in the cellular efflux of the neurotransmitter. We have elsewhere reported (Turetta et al. 2004) that the sodium ionophore monensin evoke an efflux of serotonin from platelets. We have then measured this parameter in healthy and thrombocythemic platelets. Results obtained indicated that the monensin-induced efflux of preloaded [^{14}C]5-HT from reserpine-treated platelets was not significantly different in the two types of cells suggesting no differences in outward-directed SERT activity.

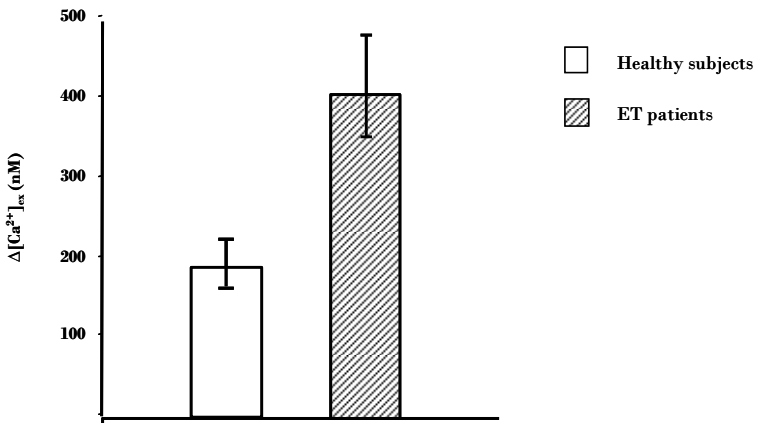

Fig. 37. Increase of $[Ca^{2+}]_c$ induced by serotonin.

A) Platelets (200 x 10^6ml) were stimulated with 1 μM serotonin and $[Ca^{2+}]$ rise was monitored with FURA-2AM, as detailed in material and methods. Values are means of twelve determinations performed in duplicate in different specimen, with S.D. indicated by vertical bars.

As synthetically described in the introduction, serotonin plays an important role in the platelet activation, which is a process widely investigated and debated in the CMPDs (Pareti et al. 1982). In the context of a research project directed at elucidating this aspect, we investigated the serotonin-induced increase in cytosolic calcium levels, chosen as activation parameter and found that the increase in $[Ca^{2+}]_{cit}$ was higher in thrombocythemic platelets (414 vs 197 nM), with respect to the control ones.

3.5 Discussion

Several studies have examined platelet function and morphology in patients with CMPDs. Platelets from patients with CMPDs, typically are characterized by impaired aggregation to certain stimuli, an increased adenosine diphosphate aggregation threshold, reduced secretion products, but a normal arachidonic acid or collagen-induced aggregation. An acquired pool disease is an hallmark of the disease, indeed the content of nucleotides, serotonin and calcium are low in platelets from people suffering for CMPDs. Despite the efforts of several investigators, is not yet clear if this is depending by an impaired abilty of platelets to uptake serotonin and nucleotides, or from a diminished number of granules, or is a defect secondary to a pre activation of circulating platelets.

In this study we found that the level of endogenous serotonin in CMPDs platelets are lower than in healthy subjects, interestingly we found that the greater difference is due by dense granules, while the cytoplasmic level, as the plasmatic ones, are not statistically different.

Serotonin uptake in platelets from CMPDs was found to be impaired from the one of heatlhy subjects (fig 31), but interestingly when uptake was evaluated in the presence of reserpine, thus inhibiting the uptake into dense granules, we found that no statistical significative difference were present. This might suggest that the difference in the endogenous levels of serotonin is likely to represent a consequence of an impaired ability to accumulate this mediator into the dense granules, or a consequence of a different number of granules.

This latter is not the case since we demonstrated with immunocytochemical assay that the number of granules doesn't differs significantly between the two groups (fig 32). Lineweaver-Burk analysis shown that platelets from MPDs have an higher Vmax while the Kd is not statistically different. This likely reflect that is the modulation of activity, more than the binding of serotonin different in platelets from CMPDs subjects. Since uptake of serotonin in dense granules is mediated by VMAT2 and is driven by a pH gradient, we used acridine orange as a probe of this gradient, and we found that no significant differences were present within the two groups. We then adresses our interest in the others consitutents of the dense granules. We found that also intragranular

concetration of Ca^{2+} and ADP were deeply lowered in the granules of platelets of CMPDs subjects. Interestingly while the ADP levels were lowered by a 40%, the difference in Ca^{2+} levels where even more evident. This might suggest that the mechanism that rules Ca^{2+} storage are more sensitive to the defect that platelets from MPDs holds.

One keystone of CMPDs is the presence of a gain of function mutation in the pseudokinase domain of JAK2 kinase. We thought interesting evaluate the potential role of tyrosine phosphorylation in the mechanism of serotonin uptake in platelets from subjects suffering from MPD`s, even in light of our recent discovery that SERT is a src family kinase substrate, thus modulating serotonin uptake. Altough JAK2 kinase is not involved in transport of serotonin, as pointed out by experiment with inhibitors, we found instead that the inhibition of uptake by src kinase inhibitors are impaired in CMPDs plaletelets. The candidate transporter that is likely to be differently modulated by kinases in CMPDs is likely to be VMAT2, since SERT uptake (as highlighted by reserpine-treated platelets uptake) and SERT efflux induced by monensin are not different in patients and controls.

All together the data obtained in this study, suggest that the well known impaired level of serotonin and the others consistuents of the granules, could depend by the inability of platelets transporter to uptake them into the granules. This inability is likely to be mediated by tyrosine kinases, and the modulation of serotonin transporter is unlikely to be the only event affected by Tyr-kinases. Wheater the defect in serotonin uptake is due to the serotonin VMAT2 transporter with the uptake of others substance been driven by that, or to a common defect in a signalling pathway that regulates uptake in dense granules, is not clear and need further studies to been fully understood.

Chapter 4
Materials and Methods

4.1.1

Reagents

Apyrase, heparin, Abalonis sulfatase, bovine serum albumin, EGTA, EDTA, IgM (mouse), fibrinogen, thyroglobulin, fibrinogen fractions, hirudin and vitronectin were purchased from Sigma-Aldrich (St. Louis, MO, USA). Human IgM was purchased from Chemicon International. Prostacyclin,RGDS, Fura 2/AM and FURA acid were obtained from Calbiochem (Darmstadt, Germany). CM5 chip, HBS-EP, P20 surfactant and coupling kit were obtained from GE Healthcare (Uppsala, Sweden). Human α-thrombin, PPACK and biotinilated PPACK human α-thrombin were purchased from HaemotologicTechnologies Inc (Essex Junction, VT). Streptavidin-RPE was purchased from Invitrogen (Carslbad CA). Hirugen was a gift of Dr. S. Yegneswaran (The Scripps Research Institute, La Jolla, CA).

All other reagents were of analytical grade.

Research project: Role of the Tyr-sulfation of platelet GpIbα in the α-thrombin binding

4.1.2

Sulfatase Treatment of Tyrosine Sulfated Proteins.

The following tyrosine sulfated proteins: IgM (mouse), fibrinogen (rat), thyroglobulin (pig), fibrinogen fraction I (bovine), fibrinogen fraction IV (bovine), hirudin (Hirudo medicinalis), and vitronectin (human) and human IgM were divided into two 0.05 mg aliquots and dissolved in 0.05 M sodium acetate at pH 5.5. 1.5 mg of the abalone sulfatase was added to one of the tubes, and both samples were placed in a heating block at 37 °C overnight. The enzyme reaction was stopped by placing the tubes on ice for 30 min followed by dilution in PBS. Only 20 units of hirudin and 5 µg of vitronectin

were used, and the sulfatase amount was reduced accordingly. Proteins were analyzed by SDS-PAGE to assess the level of degradation.

4.1.3

Preparation of PPACK-thrombin and Biotin PPACK-thrombin

Human α-thrombin was treated with a 25 fold molar excess of PPACK or PPACK-biotin for six hours at RT, then let rest overnight at 4°C.

The catalytic blocked thrombins where dialyzed over HBS buffer for 24 hrs at 4°C (2 changes), using a Slide-A-Lyzer Dialysis Cassette (ThermoLab) 10.000 MWCO.

4.1.4

Construction of a recombinant plasmid expressing the N-terminus of GP Ibα. A human GP Ibα fragment encoding the last two residues of the signal peptide and residues 1-290 of the mature GP Ibα subunit was cloned into the D. melanogaster expression vector pMT/BiP/V5-HisA (Invitrogen, Carlsbad, CA). The GP Ibα coding sequence contained a Cys to Ala substitution at position 65 generated through site-directed mutagenesis that eliminated the single unpaired Cys residue in the extracytoplasmic domain of GP Ibα. This mutation, which has no effect on function, was introduced to prevent dimerization of the purified fragment upon prolonged storage at high protein concentration. The GP Ibα fragment was cloned into the BglII/NotI restriction site of the vector to produce an in-frame synthesis of the BiP signal sequence followed by residues -2 to 290 of GP Ibα and then a termination codon. The first residue detected in the structure was His1 of GP Ibα, thus the signal peptide of the recombinant fragment was appropriately processed.

Expression of GP IbαN. Plasmid DNA was purified through a CsCl gradient prior to transfection into D. melanogaster S2 cells (Invitrogen). The cells were maintained at 22° C in Schneider's Drosophila Medium (Cambrex, Walkersville, MD) supplemented with 10% fetal bovine serum (HyClone, Logan, UT) and transfected (2-3 x 106/mL, >95% viability, 3 mL/well in 6 well plates) using the Calcium Phosphate Transfection Kit (Invitrogen). A co-transfection 2 with a second plasmid, pCoHYGRO (Invitrogen)

allowed selection of transformed cells using Hygromycin B (Calbiochem, La Jolla, CA) at 300 μg/ml. Stable cells expressing the recombinant GP Ibα fragment were selected based on immunoreactivity with an anti-humanmonoclonal antibody, LJ-P3. For large scale synthesis of GP IbαN, cells were cultured in a T162 cm2 tissue culture flask (Costar, Corning, NY). Confluent cultures were removed from flasks, sedimented by centrifugation and resuspended in serum-free, surfactant-free, detergent free medium (Invitrogen) supplemented with copper sulfate (0.5 mM). After 3 days at 22°C, cell culture supernatant was harvested and stored at -20 °C until further use.

Purification of GP IbαN.

In a typical preparation, 1.5 L of culture medium from transfected cells was dialyzed against three changes of 20 mM Tris buffer, pH 8.0 (solution A), and then applied onto an ion exchange Fast Flow Q column (1.6 x 12.5 cm; Pharmacia, Uppsala,Sweden). A gradient from 0 to 100% 1M NaCl in 20 mM Tris buffer, pH 8.0 (solution B), was then applied at a flow rate of 5ml/min (100% A for 2 min; from 0% to 60% B in 25 min; from 60% to 100% B in 3 min; 100% B for 10 min). Fractions were collected every 1 min and then analyzed by ELISA to determine their reactivity with the anti-GP Ibα monoclonal antibody, LJP3.

The positive fractions were pooled, dialyzed against 20 mM Tris, pH 8.0, and digested for 36 hours at room temperature with N-glycanase in the same buffer at a ratio of 20% w/w of the measured protein content as determined by absorbance at 280 nm. The digested GP IbαN was then purified by ion exchange chromatography using a Waters (Millipore, Milford, MA) DEAE Protein-Pak 40 HR column (1.0 x 11 cm). A gradient from 0 to 100% solution B was applied at a flow rate of 3.5 ml/min (100% A for 2 min; from 0% to 50% B in 25 min; from 50% to 100% B in 3 min; 100% B for 10 min). The eluted fractions, collected every 1 min, were analyzed by non-reduced SDS-PAGE in a 4-20% Tris-Glycine gradient gel (Invitrogen) and pooled according to the presence of GP IbαN as visualized in the gel. The pooled fractions were dialyzed against 20 mM Tris, pH 8.0, and then applied to a Mono-Q column (0.5 x 5 cm, Pharmacia). A gradient from 0 to 100% solution B was applied at a flow rate of 1.5 ml/min (100% A for 2 min; from 0% to 45% B in 25 min; from 45% to 100% B in 5 min; 100% B for 10 min), and

fractions were collected every 1 min. Four distinct peaks could be identified that contained GP IbαN with essentially identical characteristics when analyzed by SDS-PAGE and isoelectric focusing. Each GP Ibα peak was individually dialyzed against 2.5 mM Hepes, 50 mM NaCl, pH 7.4

4.1.5

GP IbαN:α-thrombin complex for functional studies

Typically, 100 µg of GP IbαN at a concentration of 0.5 mg/ml in a buffer composed of 20 mM Hepes, 150mM NaCl, pH 7.4, was mixed with different amounts of human α-thrombin at 10 mg/ml, and allowed to react for 3 hours at 37°C.

The proteins in the mixture were then separated by gel-permeation chromatography using a fastflow Superdex-200 column (1 x 30 cm; Pharmacia) equilibrated with 20 mM Hepes, 150mM NaCl, pH 7.4, and with a flow rate of 0.5 ml/min. The molecular weight markers used to calibrate the retention time as a function of molecular mass were fibronectin (450 kDa), immunoglobulin G (166 kDa), bovine serum albumin (67 kDa), ovalbumin (43 kDa) and lysozyme (14.6 kDa). Fractions were collected every 0.25 min throughout the area of absorbance at 280 nm, and were then analyzed by reversed-phase liquid chromatography. The latter was performed on a Series 4 Liquid Chromatograph system (Perkin Elmer, Wellesley, MA) using a self-packed 10 µm Poros RH-1 reversed phase column, 0.3 x 6.5 cm (Applied Biosystems, Foster City, CA). The system was equipped with a 7125 injector with a 100 ul loop (Rheodyne, Rohnert Park, CA) connected to a Waters Lambda Max 481 detector (Millipore, Milford MA). The chromatogram was recorded using the Millenium 32 software. The samples were eluted with a gradient produced by mixing varying proportions of 0.1% trifluroacetic acid in water, solution A, and in acetonitrile, solution B. The gradient used was 0.5 min at 22% B, then from 22% to 70% B in 7.5 min, followed by 0.5 min at 70% B. The quantity of each eluted protein was evaluated from the integrated area of the corresponding peaks measured at 215 nm compared to that of standard amounts of either GP IbαN or α-thrombin determined by protein assay with the bicinchoninic acid method (BCA; Pierce, Rockford, IL) calibrated with bovine serum albumin.

The protein content in the standards was also verified by amino acid analysis using the Waters PicoTag system.

4.1.6

In Flow (SPR) detection of thrombin binding to GP IbαN

Sensorgram was generated with a Biacore 3000 (Ge Healtcare, Uppsala, Sweden) with a ligand capture approach. The capturing technique has several advantages like the use of fresh ligand and preservation of the natural conformation of the ligand. Instead of bind directly GP1bαN at the surface of a carboxymethyl-dextran CM5 chip, we produced and purified LJP3 antibody (this Ab recognize the amino-terminal part of GpIbαN far enough from the residues involved in thrombin binding.) that was diluted to 100 µg/ml in 10 mM sodium acetate buffer pH 5, and immobilized on research grade CM5 sensor chips previously activated using N-ethyl-N'-(dimethylaminopropyl)carbodiimide hydrochloride and N-hydroxysuccinimide. After coupling, remaining reactive groups on the sensor chip were inactivated using 1 M ethanolamine-HCl pH 8.5.

GpIbαN where diluted in HBS-EP buffer (20 mM Hepes, 150 mM NaCl, 3 mM EDTA, 0.005% P20 surfactant) and injected over the chip at a flow rate of 20 µl/min for different time until the desired ligand concentration at the chip surface was reached.

A stock concentration of thrombin was then diluted in HBS-EP buffer at different concentration and injected over the surface to monitoring the binding to GpIbαN.

In a typical experiment nine thrombin concentration within 1µM-1 nM range was used and let them flow for 3 min (association time) and the dissociation was followed for 7 min. Two pulse of 1 minute of a 10 mM NaOH pH 12.3 solution was used as chip regeneration solution.

For the analysis of sensorgrams we used several model :

One one binding –[Rate equations: A = Conc; B[0]=Rmax; dB/dtD-(k_axAx B-k_dXAB); AB[0]=0; dAB/dtD(k_axAxB-k_dx AB); Total response: AB+RI. A and B are analyte and ligand, respectively.

Heterogenous ligand -. [Rate equations: A=Conc; B1[0]=R_{max1}; dB1/dt= - (k_{a1}xAxB1-k_{d1}xAB1); B2[0]=R_{max2}; dB2/dtD-(k_{a2}xAB2-k_{d2}AB2); AB1[0]=0; dAB1/dtD(k_{a1}xAxB1-k_{d1}xAB1);AB2[0]=0; dAB2/dtD (k_{a2}xAxB2-k_{d2}xAB2); Total response: AB1+AB2+RI.

AB1 is the complex formed by binding A to B1, AB2 is the complex formed by binding A to B2. k_{a1} is the association rate constant for A+B1=AB1 ($M^{-1}s^{-1}$), k_{d1} is the dissociation rate constant for AB1=A+B1(s^{-1}), k_{a2} is the association rate constant for A+B2=AB2 (M^{-1} s^{-1}), k_{d2} is the dissociation rate constant for AB2=A+B2 (s^{-1})].

Bivalent analite [Rate equations: A=Conc;B[0]=Rmax; dB/dt=-[(2xk_{a1})xAxB-k_{d1}xAB]; [k_{a2}xABxB-(2xk_{d2})xAB2]; AB[0]=0; dABdt= [(2xk_{a1})xAxB-k_{d1}xAB];[k_{a2}xABxB -(2xk_{d2})xAB2]; AB2[0]=0; dAB2/dt=[k_{a2}xABxB- (2xk_{d2})XAB2];Total response: AB+AB2+RI. AB is the complex formed by binding one A to B, AB2 is the complex formed by binding one A to AB. ka_1 is the association rate constant for A+B=AB (M^{-1} s^{-1}), k_{d1} is the dissociation rate constant for AB=A+B (s^{-1}), k_{a2} is the association rate constant for AB+B=AB2 ($RU^{-1}s^{-1}$). k_{d2} is the diss. rate constant for AB2=AB+B (s^{-1}).

4.1.7

Generation of transgenic mice

Generation of mice expressing human GP Ibα

Targeting Vector. The mouse GP Ibα gene was altered by site-directed mutagenesis to insert unique restriction sites flanking the coding sequence. This strategy allowed a complete replacement of GP Ibα coding sequence with a phosphoglycerate kinase-neor cassette (provided by Richard Hynes, Massachusetts Institute of Technology, Cambridge). Electroporation of embryonic stem (ES) cells was performed by Genome Systems (St. Louis), and G418-resistant colonies were screened by Southern analysis using probes from the 5' region of the mouse GP Ibα gene. Based on Southern analysis results, cell lines were chosen for microinjection into mouse blastocysts. The injections were performed by the Transgenic Core Facility at The Scripps Research Institute.

Generation of Mice Deficient in Murine GP Ibα and Expressing a Human Transgene. The generation and characterization of transgenic mice expressing the human GP Ibα polypeptide (hGpIbαTg) in the presence of two normal mouse GP Ibα alleles (mGpIbαwt) has been reported. To characterize the consequence of expressing a human transgene in the absence of an endogenous murine GP Ibα polypeptide, crosses

were made to remove the coding sequence for the mouse GP Ibα polypeptide. As a first step, GP Ibα null mice (mGpIbαnull) were bred to mice containing the human transgene (mGpIbαwt;hGpIbαTg). Southern blot analysis of the offspring confirmed the presence of heterozygous murine GpIbα alleles whereas immunologic screening using anti-human GP Ibα mAbs identified mice also expressing the human transgene product (mGPIbαhet;hGPIbαTg). Mice containing heterozygous murine GP Ibα alleles and a functional human transgene were again crossed with GP Ibαnull mice (mGpIbαhet;hGpIbαTg) × (mGpIbαnull), and the resultant offspring were genotyped and immunologically screened. This analysis identified mice with a murine GpIbαnull locus and a functional human transgene (mGpIbαnull;hGPIbαTg).

Generation of IL-4Rα/GP Ibα receptor constructs

DNA constructs encoding the ectodomain of the human IL-4 receptor (residues 1-198 of the mature α-subunit of the receptor) and residues 473 to 610 of the human GP Ibα mature subunit were generated. Specifically, a HindIII/BamHI restriction fragment of the IL-4Rα cDNA was generated in a polymerase chain reaction (PCR) using the complete IL-4Rα cDNA provided by Dr Kenji Izuhara (Saga Medical School, Japan). PCR primers for IL-4Rα generated a 5' product containing a HindIII restriction site (italics), a consensus translation initiation site (underlined), and an initiating Met codon (bold) (forward primer, 5'-GTAAGCTTGCCACCATGGGGTGGCTTTGC-3'). A reverse primer generated 3 Gly codons immediately 3' to the IL-4Rα Asn198 codon followed by a BamHI restriction site (reverse primer, 5'-CTGGATCCACCGCCGTTGTGCCACTTGGTGC-3'). A second PCR generated a BamHI/EcoRI restriction fragment containing the coding sequence of the mature GP Ibα subunit from residues Ser474 to Leu610 (forward primer, 5'-GGTGGATCCAGAAATGACCCTTTTCTC-3'; reverse primer, 5'-GCGAATTCAGAGGCTGTGGCC-3'). The PCR products were cloned and their DNA sequence confirmed. The cloned PCR products were ligated together using BamHI cohesive ends producing in a 5' to 3' direction the coding sequence for the extracytoplasmic domain of the IL4-Rα, 3 Gly residues, and the carboxyl terminus of

the GP Ibα subunit. Again, the intact coding sequence was confirmed by DNA sequence analysis. Once assembled, the IL-4Rα/GP Ibα coding sequence was cloned as a HindIII/EcoRI restriction fragment into the eukaryotic expression vector, pcDNAzeo3.1+ (Invitrogen, Carlsbad, CA). This construct was used for transfection into heterologous cells. For the generation of transgenic animals, a 3-kb GP Ibα promoter cassette was cloned as a HindIII fragment immediately 5' to the coding sequence. The generation and use of the GP Ibα promoter cassette has been previously described.11,15 Microinjection of the transgenic construct into pronuclei was performed by The Scripps Research Institute transgenic core facility.

Generation of mice expressing human GP Ibα Y279F

Transgenic founders were generated at the Mouse Genetic Core of the Scripps Research Institute by pronuclear microinjection, according to a standard protocol (Nagy A. et al. 2003). The DNA used for microinjection was a 6Kb construct containing the human blood platelet membrane glycoprotein Ibα gene (M22403) mutagenized via the QuikChange Site-directed Mutagenesis Kit (Stratagene, La Jolla, CA).

4.1.8

FACS analysis of thrombin binding to murine and human platelets.

Washed human platelets where resuspended at 33 x 10^3 / µl in modified tyrode buffer (145 mM NaCl, 5 mM KCl, 1 mM $MgCl_2$, 10 mM glucose, and 10 mM Hepes, pH 7.4), and incubated for 25 min in the presence of different concentrations of Biotin-PPACK-thrombin at room temperature, then Streptavidin-PE (Invitrogen, Carlsbad, CA) was added and allowed to bind biotin for 5 minutes.

Aliquots of plalelets suspensions were immediately analyzed. Fluorescence was measured at 585 nm using the FL-2 detector of a FACScan instrument (Becton-Dickinson, San Jose, CA) equipped with a 488 nm argon laser for excitation. The flow rate during analysis was controlled at <500 cell/s. Light scatter and fluorescence data were obtained at a fixed gain setting in the logarithmic mode.

Since blood draw in mice can locally generate thrombin that could bind to platelets, we treated animals with of Heparin (0.5U/mg), to avoid thrombin binding. Blood than was

drawed in 1:5 volume of ACD (75 mM sodium citrate, 40 mM citric acid, 130 mM dextrose, pH 4.9) and diluted with half a volume of modified tyrode Buffer pH 6.5 then centrifuged at 80g per 8 minutes, PRP was added of 1.5 U apyrase and centrifuged at 300 g per 10 minutes to pellet platelets, that was resuspended in modified tyrode bufffer pH 7.4. Binding analysis followed the same protocol above described for human platelets.

Research project : Transport and action of serotonin in healthy and thrombocythemic subjects

4.2.1

Preparation of platelet suspensions

Blood samples were collected from thrombocythemic or healthy volunteers, with their informed consent and in accordance with the Helsinki declaration. Blood was immediately mixed with one-tenth volume of citric-anticoagulant ACD (75 mM sodium citrate, 40 mM citric acid, 130 mM dextrose, pH 4.9), supplemented with 20 µg/mL apyrase and 0.8 µg/mL prostacyclin, and centrifuged for 20 min at 200 g. The supernatant platelet-rich plasma (PRP) was added with further 5% ACD and re-centrifuged for 10 min at 200 g. The latter PRP was further centrifuged for 20 min at 750 g. Spun down platelets were re-suspended, unless otherwise indicated, in the basal buffer consisting of 145 mM NaCl, 5 mM KCl, 1 mM $MgCl_2$, 10 mM glucose, and 10 mM Hepes, (pH 7.4), at a concentration of $2x10^8$ cells/mL.

4.2.2

Serotonin transport in human platelets

Serotonin uptake was determined using suspensions of platelets (2×10^8 cells/ml), prepared as described above and thermostated at 36°C for 5 min before adding labelled serotonin ([^{14}C]5-HT). Incubations were carried out under mild shaking and stopped at fixed times by withdrawing aliquots (200 µl) of the suspension, mixing them with a double volume of glutaraldehyde solution (3% in 100 mM sodium phosphate buffer, pH 7, containing 5 mM EDTA) and keeping them at 4°C for 10 min. The mixtures were

then centrifuged at 10,000 g for 5 min and the radioactivity of both pellets and supernatants was measured in a scintillation β-counter.

For the analysis of serotonin efflux, platelets were pre-loaded with 0.5 μM [^{14}C]5-HT by incubating the platelet-rich plasma for 25 min at 37°C under mild shaking. Platelets were spun down and, unless otherwise indicated, re-suspended in the basal buffer at a count of 2 x 10^8 cells/ml. At fixed times after the addition of various compounds the incubations were stopped by withdrawing aliquots (300 μl) of the suspension and mixing them with an equal volume of glutaraldehyde solution (3% in 100 mM sodium phosphate buffer, pH 7, containing 5 mM EDTA). The mixtures were centrifuged 5 min at 10,000 g and the radioactivity of both pellets and supernatants was measured in a scintillation β-counter. Each determination was carried out in triplicate.

4.2.3

Quantitative measurement of serotonin levels by ELISA

The PRP and PFP serotonin levels were measured by competitive ELISA according to the manufacturer's instructions (IBL Immuno-Biological Laboratories, Hamburg, Germany). Briefly, serotonin in samples and controls was acylated with acetic anhydride in acetone and samples, controls, and standards were applied to 96-well microtitre plates coated with goat anti-rabbit IgG. Biotinylated serotonin and rabbit antiserum to serotonin were added to each well and incubated overnight at 4°C. Para-nitrophenylphosphate in a diethanolamine solution was used as a substrate following the application of alkaline phosphatase conjugated goat anti-biotin antibody.

Samples were read at 405 nm on a Multiscan Ex (Biosystem Inc), quantified using standards supplied by the manufacturer.

4.2.4

Detection of serotonin-containing dense granules

For the cytochemical detection of serotonin-containing granules, PRP was fixed 1:1 (v/v) with 4% paraformaldehyde in PBS at room temperature for 30 min. Subsequently platelets was spunned at 800g for 20 min, then the platelets were permeabilized by the addition of Triton X-100 in water to a final concentration of 0.2% for 10 min. The

platelets were washed with a modified Hepes–Tyrode buffer (MHTB) (150 mM NaCl, 5 mM KCl, 1 mM $MgSO_4$, 10 mM Hepes–sodium salt, pH 6.5) at 1000 g for 5 min before a monoclonal mouse anti-human serotonin antibody (dilution 1:50) (Dako Diagnostics, Mississauga, ON, USA) was added. After 5 min at 37° C and two another washing steps a secondary Alexa-488-labelled goat anti-mouse IgG_1 (Cedarlane, Mississauga,ON, USA) was added at a dilution of 1:50. Coverslips were then mounted in FluorSave ReagentTM (Calbiochem) for the fluorescence microscopic observation of cells that was carried out using a Zeiss Axiovert 100 (Zeiss, Oberkochen, Germany) equipped with a digital CCD videocamera AxioCam Hr (Zeiss). Data were acquired and analyzed by Axio Vision software (Zeiss).

Samples for negative control were prepared in the same way except that the incubation with the serotonin-specific antibody was omitted.

4.2.5

Determination of the cytosolic Ca^{2+}concentration

Platelets were loaded with the fluorescent probe fura 2 acetoxymethyl ester (FURA2AM), and re-suspended at a concentration of $2x10^8$ cells/mL in the basal buffer containing 0.5 mM $Ca2^+$. The fluorescence changes were measured at 36°C in a thermostated, magnetically stirred cuvette using excitation and emission wavelengths of 340 nm and 505 nm, respectively.

4.2.6

Determination of Ca2+ release

Platelet release of Ca^{2+} was determined by means of the fluorescent probe FURA free acid (0.1 µM). Platelets were incubated in Tyrode buffer containing 30 µM EGTA for 5 min at 37°C, they were then stimulated with thrombin 500 mU/ml and the fluorescence changes was measured using excitation and emission wavelengths of 340 nm and 505 nm, respectively.

4.2.7

Acridine orange accumulation

The transport of the fluorescent probe acridine orange into human platelets was monitored by incubating the platelet suspensions (2×108 cells/ml of basal buffer) at 37 °C and using excitation and emission wavelengths of 492 and 530 nm, respectively.

4.2.8

Measurement of ATP secretion

ATP released into bulk solution was detected by means of a luciferin–luciferase bioluminescence assay. The ATP molecules released react immediately with the luciferin–luciferase and yield photons of light, which are measured in the luminometer LKB 1250-001. Excess luciferin–luciferase (50 μl) (ATP Bioluminescence Assay kit CLS II, Roche Diagnostics) was added to the platelet suspension. Then platelets were activated by thrombin (50 mU/ml) and the luminescent signal was detected. The ATP content of each sample was estimated using an internal standard addition (100 picomoles of ATP were added twice to the assay).

References

Abrams CS. Intracellular signaling in platelets. Curr Opin Hematol. 2005; 12:401-5.

Adams TE, Huntington JA. Thrombin-cofactor interactions: structural insights into regulatory mechanisms. Arterioscler Thromb Vasc Biol 2006; 26: 1738–45.

Apparsundaram S,Galli A,DeFelice LJ,Hartzell HC,Blakely RD.Acute regulation of norepinephrine transport. I. PKC-linked muscarinic receptors influence transport capacity and transporter density in SK-N-SH cells. J Pharmacol Exp Ther. 1998;287:733-743.

Apparsundaram S,Schroeter S,Blakely RD.Acute regulation of norepinephrine transport. II. PKC-modulated surface expression of human norepinephrine transporter proteins.J Pharmacol Exp Ther.1998;287:744-751.

Aughan RA, Huff RA,Uhl GR,Kuhar MJ.Protein kinase C-mediated phosphorylation and functional regulation of dopamine transporters in striatal synaptosomes.J Biol Chem.1997;272:15541-15546.

Adair BD, Xiong JP, Maddock C, Goodman SL, Arnaout MA, Yeager M. Three-dimensional EM structure of the ectodomain of integrin {alpha}V{beta}3 in a complex with fibronectin. J Cell Biol 2005;168:1109–1118.

Ahmad SS, Rawala-Sheikh R, Walsh PN. Comparative interactions of factor IX and factor IXa with human platelets. J Biol Chem 1989; 264:3244–51.

Andrews RK, Shen Y, Gardiner EE, Dong JF, López JA, Berndt MC. The glycoprotein Ib-IX-V complex in platelet adhesion and signaling. Thromb Haemost 1999; 82: 357–64.

Andrews R.K., A.D. Munday, C.A. Mitchell and M.C. Berndt. Blood 98 (2001), pp. 681–687

Andrews and J.E. Fox. J. Biol. Chem. 267 (1992), pp. 18605–18611

Ayala YM, Cantwell AM, Rose T, Bush LA, Arosio D, Di Cera E. Molecular mapping of thrombin-receptor interactions. Proteins 2001;45: 107–16.

Ayala Y, Di Cera E. Molecular recognition by thrombin. Role of the slow→fast transition, site-specific ion binding energetics and thermodynamic mapping of structural components. J Mol Biol 1994; 235: 733-746

Arias-Salgado EG, et al. PTP-1B is an essential positive regulator of platelet integrin signaling. J Cell Biol 2005;170:837–845.

Authi KS, Watson SP and Kakkar VV. Mechanisms of platelet activation and control. Plenum Press, New York, 1993.

Babich M, King KL and Nissenson RA (1990) Thrombin stimulates inositol phosphate production and intracellular free calcium by a pertussis toxin-insensitive mechanism in osteosarcoma cells. Endocrinology 126: 948-954

Baffy G, Yang L, Raj S, Manning DR and Williamson JR (1994) G protein coupling to the thrombin receptor in Chinese hamster lung fibroblasts. J Biol Chem 269: 8483-8487

Bellucci S, Michiels JJ. Spontaneous proliferative megakaryopoiesis and platelet hyperactivity in essential thrombocythemia: is thrombopoietine the link?. Ann Hematol 2000; 79: 51-58

Berlin NI: Diagnosis and classification of the polycythemias. Semin Hematol 1975; 12: 339–351.

Bennett JS, Vilaire G. Exposure of platelet fibrinogen receptors by ADP and epinephrine. J Clin Invest 1979;64:1393–1401.

Beuming, T., Shi, L., Javitch, J.A., Weinstein, H. 2006. A comprehensive structure-based alignment of prokaryotic and eukaryotic neurotransmitter/Na+ symporters (NSS) aids in the use of the LeuT structure to probe NSS structure and function. Mol. Pharmacol. 70:1630–1642

Bernatowicz MS, Klimas CE, Hartl KS, Peluso M, Allegretto NJ, Seiler SM. Development of potent thrombin receptor antagonist peptides. J Med Chem 1996; 39: 4879– 87.

Bergmeier W, et al. The role of platelet adhesion receptor GPIb{alpha} far exceeds that of its main ligand, von Willebrand factor, in arterial thrombosis. Proc Natl Acad Sci USA 2006;103:16900–16905.

Benka ML, Lee M, Wang GR, Buckman S, Burlacu A, Cole L, DePina A, Dias P, Granger A, Grant B, Haywardlester A, Karki S, Mann S, Marcu O, Nussenzweig A, Piepenhagen P, Raje M, Roegiers F, Rybak S, Salic A, Smithhall J, Waters J, Yamamoto N, Yanowitz J, Yeow K, Busa WB and Mendelsohn ME (1995) The thrombin receptor in human platelets is coupled to a GTP binding protein of the G alpha q family. FEBS Lett 363: 49-52

Bhatt DL, Topol EJ. Scientific and therapeutic advances in antiplatelet therapy. Nat Rev Drug Discov 2003;2:15–28.

Bode W, Mayr I, Baumann U. The refined 1.9 A crystal structure of human alpha-thrombin: interaction with D-Phe-Pro-Arg chloromethylketone and significance of the Tyr-Pro-Pro-Trp insertion segment. EMBO J 1989; 8: 3467-3475

Brass LF, Manning DR, Cichowski K, Abrams CS. Signaling through G proteins in platelets: to the integrins and beyond. Thromb Haemost 1997;78:581–589.

Brunk I, Höltje M, von Jagow B, Winter S, Sternberg J, Blex C, Pahner I, Ahnert-Hilger G. Regulation of vesicular monoamine and glutamate transporters by vesicle-associated trimeric G proteins: new jobs for long-known signal transduction molecules. Handb Exp Pharmacol. 2006;(175):305-25.

D.C. Calverley, T.J. Kavanagh and G.J. Roth. Blood 91 (1998), pp. 1295–1303.

Carter WJ, Cama E, Huntington JA. Crystal structure of thrombin bound to heparin. J Biol Chem 2005; 280: 2745–9.

Chang CP, Zhao J, Wiedmer T, Sims PJ. Contribution of platelet microparticle formation and granule secretion to the transmembrane migration of phosphatidylserine. J Biol Chem 1993;268:7171–7178.

Coller BS. Blockade of platelet GPIIb/IIIa receptors as an antithrombotic strategy. Circulation 1995;92:2373–2380.

ChamberlainLH,GouldGW.The vesicle- and target-SNARE proteins that mediate Glut4 vesicle fusion are localized in detergent-insoluble lipid rafts present on distinct intracellular membranes. J Biol Chem. 2002; 277: 49750-49754.

Chen J.G., Liu-Chen S., Rudnick G. 1998. Determination of external loop topology in the serotonin transporter by site-d Androutsellis-Theotokis A., Rudnick G. 2002. Accessibility and conformational coupling in serotonin transporter predicted internal domains. J. Neurosci. 22:8370–8378

N. Christodoulides, S. Feng, J.C. Resendiz, M.C. Berndt and M.H. Kroll. Thromb. Res. 102 (2001), pp. 133–142

Connolly AJ, Ishihara H, Kahn ML, Farese RV Jr, Coughlin SR. Role of the thrombin receptor in development and evidence for a second receptor. Nature 1996; 381: 516– 9.

Covic L, Gresser AL. Kuliopulos A. Biphasic kinetics of activation and signaling for PAR1 and PAR4 thrombin receptors in platelets. Biochemistry 2000; 39: 5458– 67.

Cesar JM, de Miguel D, Garcia Avello A, Burgaleta C. Platelet dysfunction in primary thrombocythemia using the platelet function analyzer, PFA-100. Am J Clin Pathol 2005; 123: 772-777

Caranobe C, Sie P, Fernandez F, Pris J, Moatti S, Boneu B. (1984) Abnormal platelet serotonin uptake and binding sites in myeloproliferative disorders. Thromb Haemost 51; 349-53.

Cortellazzo S, Viero P, Buczko W, Barbui T, De Gaetano G. (1985) Platelet 5-hydroxytryptamine transport and storage in myeloproliferative disorders. Scand J Haematol 34; 146-151.

Casadevall N, Vainchenker W: A unique clonal JAK2 mutation leading to constitutive signalling causes polycythaemia vera. Nature 2005; 434: 1144–1148.

Cools J, Peeters P, Voet T, Aventin A, Mecucci C, Grandchamp B, Marynen P: Genomic organization of human JAK2 and mutation analysis of its JH2-domain in leukemia. Cytogenet Cell Genet 1999; 85: 260–266.

Dahlback B, Stenflo J. Binding of bovine coagulation factor Xa to platelets. Biochemistry 1978; 17: 4938–45.

Dameshek W: Some speculations on the myeloproliferative syndromes. Blood 1951; 6: 372–375.

Dameshek W: Physiopathology and course of polycythemia vera as related to therapy. J Am Med Assoc 1950; 142: 790–797.

De Candia E, Hall SW, Rutella S, Landolfi R, Andrews RK, De Cristofaro R. Binding of thrombin to glycoprotein Ib accelerates the hydrolysis of Par-1 on intact platelets. J Biol Chem 2001; 276: 4692– 8.

De Cristofaro R, De Candia E, Landolfi R, Rutella S, Hall SW. Structural and functional mapping of the thrombin domain involved in the binding to the platelet glycoprotein Ib. Biochemistry 2001; 40: 13268–73.

De Gaetano G. Historical overview of the role of platelets in hemostasis and thrombosis. Haematologica 2001; 86:349-56.

De Marco L, Mazzucato M, Fabris F, De Roia D, Coser P, Girolami A, Vicente V, Ruggeri ZM. Variant Bernard-Soulier syndrome type bolzano. A congenital bleeding disorder due to a structural and functional abnormality of the platelet glycoprotein Ib-IX complex. J Clin Invest 1990; 86: 25– 31.

De Marco L, Mazzucato M, Masotti A, Fenton JWd, Ruggeri ZM. Function of glycoprotein Ib alpha in platelet activation induced by alpha-thrombin. J Biol Chem 1991; 266: 23776– 83.

De Marco L, Mazzucato M, Masotti A, Ruggeri ZM. Localization and characterization of an alpha-thrombin-binding site on platelet glycoprotein Ib alpha. J Biol Chem 1994; 269: 6478– 84.

De Virgilio M, Kiosses WB, Shattil SJ. Proximal. selective, and dynamic interactions between integrin alphaIIbbeta3 and protein tyrosine kinases in living cells. J Cell Biol 2004;165:305–311.

J.F. Dong, G. Sae-Tung and J.A. Lopez. Blood 89 (1997), pp. 4355–4363

C.Q. Li, J.F. Dong, F. Lanza, D.A. Sanan, G. Sae-Tung and J.A. Lopez. J. Biol. Chem. 270 (1995), pp. 16302–16307

Dumas JJ, Kumar R, Seehra J, Somers WS, Mosyak L. Crystal structure of the GpIbalpha-thrombin complex essential for platelet aggregation. Science 2003; 301: 222–6.

J.F. Dong, C.Q. Li and J.A. Lopez. Biochemistry 33 (1994), pp. 13946–13953

Du XP, Plow EF, Frelinger AL III, O'Toole TE, Loftus JC, Ginsberg MH. Ligands "activate" integrin alpha IIb beta 3 (platelet GPIIb-IIIa). Cell 1991;65:409–416.

X. Du, J.E. Fox and S. Pei.J. Biol. Chem. 271 (1996), pp. 7362–7367.

G.D. Englund, R.J. Bodnar, Z. Li, Z.M. Ruggeri and X. Du. J. Biol. Chem. 276 (2001), pp. 16952–16959.

Erickson, J.-D., Eiden, L.-E., and Hoffman, B.-J. (1992) Proc. Natl. Acad. Sci. U. S. A. 89, 10993-10997

Faull RJ, Du X, Ginsberg MH. Receptors on platelets. Methods Enzymol 1994;245:183–194.

Flaumenhaft R. Molecular basis of platelet granule secretion. Arterioscler Thromb Vasc Biol 2003; 23:1152-60.

Fee JA, Monsey JD, Handler RJ, Leonis MA, Mullaney SR, Hope HM and Silbert DF (1994) A Chinese hamster fibroblast mutant defective in thrombin-induced signaling has a low level of phospholipase C-beta 1. J Biol Chem 269: 21699-21708

Finazzi G, Budde U, Michiels JJ. Bleeding time and platelet function in essential thrombocythemia and other myeloproliferative disorders. Leuk Lymphoma 1996; 22 (supl1): 71-78

Fabris F, Randi M, Casonato A, Scattolo N, Girolami A. (1982) Platelet serotonin and platelet aggregation in the differential diagnosis of thrombocythosis. Thromb. Haemost. 48; 343-8.

Fabris F, Randi M, Sbrojavacca R, Casonato A, Girolami A: The possible value of platelet aggregation studies in patients with increased platelet count . Blut 1981;43:279-285

S. Feng, J.C. Resendiz, X. Lu and M.H. Kroll. Blood 102 (2003), pp. 2122–2129.

Fredenburgh JC, Stafford AR, Weitz JI. Evidence for allosteric linkage between exosites 1 and 2 of thrombin. J Biol Chem 1997; 272: 25493-25499

Geiger J. Inhibitors of platelet signal transduction as anti-aggregatory drugs. Expert Opin Investig Drugs 2001;10:865–890.

Goncalves I, Hughan SC, Schoenwaelder SM, Yap CL, Yuan Y, Jackson SP. Integrin alpha IIb beta 3-dependent calcium signals regulate platelet-fibrinogen interactions under flow. Involvement of phospholipase C gamma 2. J Biol Chem 2003;278:34812–34822.

Gachet C. The platelet P2 receptors as molecular targets for old and new antiplatelet drugs. Pharmacol Ther 2005; 108:180-92.

Ginsberg MH, Forsyth J, Lightsey A, Chediak J, Plow EF. Reduced surface expression and binding of fibronectin by thrombin-stimulated thrombasthenic platelets. J Clin Invest 1983;71:619–624.

Greengard JS, Heeb MJ, Ersdal E, Walsh PN, Griffin JH. Binding of coagulation factor XI to washed human platelets. Biochemistry 1986; 25: 3884–90.

Gavrilovskaya IN, Brown EJ, Ginsberg MH, Mackow ER. Cellular entry of hantaviruses which cause hemorrhagic fever with renal syndrome is mediated by beta3 integrins. J Virol 1999;73:3951–3959.

Hamilton JR,Cornelissen I,Coughlin SR. Impaired hemostasis and protection against thrombosis in protease-activated receptor 4-deficient mice is due to lack of thrombin signaling in platelets. J Thromb Haemost 2004; 2: 1429– 35.

Hung DT, Wong YH, Vu TK and Coughlin SR (1992) The cloned platelet thrombin receptor couples to at least two distinct effectors to stimulate phosphoinositide hydrolysis and inhibit adenylyl cyclase. J Biol Chem 267: 20831-20834

Hung DT, Vu TK, Wheaton VI, Ishii K, Coughlin SR. Cloned platelet thrombin receptor is necessary for thrombin-induced platelet activation. J Clin Invest 1992; 89: 1350– 3.

Hogg PJ, Jackson CM, Labanowski JK, Bock PE. Binding of fibrin monomer and heparin to thrombin in a ternary complex alters the environment of the thrombin catalytic site, reduces affinity for hirudin, and inhibits cleavage of fibrinogen. J Biol Chem 1996; 271:26088–95.

Huntington JA. Molecular recognition mechanisms of thrombin. J Thromb Haemost 2005; 3: 1861–72

Hawiger J, Kloczewiak M, Timmons S, Strong D, Doolittle RF. Interaction of fibrinogen with staphylococcal clumping factor and with platelets. Ann NY Acad Sci 1983;408:521–535.

Heuck G: Zwei Fälle von Leukämie mit eigentümlichem Blut resp. Knochenmarksbefund. Virchows Arch 1879; 78: 475.

Henry L.K., Adkins E.M., Han Q., Blakely R.D. 2003. Serotonin and cocaine-sensitive inactivation of human serotonin transporters by methanethiosulfonates targeted to transmembrane domain I. J. Biol. Chem. 278:37052–37063

Hantgan RR. Fibrin protofibril and fibrinogen binding to ADP-stimulated platelets: evidence for a common mechanism. Biochim Biophys Acta 1988;968:24–35.

M.J. Hickey, S.A. Williams and G.J. Roth. Proc. Natl. Acad. Sci. U. S. A. 86 (1989), pp. 6773–6777.

F. Lanza, M. Morales, C. de La Salle, J.P. Cazenave, K.J. Clemetson, T. Shimomura and D.R. Phillips. J. Biol. Chem. 268 (1993), pp. 20801–20807.

Jackson SP, Yap CL, Anderson KE. Phosphoinositide 3-kinases and the regulation of platelet function. Biochem Soc Trans 2004;32:387–392.

Jardetzky O. 1966. Simple allosteric model for membrane pumps. Nature 211:969–970

Jencks W.P. 1980. The utilization of binding energy in coupled vectorial processes. Adv. Enzymol. Relat Areas Mol. Biol. 51:75–106

James C, Ugo V, Le Couedic JP, Staerk J, Delhommeau F, Lacout C, Garcon L, Raslova H, Berger R, Bennaceur-Griscelli A, Villeval JL, Constantinescu SN,

Jones AV, Kreil S, Zoi K, Waghorn K, Curtis C, Zhang L, Score J, Seear R, Chase AJ, Grand FH, White H, Zoi C, Loukopoulos D, Terpos E, Vervessou EC, Schultheis B, Emig M, Ernst T, Lengfelder E, Hehlmann R, Hochhaus A, Oscier D, Silver RT, Reiter A, Cross NC: Widespread occurrence of the JAK2 V617F mutation in chronic myeloproliferative disorders. Blood 2005; 106: 2162–2168.

Jaffe SS, Harris NL, Sterm A, Vardiman JW:WHO Classification of Tumours: Tumours of Haematopoiesis and Lymphoid Tissues. Lyon, IARC, 2001, pp 31–42.

JayanthiLD,SamuvelDJ,RamamoorthyS.Regulated internalization and phosphorylation of the native norepinephrine transporter in response to phorbol esters: evidence for

localization in lipid rafts and lipid raft mediated internalization.J Biol Chem.2004;279:19315-19326.

Kanthou C, Kanse SM, Kakkar VV and Benzakour O (1996) Involvement of pertussis toxin-sensitive and -insensitive G proteins in alpha-thrombin signalling on cultured human vascular smooth muscle cells. Cell Signalling

Kanner, B. I., and Schuldiner, S. (1987) CRC Crit. Rev. Biochem. 22, 1-38

Kralovics R, Passamonti F, Buser AS, Teo SS, Tiedt R, Passweg JR, Tichelli A, Cazzola M, Skoda RC: A gain-of-function mutation of JAK2 in myeloproliferative disorders. N Engl J Med 2005; 352: 1779–1790.

Kahn ML, Nakanishi-Matsui M, Shapiro MJ, Ishihara H, Coughlin SR. Protease-activated receptors 1 and 4 mediate activation of human platelets by thrombin. J Clin Invest 1999; 103: 879– 87.

Kane WH, Lindhout MJ, Jackson CM, Majerus PW. Factor Va dependent binding of factor Xa to human platelets. J Biol Chem 1980; 255: 1170–4.

Karakantza M, Giannakoulas NC, Zikos P. Markers of endothelial and in vivo platelet activation in patients with essential thrombocythemia vera. Int J Hematol 2004; 79: 253-259

Kane WH, Majerus PW. The interaction of human coagulation factor Va with platelets. J Biol Chem 1982; 257: 3963–9.

Kauffenstein G, et al. The P2Y(12) receptor induces platelet aggregation through weak activation of the alpha(IIb)beta(3) integrin – a phosphoinositide 3-kinase-dependent mechanism. FEBS Lett 2001;505:281–290.

Karczewski J, Knudsen KA, Smith L, Murphy A, Rothman VL, Tuszynski GP. The interaction of thrombospondin with platelet glycoprotein GPIIb-IIIa. J Biol Chem 1989;264:21322–21326

Kasirer-Friede A, Cozzi MR, Mazzucato M, De Marco L, Ruggeri ZM, Shattil SJ. Signaling through GP Ib-IX-V activates alpha IIb beta 3 independently of other receptors. Blood 2004;103:3403–3411.

D. Kenny, P.A. Morateck and R.R. Montgomery. Blood 99 (2002), pp. 4428–4433.

S.A. Korrel, K.J. Clemetson, H. Van Halbeek, J.P. Kamerling, J.J. Sixma and J.F. Vliegenthart. Eur. J. Biochem. 140 (1984), pp. 571–576.

F. Lanza, M. Morales, C. de La Salle, J.P. Cazenave, K.J. Clemetson, T. Shimomura and D.R. Phillips. J. Biol. Chem. 268 (1993), pp. 20801–20807.

Le Bonniec BF, Esmon CT. Glu-192-Gln substitution in thrombin mimics the catalytic switch induced by thrombomodulin. Proc Natl Acad Sci 1991; 88: 7371-7375

Lefkovits J, Plow EF, Topol EJ. Platelet glycoprotein IIb/IIIa receptors in cardiovascular medicine. N Engl J Med 1995;332:1553–1559.

Lopez J. J., A. Camello-Almaraz, J.A. Pariente, G.M. Salido and J.A. Rosado, Ca2+ accumulation into acidic organelles mediated by Ca2+- and vacuolar H+-ATPases in human platelets, Biochem. J. 390 (2005), pp. 243–252.

J.A. Lopez, D.W. Chung, K. Fujikawa, F.S. Hagen, T. Papayannopoulou and G.J. Roth. Proc. Natl. Acad. Sci. U. S. A. 84 (1987), pp. 5615–5619.

J.A. Lopez, D.W. Chung, K. Fujikawa, F.S. Hagen, E.W. Davie and G.J. Roth. Proc. Natl. Acad. Sci. U. S. A. 85 (1988), pp. 2135–2139.

Luo H, Rose P, Barber D, Hanratty WP, Lee S, Roberts TM, D'Andrea AD, Dearolf CR: Mutation in the Jak kinase JH2 domain hyperactivates Drosophila and mammalian Jak-Stat pathways. Mol Cell Biol 1997; 17:1562–1571.

Landolfi R, Ciabattoni G, Patrinani P. Increased thromboxane biosynthesis in patients with polycythemia vera: evidence for aspirin-suppressible platelet activation in vivo. Blood 1992; 80: 1965-1971

Lian L, Wang Y, Draznin J, Eslin D, Bennett JS, Poncz M, Wu D, Abrams CS. The relative role of PLCβ and PI3Kγ in platelet activation. Blood 2005 106:110-7.

Lacout C, Pisani DF, Tulliez M, Moreau Gachelin F, Vainchenker W, Villeval JL: JAK2V617F expression in murine hematopoietic cells leads to MPD mimicking human PV with secondary myelofibrosis. Blood 2006; 108: 1652–1660.

Levine RL, Wadleigh M, Cools J, Ebert BL, Wernig G, Huntly BJ, Boggon TJ, Wlodarska I, Clark JJ, Moore S, Adelsperger J, Koo S, Lee JC, Gabriel S, Mercher T, D'Andrea A, Frohling S, Dohner K, Marynen P, Vandenberghe P, Mesa RA, Tefferi A, Griffin JD, Eck MJ, Sellers WR, Meyerson M, Golub TR, Lee SJ, Gilliland DG: Activating mutation in the tyrosine kinase JAK2 in polycythemia vera, essential thrombocythemia and myeloid metaplasia with myelofibrosis. Cancer Cell 2005; 7: 387–397.

Liu, Y., Peter, D., Roghani, A., Schuldiner, S., Prive, G. G., Eisenberg, D., Brecha, N., and Edwards, R. H. (1992) Cell 70, 539-551

Litvinov RI, Shuman H, Bennett JS, Weisel JW. Binding strength and activation state of single fibrinogen-integrin pairs on living cells. Proc Natl Acad Sci USA 2002;99:7426–7431

Malkowski MG,Martin PD, Guzik JC, Edwards BF. The co-crystal structure of unliganded bovine alpha-thrombin and prethrombin-2: movement of the Tyr-Pro-Pro-Trp segment and active site residues upon ligand binding. Protein Sci 1997; 6: 1438–48.

P. Marchese, M. Murata, M. Mazzucato, P. Pradella, L. De Marco, J. Ware and Z.M. Ruggeri. J. Biol. Chem. 270 (1995), pp. 9571–9578.

McNicol A, Israels SJ. Platelet dense granules: structure, function and implications for haemostasis. Thromb Res 1999; 95:1-18.

Mondoro TH, Wall CD, White MM, Jennings LK. Selective induction of a glycoprotein IIIa ligand-induced binding site by fibrinogen and von Willebrand factor. Blood 1996;88:3824–3830.

Mendolicchio GL, Ruggeri ZM. New perspectives on von Willebrand factor functions in hemostasis and thrombosis. Semin Hematol 2005;42:5–14.

Marguerie GA, Plow EF, Edgington TS. Human platelets possess an inducible and saturable receptor specific for fibrinogen. J Biol Chem 1979;254:5357–5363.

Mitchell S.M., Lee E., Garcia M.L., Stephan M.M. 2004. Structure and function of extracellular loop 4 of the serotonin transporter as revealed by cysteine-scanning mutagenesis. J. Biol. Chem. 279:24089–24099

Michiels JJ, Abels J, Steketee J, van Vliet HHDM, Vuzevski VD. Erythromelalgia caused by platelet-mediated arteriolar inflammation and thrombosis in thrombocythemia. Ann Intern Med 1985; 102: 466-471

Michiels JJ, van Genderen PJJ, Lindemans J, van Vliet HHDM. Erythromelalgic, thrombotic and hemorrhagic thrombocythemia. Leuk Lymphoma 1996; 22(suppl 1): 47-56

Merickel A, Rosandich P, Peter D, Edwards RH. Identification of residues involved in substrate recognition by a vesicular monoamine transporter. J Biol Chem. 1995;270:25798-25804.

Miletich JP, Jackson CM, Majerus PW. Properties of the factor Xa binding site on human platelets. J Biol Chem 1978; 253: 6908–16

Myles T, Yun TH, Hall SW, Leung LL. An extensive interaction interface between thrombin and factor V is required for factor V activation. J Biol Chem 2001; 276: 25143–9.

S. Moog, P. Mangin, N. Lenain, C. Strassel, C. Ravanat, S. Schuhler, M. Freund, M. Santer, M. Kahn, B. Nieswandt, C. Gachet, J.P. Cazenave and F. Lanza. Blood 98 (2001), pp. 1038–1046.

Nakanishi-Matsui M, Zheng YW, Sulciner DJ, Weiss EJ, Ludeman MJ, Coughlin SR. PAR3 is a cofactor for PAR4 activation by thrombin. Nature 2000; 404: 609– 13

Nelson P.J., Rudnick G. 1979. Coupling between platelet 5-hydroxytryptamine and potassium transport. J. Biol. Chem. 254:10084–10089

Nurden AT. Glanzmann thrombasthenia. Orphanet J Rare Dis 2006;1:10.

Offermanns S, Toombs CF, Hu YH, Simon MI. Defective platelet activation in G alpha(q)-deficient mice. Nature 1997; 389: 183– 6.

O'Brien JR: "Exausted"platelets continue to circulate. Lancet 1978;ii:1316-1317

Offermanns S, Laugwitz KL, Spicher K, Schultz G. G proteins of the G12 family are activated via thromboxane A2 and thrombin receptors in human platelets. Proc Natl Acad Sci U S A 1994; 91: 504– 8.

Ogino Y, Tanaka K and Shimizu N (1996) Direct evidence for two distinct G proteins coupling with thrombin receptors in human neuroblastoma SH-EP cells. Eur J Pharmacol 316: 105-109

Okamura T, Hasitz M, Jamieson GA. Platelet glycocalicin: interaction with thrombin and role as thrombin receptor on the platelet surface. J Biol Chem 1978; 253: 3435– 43.

Ozaki Y, Asazuma N, Suzuki-Inoue K, Berndt MC. Platelet GPIb-IX-V-dependent signaling. J Thromb Haemost 2005;3:1745–1751.

Panizzi P, Friedrich R, Fuentes-Prior P, Kroh HK, Briggs J, Tans G, Bode W, Bock PE. Novel fluorescent prothrombin analogs as probes of staphylocoagulase-prothrombin interactions. J Biol Chem 2006; 281: 1169–78.

Parton RG,Richards AA.Lipid rafts and caveolae as portals for endocytosis: new insights and common mechanisms.Traffic.2003;4:724-738.

Peter, D., Jimenez, J., Liu, Y., Kim, J., and Edwards, R. H. (1994) J. Biol. Chem. 269, 7231-7237

Pareti FI, Gugliotta L. Mannucci L, Guarini A, Mannucci PM. (1982) Biochemical and metabolic aspects of platelet dysfunctions in chronic myeloproliferative disorders. Thromb. Haemost. 47; 84-9.

Priestle JP, Rahuel J, Rink H, Tones M, Grutter MG. Changes in interactions in complexes of hirudin derivatives and human alpha-thrombin due to different crystal forms. Protein Sci 1993; 2: 1630–42.

Ramakrishnan V, DeGuzman F, Bao M, Hall SW, Leung LL, Phillips DR. A thrombin receptor function for platelet glycoprotein Ib-IX unmasked by cleavage of glycoprotein V. Proc Natl Acad Sci U S A 2001; 98: 1823– 8.

Rawala-Sheikh R, Ahmad SS, Ashby B, Walsh PN. Kinetics of coagulation factor X activation by platelet-bound factor IXa. Biochemistry 1990; 29: 2606–11.

Rosado J.A. , J.J. Lopez, A.G. Harper, M.T. Harper, P.C. Redondo, J.A. Pariente, S.O. Sage and G.M. Salido, Two pathways for store-mediated calcium entry differentially dependent on the actin cytoskeleton in human platelets, J. Biol. Chem. 279 (2004), pp. 29231–29235.

RamamoorthyS,BlakelyRD.Phosphorylation and sequestration of serotonin transporters differentially modulated by psychostimulants.Science.1999;285:763-766.

Rudnick G. 2002. Mechanisms of Biogenic Amine Neurotransmitter Transporters. In: Reith MEA, editor. Neurotransmitter Transporters, Structure, Function, and Regulation. Humana Press, Totowa, New Jersey, pp. 25–52

Rao AK. Molecular and biochemical basis for the platelet dysfunction in myeloproliferative disorders. Semin Hematol 2004 ; 41: 6-9.

RudnickG, Fishkes H, Nelson PJ, Shuldiner S. (1980) Evidence for two distinct serotonin transport systems in platelets. J Biol Chem 255; 3638-41.

Rocca B, Ciabattoni G, Tartaglione R. Increased thromboxane biosynthesis in essential thrombocythemia. Thromb Haemost 1995; 74: 1225-1230
RamamoorthyS,GiovanettiE,QianY,BlakelyRD.Phosphorylation and regulation of antidepressant-sensitive serotonin transporters.J Biol Chem.1998;273:2458-2466.

Rudnick G., Nelson P.J. 1978. Platelet 5-hydroxytryptamine transport - an electroneutral mechanism coupled to potassium. Biochemistry 17:4739–4742

Ruggeri ZM. Mechanisms initiating platelet thrombus formation. Thromb Haemost 1997;78:611–616.

Ruggeri ZM, Bader R, de Marco L. Glanzmann thrombasthenia: deficient binding of von Willebrand factor to thrombin-stimulated platelets. Proc Natl Acad Sci USA 1982;79:6038–6041.

Rendu F, Brohard-Bohn B. The platelet release reaction: granules' constituents, secretion and functions. Platelets 2001; 12:261-73.

Schoenwaelder SM, Yuan Y, Cooray P, Salem HH, Jackson SP. Calpain cleavage of focal adhesion proteins regulates the cytoskeletal attachment of integrin alphaIIbbeta3

(platelet glycoprotein IIb/IIIa) and the cellular retraction of fibrin clots. J Biol Chem 1997;272:1694–1702.

Sambrano GR, Huang W, Faruqi T, Mahrus S, Craik C, Coughlin SR. Cathepsin G activates protease-activated receptor-4 in human platelets. J Biol Chem 2000; 275: 6819– 23.

Sambrano GR, Weiss EJ, Zheng YW, Huang W, Coughlin SR. Role of thrombin signalling in platelets in haemostasis and thrombosis. [Comment In: Nature. 2001 Sep 6;413(6851):26–7 UI: 21429411]. Nature 2001; 413: 74– 8.

Scandura JM, Ahmad SS, Walsh PN. A binding site expressed on the surface of activated human platelets is shared by factor X and prothrombin. Biochemistry 1996; 35: 8890–902

Schechter I, Berger A. On the size of the active site in proteases. I. Papain. Biochem Biophys Res Commun 1967; 27: 157-162

Savage B, Almus-Jacobs F, Ruggeri ZM. Specific synergy of multiple substrate-receptor interactions in platelet thrombus formation under flow. Cell 1998;94:657–666.

Scarborough RM, Kleiman NS, Phillips DR. Platelet glycoprotein IIb/III antagonists. What are the relevant issues concerning their pharmacology and clinical use? Circulation 1999;100:437–444.

Shattil SJ, Newman PJ. Integrins: dynamic scaffolds for adhesion and signaling in platelets. Blood 2004;104:1606–1615.

SamuvelDJ,JayanthiLD,BhatNR,RamamoorthyS.A role for p38 mitogen-activated protein kinase in the regulation of the serotonin transporter: evidence for distinct cellular mechanisms involved in transporter surface expression.J Neurosci.2005;25:29-41.

Sato Y., Zhang Y.-W., Androutsellis-Theotokis A., Rudnick G. 2004. Analysis of transmembrane domain 2 of rat serotonin transporter by cysteine scanning mutagenesis. J. Biol. Chem. 279:22926–22933

Smith JW, Piotrowicz RS, Mathis D. A mechanism for divalent cation regulation of beta 3-integrins. J Biol Chem 1994;269:960–967.

Selheim F, Froyset AK, Strand I, Vassbotn FS, Holmsen H. Adrenaline potentiates PI 3-kinase in platelets stimulated with thrombin and SFRLLN: role of secreted ADP. FEBS Lett 2000;485:62-6.

Shattil SJ, Hoxie JA, Cunningham M, Brass LF. Changes in the platelet membrane glycoprotein IIb.IIIa complex during platelet activation. J Biol Chem 1985;260:11107–11114.

Shapiro MJ, Weiss EJ, Faruqi TR, Coughlin SR. Protease-activated receptors 1 and 4 are shut off with distinct kinetics after activation by thrombin. J Biol Chem 2000; 275: 25216– 21.

Y. Shen, J.F. Dong, G.M. Romo, W. Arceneaux, A. Aprico, E.E. Gardiner, J.A. Lopez, M.C. Berndt and R.K. Andrews. Blood 99 (2002), pp. 145–150

Siess W, Grunberg B, Luber K. Functional relationship between cyclic AMP-dependent protein phosphorylation and platelet inhibition. Adv Exp Med Biol 1993;344:229–235.

Sinha D, Seaman FS, Koshy A, Knight LC,Walsh PN. Blood coagulation factor XIa binds specifically to a site on activated human platelets distinct from that for factor XI. J Clin Invest 1984; 73: 1550–6.

Selak MA, Chignard M, Smith JB. Cathepsin G is a strong platelet agonist released by neutrophils. Biochem J 1988; 251: 293– 9.

Suzuki A, Kozawa O, Shinoda J, Watanabe Y, Saito H and Oiso Y (1996) Thrombin induces proliferation of osteoblast-like cells through phosphatidylcholine hydrolysis. J Cell Physiol 168: 209-216

Swift S, Sheridan PJ, Covic L and Kuliopulos A (2000) Par1 thrombin receptor-G protein interactions—separation of binding and coupling determinants in the G alpha subunit. J Biol Chem 275: 2627-2635

Talvenheimo J., Fishkes H., Nelson P.J., Rudnick G. 1983. The serotonin transporter-imipramine 'receptor': Different sodium requirements for imipramine binding and serotonin translocation. J. Biol. Chem. 258:6115–6119
Rudnick G. 1998. Bioenergetics of neurotransmitter transport. J. Bioenerget. Biomembr. 30:173–185

Takagi J, Petre BM, Walz T, Springer TA. Global conformational rearrangements in integrin extracellular domains in outside-in and inside-out signaling. Cell 2002;110:599–511.

Tanford C. 1983. Translocation pathway in the catalysis of active transport. Proc. Natl. Acad. Sci. USA 80:3701–3705

Tate C., Blakely R. 1994. The effect of N-linked glycosylation on activity of the Na^+-and Cl–-dependent serotonin transporter expressed using recombinant baculovirus in insect cells. J. Biol. Chem. 269:26303–26310

Thiagarajan P, Kelly KL. Exposure of binding sites for vitronectin on platelets following stimulation. J Biol Chem 1988;263:3035–3038.

Thiele J, Kvasnicka HM, Diehl V: Initial (latent) polycythemia vera with thrombocytosis mimicking essential thrombocythemia. Acta Haematol 2005; 113: 213–219.

Tracy PB, Peterson JM, Nesheim ME, McDuffie FC, Mann KG. Interaction of coagulation factor Vand factor Va with platelets. J Biol Chem 1979; 254: 103541.

Tsiang M, Jain AK, Dunn KE, Rojas ME, Leung LL, Gibbs CS. Functional mapping of the surface residues of human thrombin. J Biol Chem 1995; 270: 16854–63.

Tomiyama Y, Kunicki TJ, Zipf TF, Ford SB, Aster RH. Response of human platelets to activating monoclonal antibodies: importance of Fc gamma RII (CD32) phenotype and level of expression. Blood 1992;80:2261–2268.

Turetta L, Bazzan E, Bertagno K, Musacchio E, Deana R. Role of Ca(2+) and protein kinase C in the serotonin (5-HT) transport in human platelets.Cell Calcium. 2002 May;31(5):235-44.

Van Genderen PJJ, Prins F, Michiels JJ, Schrör K. Thromboxane-dependent platelet activation in vivo precedes arterial thrombosis in thrombocythaemia: a rationale for the use of low-dose aspirin as an antithrombotic agent. Br J Haematol 1999; 104: 438-441

Verhamme IM, Olson ST, Tollefsen DM, Bock PE. Binding of exosite ligands to human thrombin. Re-evaluation of allosteric linkage between thrombin exosites I and II. J Biol Chem 2002; 277: 6788–98

Vindigni A,Di Cera E. Release of fibrinopeptides by the slow and fast forms of thrombin. Biochemistry 1996; 35: 4417–26.

Vu TK, Hung DT, Wheaton VI, Coughlin SR. Molecular cloning of a functional thrombin receptor reveals a novel proteolytic mechanism of receptor activation. Cell 1991; 64: 1057– 68.

Ware J, Russell SR, Vicente V, Scharf RE, Tomer A, McMillan R, Ruggeri ZM. Nonsense mutation in the glycoprotein Ib alpha coding sequence associated with Bernard-Soulier syndrome. Proc Natl Acad Sci U S A 1990; 87: 2026– 30.

Watson SP, Auger JM, McCarty OJ, Pearce AC. GPVI and integrin alphaIIb beta3 signaling in platelets. J Thromb Haemost 2005;3:1752–1762.

Wagner CL, Mascelli MA, Neblock DS, Weisman HF, Coller BS, Jordan RE. Analysis of GPIIb/IIIa receptor number by quantification of 7E3 binding to human platelets. Blood 1996;88:907–914.

M.R. Wardell, C.C. Reynolds, M.C. Berndt, R.W. Wallace and J.E. Fox. J. Biol. Chem. 264 (1989), pp. 15656–15661

Weiss HJ, Turitto VT, Baumgartner HR. Platelet adhesion and thrombus formation on subendothelium in platelets deficient in glycoproteins IIb-IIIa, Ib, and storage granules. Blood 1986;67:322–330.

Wernig G, Mercher T, Okabe R, Levine RL, Lee BH, Gilliland DG: Expression of Jak2V617F causes a polycythemia vera-like disease with associated myelofibrosis in a murine bone marrow transplant model.
Blood 2006; 107: 4274–4281.

Wonerow P, Pearce AC, Vaux DJ, Watson SP. A critical role for phospholipase Cgamma2 in alphaIIbbeta3-mediated platelet spreading. J Biol Chem 2003;278:37520–37529.

Xu WF, Andersen H, Whitmore TE, Presnell SR, Yee DP, Ching A, Gilbert T, Davie EW, Foster DC. Cloning and characterization of human protease-activated receptor 4. Proc Natl Acad Sci U S A 1998; 95: 6642– 6.

J.C. Whisstock, Y. Shen, J.A. Lopez, R.K. Andrews and M.C. Berndt. Thromb. Haemost. 87 (2002), pp. 329–333

Winitz S, Gupta SK, Qian NX, Heasley LE, Nemenoff RA and Johnson GL (1994) Expression of a mutant Gi2 alpha subunit inhibits ATP and thrombin stimulation of cytoplasmic phospholipase A2-mediated arachidonic acid release independent of Ca2+ and mitogen-activated protein kinase regulation. J Biol Chem 269: 1889-1895

Yelin R, Schuldiner S. Vesicular neurotransmitter transporters: pharmacology, biochemistry, and molecular analysis. In: Reith MEA, ed. Neurotransmitter Transporters; Structure, Function, and Regulation. 2nd ed. Totowa, NJ: Humana Press; 2002:313-354.

Yun TH, Baglia FA, Myles T, Navaneetham D, Lopez JA, Walsh PN, et al. Thrombin activation of factor XI on activated platelets requires the interaction of factor XI and platelet glycoprotein Ib alpha with thrombin anion-binding exosites I and II, respectively. J Biol Chem 2003; 278: 48112–9.

Zarpellon A, Donella-Deana A, Folda A, Turetta L, Pavanetto M, Deana R. Serotonin (5-HT) Transport in Human Platelets is Modulated by Src-Catalysed Tyr-Phosphorylation of the Plasma Membrane Transporter SERT. Cell Physiol Biochem 2008;21:87-94.

Abbreviations

AA, Arachidonic acid
BSA, Albumin from bovine serum
cAMP, Adenosine 3',5'-cyclic monophosphate
cGMP, Guanosine 3',5'-cyclic monophosphate
COX, Cyclooxygenase
Da, Daltons
DAG, Diacylglycerol
DMSO Dimethyl sulfoxide
DTS Dense tubular system
EDTA Ethylenediaminetetraacetic acid
ER Endoplasmic reticulum
ERK Extracellular signal-regulated kinase
FACS Fluorescence-activated cell sorting
GP Glycoprotein
GTP Guanosine 5'-triphosphate
HEPES (4-(2-hydroxyethyl)-1-piperazineethanesulfonic acid)
IP3 Inositol 1,4,5-trisphosphate
LDH Lactate dehydrogenase
MAPK Mitogen-activated protein kinase
MEK MAP kinase kinase
MLC Myosin light chain
MMP Matrix metallo-protease
NO Nitric oxide
OCS Open canalicular system
PGI2 Prostacyclin
PI-3K Phosphatidylinositol 3-kinase
PIP2 Phosphatidylinositol bisphosphate
PK Protein kinase
PKC Protein kinase C
PLC Phospholipase C
PMA Phorbol 12-myristate 13-acetate
PMCA Plasma membrane calcium pump
PPP Platelet poor plasma
PRP Platelet rich plasma
PTK Protein tyrosine kinase
SDS-PAGE Sodium dodecyl sulfate polyacrylamide gel electrophoresis
SERCA Sarcolendoplasmic reticulum calcium ATPase
SMCE Store-mediated calcium entry
SPR Surface plasmon resonance
Tg Thapsigargin
TRAP Thrombin receptor activator peptide
TRIS Tris(hydroxymethyl)aminomethane
TXA2 Thromboxane A2
VWF Von Willebrand factor